Low-complexity and filter-tap memory optimized channel estimation in multi-mode and multi-standard OFDM systems

Farzad Foroughi Abari

Thesis for the degree of
Licentiate in Engineering

Lund University
Lund, Sweden
2011

Licentiate in Engineering (LicEng) is an intermediate academic degree between MSc and PhD awarded by Swedish and Finnish universities, likened to a Master of Philosophy (MPhil) degree in the British system.

Department of Electrical and Information Technology
Radio Systems Group
Lund University
P.O. Box 118, S-221 00 Lund, Sweden

Series of licentiate and doctoral theses
No. 29
ISSN: 1654-790X
ISBN: 978-91-7473-119-4

Printed in Sweden by Tryckeriet i E-huset, Lund University, Lund.
November 2011

Abstract

Communication over orthogonal pulses in frequency (e.g., OFDM) has become a dominant choice for the emerging high speed wireless standards. One of the main processing blocks in such systems is dedicated to combating and compensating for the fading frequency selective wireless channels. Thus, channel estimation is a crucial signal processing operation in modern wireless transceivers. To assist channel estimation, it is a common practice in wireless communications jargon to use pilots. Scattered pilots have been used in a number of existing state-of-the-art communications systems. For instance, LTE and DVB-H benefit from different forms of scattered pilots in their downlink transmission. Considering the very fact that it is desired to use low-complexity algorithms to address the channel estimation needs of the mobile terminals, a number of approaches to low-complexity estimators have been probed and discussed in this thesis. The focus of the work has been on developing algorithms with low hardware requirements in terms of processing elements as well as on-chip memory, when possible. In particular, it is shown how certain families of linear estimators can be manipulated into low-complexity variants which can be used as alternatives for channel estimation with a certain amount of performance degradation. Besides, the estimators have been tailored to the needs of two existing OFDM standards, i.e., LTE and DVB-H. In the event of co-integration of these standards, the innate analogy between them, in terms of OFDM system parameters and their respective pilot patterns, is exploited to reduce the overall hardware requirements for channel estimation purposes. For instance, it is shown that by exploiting the similarities in 2nd-order channel statistics, the employed channel estimators can be shared between LTE and DVB-H across their modes of operation. Furthermore, a certain strategy can be pursued for pilot pattern design in OFDM systems such that it is possible to reuse the designed estimators in multi-mode or/and multi-standard environments.

Contents

Preface

This thesis consists of a General Introduction and the following scientific papers which are referred to in the text by their roman numerals:[1]

I. Farzad Foroughi Abari, Johan Löfgren, and Ove Edfors, "Channel estimation for a mobile terminal in a multi-standard environment (LTE and DVB-H)", in *Proc. of IEEE Int. Conf. on Signal Process. and Commun. Syst.*, Omaha, NE, Sep. 2009.

II. Farzad Foroughi Abari, Farnaz Sharifabad, and Ove Edfors, "Low-complexity channel estimation for LTE in fast fading environments for implementation on multi-standard platforms", in *Proc. of IEEE Veh. Tech. Conf.*, Ottawa, Canada, Sep. 2010.

III. Farzad Foroughi Abari, Fredrik Rusek, and Ove Edfors, "On coefficient memory co-optimization for channel estimation in a multi-standard environment (LTE and DVB-H)", in *Proc. IEEE 8th Int. Workshop Multi-Carrier Syst. and Solutions*, Herrsching, Germany, May 2011.

IV. Farzad Foroughi Abari, Fredrik Rusek, and Ove Edfors, "Channel estimation filter-tap memory optimized pilot pattern design for OFDM systems in multi-mode and multi-standard environments", Tech. Rep., Dept. of Elec. and Info. Technology (EIT), Lund, Sweden, June 2011.

Other publications by the author

I. Farnaz Sharifabad, Farzad Foroughi Abari, and Ove Edfors, "Low-complexity channel estimation for low-mobility LTE using 4×4 MIMO", in *Proc. the 6th IEEE Conf. Ind. Electron. and Applicat.*, Beijing, China, June 2011.

II. Isael Diaz, Balaji Sathyanarayanan, Alirad Malek, Farzad Foroughi, and Joachim Neves Rodrigues, "Highly Scalable Implementation of a Robust MMSE Channel Estimator for OFDM multi-standard Environment", accepted to *IEEE Workshop Signal Process. Syst.*, Beirut, Lebanon, Oct. 2011.

[1] The order of the authors names indicates their relative contributions to the publications.

General Introduction

Farzad Foroughi Abari

1 Introduction

Gradually replacing single-carrier communications systems, orthogonal frequency division multiplexing (OFDM) has been a driving force behind the latest high speed standards in wired as well as wireless communications. The ability to divide a wide spectrum into narrowband subchannels, where data could possibly be multiplexed for different users, has provided a number of different possibilities, including but not limited to, reducing or eliminating the inter symbol interference (ISI), using simple equalizers and employing flexible channel estimators.

Although the narrowband characteristics of tones in a given OFDM system simplifies the equalization at the receiver side, the effects of the wireless channel experienced by the tones still needs to be compensated. As a result, channel state information (CSI) needs to be supplied to or estimated at the receiver. A number of approaches are suggested in literature to aid channel estimation at the receiver in the presence of additive white Gaussian noise (AWGN). These approaches range from simple linear to complex nonlinear alternatives, each having a certain complexity/performance characteristic attached to them. Thus, the estimators can be tailored to the characteristics of each standard. One of the dominating decision criteria is the availability (and the pattern) of pilot data which can be used to aid channel estimation in a given system.

The pilot patterns are usually categorized into continuous and scattered variants. For instance, continuous pilots in the form of preamble have been proposed in IEEE 802.11n [1] for high speed data communications through Wireless Local Area Network (WLAN). For systems experiencing higher amount of fading, such as Long Term Evolution (LTE) [2], scattered pilots are usually employed. The presence of scattered pilots not only aids instantaneous estimation of the channel but also provides the possibility for tracking channel variations in time.

Scattered pilots can be thought of sampling a 2-D grid. For example, if a number of consecutive OFDM symbols, extending over the time axis, are unfolded in the frequency direction a 2-D time-frequency grid is constructed. The building blocks in the constructed grid are tones where one tone is a subchannel in a given OFDM symbol. In addition, if the grid is sampled according to some random or deterministic pattern, a subset of points, called pilot tones, is collected which can be used to assist a number of signal processing operations in a transceiver. For instance, one of the main applications is to aid the estimation of the wireless channel, known as pilot-aided channel estimation by convention.

Thus, pilot-aided channel estimation can be described as a mapping operation between the sampled time-frequency space, i.e., the pilots space, to the full 2-D space where all the required tones are estimated or interpolated. The mapping function may denote a linear or nonlinear operation and depending on its characteristics, the pilot pattern can be optimized for a certain system. For instance, the pilot sampling frequency should comply with the Nyquist criteria if a linear mapping is desired. On the other hand, Nyquist criteria may be violated for some nonlinear operations, e.g., iterative joint channel estimation and data detection [3, 4].

Conventionally, the pilots are designed for a certain system constrained by a

number of requirements. The design parameters can cover a wide range of requirements such as high performance in fast-fading environments, low latency, and high capacity, just to name a few. However, to the best of the author's knowledge, little work has been done with respect to designing pilot patterns which are optimized for co-implementation and integration of several OFDM systems in one single platform. The idea deserves a growing attention especially when the astonishing number of different standards that future mobile terminals need to handle are taken into account. In fact, it is no longer far fetched to imagine a smart phone handling high rate data communications under one standard while simultaneously streaming high resolution multimedia content.

On the other hand, hardware technology does not usually keep pace with the exponential growth in signal processing requirements in mobile terminals. Thus, it is at times inevitable to relax the stringent requirements on the performance of the optimal algorithms to achieve a certain performance/complexity trade-off. For instance, optimal linear estimators designed for channel estimation purposes may find little interest when their application in low-power terminals, with limited hardware resources, is taken into consideration. In this thesis, an effort has been made to address some of the performance/computational complexity trade-offs with respect to low-complexity channel estimators.

The main contribution of this thesis covers the following.

- A number of low-complexity channel estimators for LTE and Digital Video Broadcasting-Handheld (DVB-H) [5] are probed and their performance in terms of mean square error and bit error rate is evaluated. The studied estimators include the MMSE and DFT-based variants where MMSE estimators have been more thoroughly analyzed.

- Depending on the fading characteristic of the wireless channel, a number of strategies, e.g., pilot merging, for alleviating the time-domain filtering are proposed. Furthermore, The effect of pilot merging on the performance of the channel estimator is evaluated. Taking the performance degradation into account, various strategies for pilot merging are proposed.

- It is shown how similarities between channel estimation filter taps can be used to reduce the on-chip memory needed for the storage of the filter coefficients. Moreover, it is shown that by seeking certain pilot merging schemes the on-chip memory for the storage of filter taps can be optimized for LTE and DVB-H across their various modes of operation.

- Last but not least, a new approach to pilot pattern design in OFDM systems is proposed. The suggested strategy maximizes the number of OFDM systems which can be co-integrated in the same platform by employing similar filters for channel estimation purposes.

As a result, the following structure has been adopted in this thesis. In Sec. 2 a brief introduction to wireless OFDM systems is provided and their prominent advantages and possible shortcomings are discussed. In Sec. 3, a mathematical

description of minimum mean square error (MMSE) family of channel estimators is given. Furthermore, it will be shown how a certain family of low-complexity estimators can be derived through relaxing the stringent requirements on the estimators' performance. Moreover, The performance of the estimators at various simplifying stages is probed. Also, simple methods to avoid time-domain filtering for moderately fast fading wireless channels are discussed. The nuts and bolts of filter memory optimization are elaborated in Sec. 3.5.

After the general introduction three papers and a technical report, attached as separate chapters, finalize the discussions in this thesis. Papers I-III elaborate on the principles for channel estimation and filter memory optimization discussed in the general introduction. The final chapter, i.e., the attached technical report, however, wraps up the thesis by providing a novel and methodological approach to pilot pattern design for OFDM systems. The design criteria is to enable the proposed estimators to be shared among a maximum number of modes in the same system. Besides, it provides the feasibility to apply the filters to other compatible OFDM systems co-implemented in multi-standard platforms. Furthermore, the pilot pattern design for OFDM systems in a multi-standard platform, where one OFDM system is already fixed (standardized), will be discussed in 5.2. Remaining a dominant high-rate data communications standard for the foreseeable future, compatible pilot-pattern design for systems co-implemented with LTE is discussed through an example in Sec. 5.2.

2 Wireless OFDM systems

The communications channels in wireless environments are characterized by the reflection of the transmitted radio signal from the objects in the environment. In the event of a line-of-sight (LOS) communications, the secondary reflections from the objects in the environment may have a negligible effect on the performance of the radio communication. However in many scenarios, there is either no LOS component or the reflections from the objects are too strong to be ignored.

There are different approaches to the characterization of the wireless channels. In ray tracing [6], e.g., a deterministic channel model is usually sought. Although ray tracing provides a good insight into certain properties of the wireless environment, it cannot precisely describe and track the time-variations as well as object movements in the environment. Specifically, it is quite complicated to characterize the reflections when the number of existing objects increases. Thus, another approach, based on probability theory, has been adopted to describe the wireless channels and their properties. In the following, a concise and statistical description of narrowband and wideband wireless channels is provided.

2.1 Narrowband wireless channels

In the event of no line of sight (NLOS), the simplest example of a narrowband channel is the existence of one reflecting object in the wireless environment. As a result,

the wireless channel response is composed of a single tap. However, in the majority of practical cases, multiple reflecting objects exist. But, if the reflections from the objects arrive at the receiver in a sufficiently narrow time interval such that the receiver cannot resolve the individual reflections, the sum of the reflections constitute a single tap which categorizes it as a narrowband channel. Thus, a simplified baseband representation of a narrowband channel can be described as

$$h_{\text{cont.}}(\tau, t) = \alpha_0(t)\delta(\tau - \tau_0), \tag{2.1}$$

where $\alpha_0(t) = \mathbb{E}\left[|\alpha_0(t)|^2\right] \exp\left(2\pi f_D t - 2\pi f_c \tau_0\right)$ and τ_0 is the arrival time. Furthermore, f_D and f_c are the Doppler and carrier frequencies, respectively.

2.2 Wideband wireless channels

In the event of multiple resolvable reflections, the single-tap channel model does not hold any more and a more general description needs to be sought. Thus, for a wide sense stationary uncorrelated scattering (WSSUS) wireless channel with M resolvable components, (2.1) becomes [7]

$$h_{\text{cont.}}(\tau, t) = \sum_{l=0}^{M-1} \alpha_l(t)\delta(\tau - \tau_l), \tag{2.2}$$

where the lth component in (2.2) is either a single reflection or the sum of a cluster of non-resolvable reflections, as mentioned in Sec. 2.1. Besides, $\alpha_l(t)$ are independent zero-mean complex Gaussian processes with Rayleigh distributed amplitudes. Furthermore, the power delay profile (PDP) associated with (2.2) is defined as $\theta(\tau) = \sum_{l=0}^{M-1} \mathbb{E}\left[|\alpha_l|^2\right] \delta(\tau - \tau_l)$ where $\mathbb{E}\left[|\alpha_l|^2\right]$ is the variance of tap l.

Due to the fact that the majority of signal processing in today's transceivers is performed in discrete time, a discrete-time format of (2.2) needs to be sought. Thus, if the wireless channel remains time-invariant during the transmission of a single data symbol m, (2.2) can be written as

$$h_{\text{cont.}}(\tau, m) = \sum_{l=0}^{M-1} \alpha_l(m)\delta(\tau - \tau_{l\text{n}} T_{\text{s}}), \tag{2.3}$$

where T_{s} is the sampling interval at the transceiver and $\tau_{l\text{n}}$ is the normalized arrival time, i.e., $\tau_{l\text{n}} = \tau_l / T_{\text{s}}$. Moreover, if the available symbol bandwidth (BW) is divided into N equal frequency intervals of Δf, the discrete-time frequency response of (2.3) at discrete time m becomes

$$h[k, m] = \sum_{l=0}^{M-1} \alpha_l(m) \exp(-2\pi j (k/N) \tau_{l\text{n}}). \tag{2.4}$$

where $h[k, m]$ is the channel attenuation on discrete tone k at time m.

2.3 Second-order wireless channel statistics

For the presumed WSSUS channel in (2.4), the cross correlation between subcarriers k and k' corresponding to channels associated with data symbols m and m' respectively is

$$r_{\mathrm{h}}\left[k-k', m-m'\right] = \mathbb{E}\left\{h[k,m]h^*[k',m']\right\}, \tag{2.5}$$

where $(\cdot)^*$ denotes the complex conjugate operation.

After some mathematical manipulation it can be deduced that

$$r_{\mathrm{h}}[k-k', m-m'] = r_{\mathrm{h,f}}[k-k']r_{\mathrm{h,t}}[m-m'] \tag{2.6}$$

where $r_{\mathrm{h,f}}$ is the correlation among subcarriers at a fixed time instance in frequency direction and $r_{\mathrm{h,t}}$ is the correlation between two instances of the same subcarrier at times m and m'. It can be observed from (2.6) that the channel correlation is the product of correlation in time and frequency. This is known as separable correlation in literature.

The channel correlation in frequency, $r_{\mathrm{h,f}}\left[k-k'\right]$, is a function of the PDP. For example, it can be shown [8] that for a uniformly distributed PDP, $\theta(\tau)$, where all taps constitute equal energy $r_{\mathrm{h,f}}$ reduces to

$$r_{\mathrm{h,f}}\left[\Delta k\right] = \frac{1-\exp(-2j\pi L\Delta k/N)}{2j\pi L\Delta k/N}, \tag{2.7}$$

where $\Delta k = k-k'$ is the distance between two subcarriers, e.g., a pilot and estimated tone, and L is the PDP spread in discrete time samples.

The channel correlation in time, $r_{\mathrm{h,t}}\left[m-m'\right]$, may be characterized in various forms depending on the properties of the fading environment. For instance, if the zeroth-order Bessel function of the 1st kind is denoted as $J_0(\cdot)$, then

$$r_{\mathrm{h,t}}[m-m'] = J_0(2\pi f_{\mathrm{d}}(m-m')) \tag{2.8}$$

for a 2-D scattering environment meeting certain conditions [9]. In addition, if $\mathrm{sinc}(x) = \frac{\sin(x)}{x}$ it has been shown that

$$r_{\mathrm{h,t}}[m-m'] = \mathrm{sinc}(2\pi f_{\mathrm{d}}(m-m')) \tag{2.9}$$

for a 3-D scattering environment constraint to certain conditions [10]. Furthermore, f_{d} in (2.8) and (2.9) denotes the normalized Doppler spread, i.e., $f_{\mathrm{d}} = D_{\mathrm{p}}T_{\mathrm{u}}/2$, where T_{u} is the data symbol duration and D_{p} is the Doppler spread. Besides, it is worthwhile to remind the reader that the channel variations in time are presumed to be negligible for T_{u}.

It can be observed from (2.9) that f_{d} has a significant effect on the correlation in time. In fact, the lower the f_{d}, the higher the correlation in time. For instance, Fig. 1 illustrates the time correlation, for a 3-D scattering environment, versus time for a number of different terminal velocities where the carrier frequency, $f_{\mathrm{c}} = 2.6$ GHz. It can be seen that the wireless channel exhibits a quite strong time correlation even for high terminal speeds. As will be elaborated in subsequent sections, LTE's

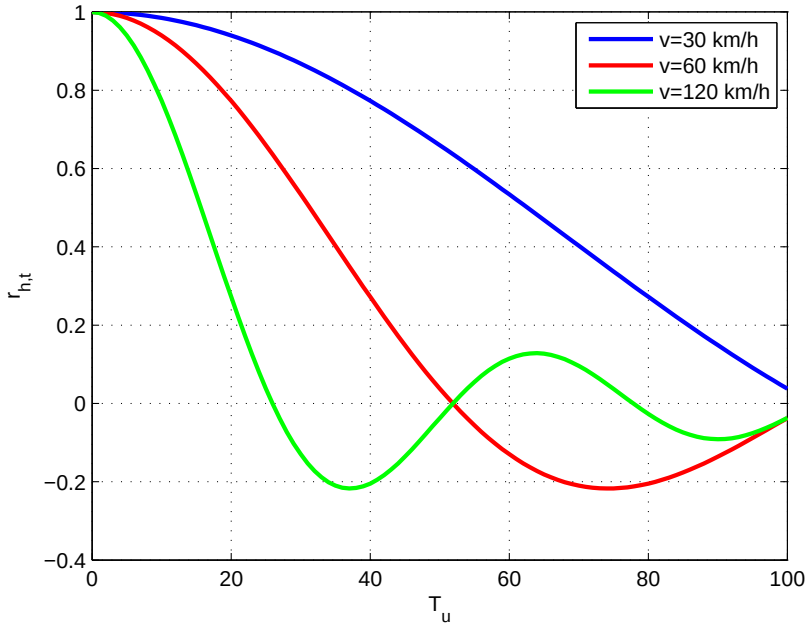

Figure 1: Time correlation versus time. The time axis is scaled by the LTE's symbol time duration, i.e., $T_{\mathrm{u}} = 66.7\,\mu$s, for illustration purposes. It can be observed that for terminal velocities as high as 120 km/h, there is still a strong time correlation among a few consecutive OFDM symbols.

symbol duration is $T_{\mathrm{u}} = 66.7\,\mu$s. Thus, the time correlation remains almost strong during the transmission of a few OFDM symbols even when the terminal speed approaches as high a velocity as 120 km/h. As will be discussed in the following sections, this important property has been exploited to contemplate low-complexity channel estimators where time-domain filtering may be avoided.

Meanwhile, Fig. 2 illustrates the absolute value of correlation in frequency associated with (2.7) for a number of different $\frac{L}{N}$, where N is the number of DFT points. An interesting observation can be made from this figure. The subcarriers decorrelate quite fast for the exemplary values, which are typical of the ones expected in LTE and DVB-H, as elaborated in Secs. 4.1 and 4.2. The above mentioned fact will be used in the subsequent sections to facilitate the derivation of low-complexity channel estimators.

2.4 Multi-carrier communications

Single-carrier communications were once dominating the high-speed wireless communications arena. In a single-carrier system binary data, after going through various source and channel coding stages, is modulated and and transmitted over the air. To maximize the throughput the symbols are inserted sequentially in a compact pulse train before transmission. In the meantime, the symbol duration in a conventional single-carrier system is reduced to provide the opportunity for high rate

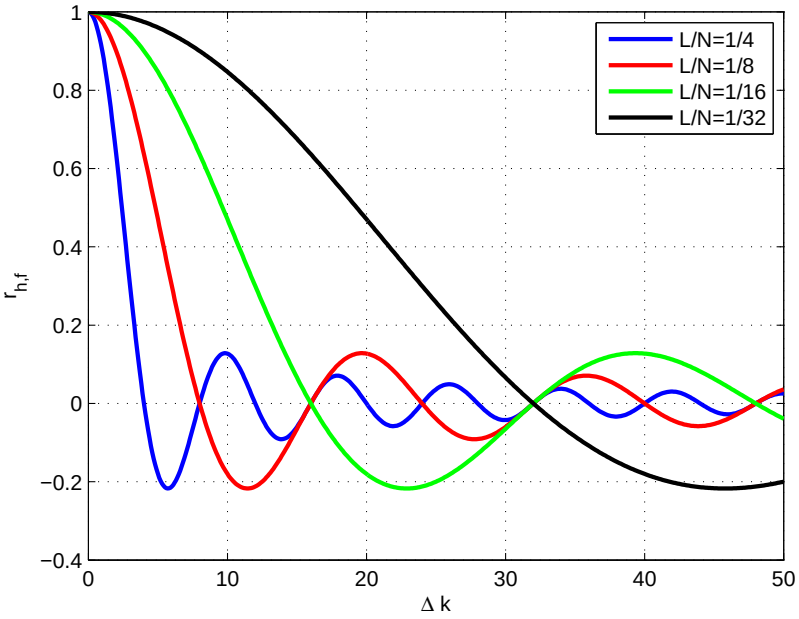

Figure 2: Frequency correlation versus tone separation, Δk. It can be observed that there is a substantial correlation loss among subcarriers which are located far apart, especially for larger values of $\frac{L}{N}$.

signaling. Had the transmission been materialized in a flat-fading wireless channel, this method would have provided an efficient alternative for fast data transmission. However, the majority of wireless channels in practice are frequency selective and exhibit a substantial amount of fading. As a result, the symbols experience severe inter symbol interference (ISI) before arriving at the receiving end, requiring sophisticated equalization techniques to retrieve the data. The effect of ISI would become more detrimental in the event of a higher frequency selectivity and a shorter symbol interval.

To combat the frequency selectivity in wide-band channels, multi-carrier modulation was proposed an an alternative [11]. The idea behind multi-carrier modulation is to restrict the occupied BW of each symbol to a sufficiently narrowband, called subchannel, subband, or tone so that each symbol experiences little or no fading upon transmission through a frequency selective channel. In other words, the symbol time is increased so much as the wireless channel's delay spread becomes negligible in comparison. The original idea behind multi-carrier modulation, as described above, suffered from the fact that one cannot arbitrarily narrow down the symbol BW without increasing its length in time. Considering the fact that the symbol duration in time has to be limited, a penalty factor in terms of increased BW needs to be paid. Besides, such a scheme suffers from expensive narrowband filters while requiring a large number of modulators/demodulators at the transceiver.

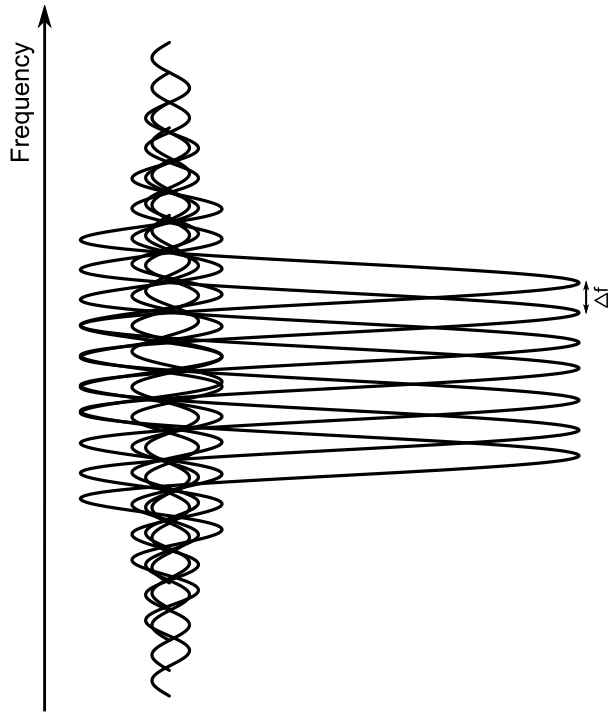

Figure 3: The concept of orthogonal signaling in frequency. The peculiar spacing of signals insures no ICI.

2.5 OFDM

Following the multi-carrier concept, during the 60s [12, 13], it was realized that the pulses (data symbols) may overlap each other in frequency without interference. The overlap operation needs to be done in such a way that the pulses remain orthogonal to one another. As a result, the penalty in BW for a sufficiently large number of subchannels becomes insignificant [11]. Inserting a number of data symbols on a number of overlapping orthogonal pulses is known as orthogonal frequency data multiplexing, i.e., OFDM, and is the principle behind high rate multi-carrier communications. Fig. 3 illustrates how a number of well-known sinc pulses can overlap each other while remaining orthogonal. Moreover, N such symbols can be collected into a single OFDM symbol and modulated to the desired carrier frequency for transmission. In other words, OFDM converts a frequency selective channel into a non-frequency selective one [14]. Considering the fact that the encapsulated OFDM symbols can be much longer in time when compared to their single-carrier counter parts, they experience less severe ISI when transmitted over a frequency selective wireless channel. Moreover, to eliminate the effect of ISI, a cyclic prefix (CP), also known as guard interval (GI), whose length is equal to the maximum expected delay spread of the channel is appended to each symbol before carrier modulation and final transmission [15].

The CP can appear in one of the following two forms. Either the last M samples, where M equals the delay spread of the wireless channel, in each OFDM symbol

are copied and appended to the beginning of the symbol or M zeros are appended instead. The former converts the linear convolution into a circular convolution without additional operation at the receiver. In the latter, however, the receiver needs to collect the last M samples of the received symbol and copy it into the beginning of the corresponding symbol, converting a linear convolution to a circular convolution [16]. Both approaches allow the partitioning of the frequency selective channel into a number of parallel flat-fading subchannels without requiring the CSI at the transmission side. In retrospect, there are other approaches such as vector coding (VC), also known as precoding, where the CSI is needed at the transmitter to allow a similar operation [16].

Although more robust against ISI, OFDM systems may suffer from a number of drawbacks. For instance, the presence of inter carrier interference (ICI) results in a loss of orthogonality among subcarriers in OFDM systems. In other words, the orthogonality among the signals may be jeopardized due a multitude of reasons including but not limited to fast fading environments, carrier frequency offset, and timing jitter. If hardware imperfections at the transmitter or receiver, e.g., I/Q imbalance [17], are neglected, fast fading is the main reason behind loss of orthogonality resulting in performance degradation of the system. A simple way to combat ICI is to adjust the OFDM symbol duration so that each symbol experiences little or no fading during its transmission. Thus, fading places a limit on the duration of OFDM symbols and its resilience to ISI. High peak-to-average power ratio (PAPR) is another prohibiting factor in practical OFDM system implementations. High PAPR can place stringent requirements on the linearity of power amplifiers both at the receiving and transmitting sides requiring costly design and components.

Practical implementations of OFDM systems were not realized during the early days of telecommunications due to hardware shortcomings. As digital hardware design became more mature and digital signal processors (DSP) became more powerful and efficient, OFDM systems became more popular. Probably, the most critical burden associated with the practical implementation of OFDM systems has been the insertion of overlapping pulses in specific intervals such that the orthogonality of the whole pulse train is secured. Implementing such system in analogue domain is cumbersome due to deviations of analogue electronics from precise mathematical descriptions. However, if available, OFDM modulation/demodulation may be carried out in digital domain through a conventional inverse fast Fourier transform (IFFT)/fast Fourier transform (FFT) operations.

The baseband equivalent of OFDM modulation can be stated as

$$s(t) = \sum_{k=0}^{N-1} x[k] \exp(j2\pi k \Delta f t), \tag{2.10}$$

where Δf is the inter-carrier distance between the modulation frequencies, k refers to the kth subchannel and $x(k)$ corresponds to the data selected from a constellation map, e.g., 16QAM. In the event of proper sampling, i.e., $f_\mathrm{s} = N\Delta f$, (2.10) becomes

an inverse discrete Fourier transform (IDFT) and may be written as

$$s[n] = \sum_{k=0}^{N-1} x[k] \exp(j2\pi kn/N), \tag{2.11}$$

where N is the number of samples in an OFDM symbol. DFT/IDFT can be efficiently carried out by FFT and IFFT algorithms. Furthermore, exponential growth in integrating more area-efficient transistors on the same chip provided the opportunity to integrate dedicated fast and power-efficient FFT/IFFT accelerators on a transceiver. Thus, commercial interest in OFDM was ignited as digital hardware technology became more mature and made its practical implementation feasible.

As a result of orthogonal modulation, each transmitted data symbol experiences flat fading due to its narrow-band characteristics. However, due to frequency-flat fading, subcarriers experiencing low signal to noise ratios (SNR), result in considerable bit error rate (BER) degradation. This phenomenon is similar to single-carrier systems in flat-fading environments. Thus, various coding and interleaving schemes, over time and frequency, can be practiced to mitigate or reduce the detrimental effects. Examples of such coding and interleaving schemes in practical applications can be found in [2, 5]. A detailed description of such operations, however, is beyond the scope of this thesis.

2.6 System model

The adopted system model in this thesis is a single-input single-output (SISO) OFDM system operating in a fading and frequency-selective wireless environment. The choice of SISO system is due to its simplicity for illustration of the introduced concepts . However, the acquired results may be easily extended to multiple-input multiple-output (MIMO) OFDM systems. The proposed OFDM system is characterized by the following parameters,

- $T_{\mathrm{u}}, [\mu s]$ = useful OFDM symbol duration,
- $T_{\mathrm{CP}}, [\mu s]$ = CP duration,
- Doppler spread (D_{p}) and delay spread (D_{s}),
- N = number of DFT points, where $N = 2^q$ and q is a positive integer.

Furthermore, other parameters of interest associated with the system can be easily deduced from the above system specifications. For instance, one may figure out that $\Delta f = 1/T_{\mathrm{u}}$, $BW = f_{\mathrm{s}} = N/T_{\mathrm{u}}$, where Δf is the subcarrier spacing, f_{s} is the transceivers sampling frequency, and BW is the occupied bandwidth.

Fig. 4 illustrates a possible configuration for the proposed system model. The adopted wireless channel is a wide-band channel similar to (2.2). Following the signal flow depicted in Fig. 4, data corresponding to one OFDM symbol are inserted on the designated tones at the transmitter and fed into an N-point IFFT whose output is given by (2.11). Then, the CP is inserted at the output of the IFFT block and after going through digital-to-analogue (D/A) conversion and modulation to the proper

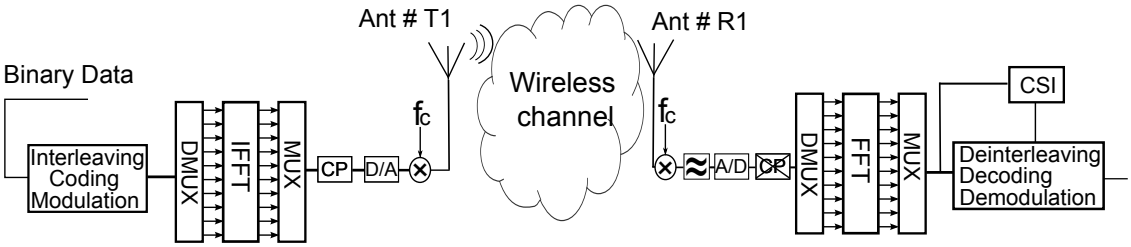

Figure 4: The adopted SISO OFDM system model.

carrier frequency the outcome is transmitted over the wireless channel modeled by (2.2).

Upon reception at the receiver, the signal is picked up by the receiving antenna and after carrier demodulation, low-pass filtering, analogue-to-digital (A/D) conversion, and CP removal, the result is fed into an N-point FFT. If the signal samples before FFT block are collected into the column vector $\mathbf{r}$ of size N, then

$$\mathbf{r} = \mathbf{H}\mathbf{s} + \boldsymbol{\eta}, \tag{2.12}$$

where $\mathbf{H}$ is a $N \times N$ circulant matrix associated with (2.4) for the mth OFDM symbol, $\mathbf{s}$ corresponds to the $N \times 1$ vector of data in (2.11) and $\boldsymbol{\eta}$ is the $N \times 1$ vector of AWGN. The circulant matrix $\mathbf{H}$ is the direct result of employing CP in OFDM systems. Furthermore, if the unitary Fourier matrix of size N is denoted by $\mathbf{T}_{\mathrm{n}}$, the output of FFT equals

$$\mathbf{y} = \mathbf{T}_{\mathrm{n}}\mathbf{r} = \mathbf{T}_{\mathrm{n}}\mathbf{H}\mathbf{s} + \mathbf{T}_{\mathrm{n}}\boldsymbol{\eta}. \tag{2.13}$$

However, it can be shown that following (2.11), $\mathbf{s} = \mathbf{T}_{\mathrm{n}}^{H}\mathbf{x}$, where $\mathbf{x}$ is the column vector of transmit data having size N. Considering the fact that the unitary Fourier matrix $\mathbf{T}_{\mathrm{n}}$ and its Hermitian, i.e., $\mathbf{T}_{\mathrm{n}}^{H}$, diagonalize any circulant matrix [18], (2.13) can be written as

$$\mathbf{y} = \boldsymbol{\Lambda}\mathbf{x} + \boldsymbol{\eta}, \tag{2.14}$$

where $\boldsymbol{\Lambda} = \mathbf{T}_{\mathrm{n}}\mathbf{H}\mathbf{T}_{\mathrm{n}}^{H}$ is a diagonal matrix containing the channel attenuations corresponding to (2.4) for a fixed OFDM symbol, i.e., discrete time instance m. Moreover, (2.14) can be rewritten as

$$\mathbf{y} = \mathbf{X}\mathbf{h} + \boldsymbol{\eta}, \tag{2.15}$$

where $\mathbf{X}$ is a diagonal matrix of size $N \times N$ encompassing the transmitted data $x(k)$, and $\mathbf{h}$ is a column vector of size N containing the channel attenuations in frequency.

3 Channel estimation

Channel estimation is an essential part of coherent data detection in OFDM systems [19]. A lot of work has been carried out for channel estimation in wireless communications. With the advent of OFDM and its practical realization through FFT/IFFT hardware accelerators, channel estimation research picked up for such

systems and ever since various methods have been suggested in literature [7, 8, 20–22]. The proposed methods range from simple linear estimators to complicated iterative estimation in the presence of channel coding [4, 23]. In general, one may categorize the channel estimation algorithms as linear and nonlinear estimators.

Quite contrary to a linear approach where the CSI can be obtained through, e.g., a matrix multiplication, nonlinear methods are characterized by multi-stage processing blocks where at least one of the stages encompasses certain nonlinear operations. For instance, joint estimation and detection approaches comprise iterative information passage between the decoder as well as the channel estimation blocks. These approaches usually have a higher performance when compared to the conventional linear methods at the expense of higher computational complexity. Meanwhile, in the event of pilot-aided channel estimation, these approaches may need less pilot overhead, even below the threshold set by the Nyquist sampling criteria [4]. An elaborate analysis of nonlinear channel estimation approaches needs a book of its own and is well beyond the scope of this thesis.

Due to their inherent simplicity and low complexity, linear estimators have been of high interest in practical system implementations. Besides, their existence is often independent of other transceiver subsystems, e.g., decoders when compared to some nonlinear methods. A linear estimation operation can be described as a simple matrix multiplication such as

$$\hat{\mathbf{h}} = \mathbf{W}\hat{\mathbf{y}}, \tag{3.1}$$

where $\hat{\mathbf{y}}$ is a column vector whose elements are the measured signal values and $\mathbf{W}$ is the estimation filter matrix.

3.1 Pilot-aided channel estimation

To be able to capture the CSI in a communications system, one often needs to rely on the (noisy) observations of the received signal values. Moreover, the estimator, e.g., at the receiver, usually needs to know the transmitted signal values to estimate the channel. Yet, there are classes of estimators, known as blind estimators, which rely only on the received signal and its pseudo-stationary properties to do the estimation [24–27]. Their application, however, is prohibitive in low-power terminals with limited processing resources due to their high computational complexity.

In the majority of practical cases the transmitter and receiver should have a priori knowledge of the transmitted data for the purposes of channel estimation. Thus, the transmitter and receiver agree on a subset of data which is called pilot-data by convention and is extensively used in practical system implementations. The pilots are inserted in specific locations in the transmitted signal. They appear either in continuous or scattered patterns. The contiguous scheme is usually employed in wireless systems where little fading is expected. For instance, IEEE 802.11n [1] uses continuous transmission of pilots for the purposes of channel estimation in its preamble. Contrary, if the wireless channel experiences a considerable amount of fading, e.g., movements in the environment, scattered pilots distributed both in time and frequency need to be used so that the channel variations over time and frequency can be tracked.

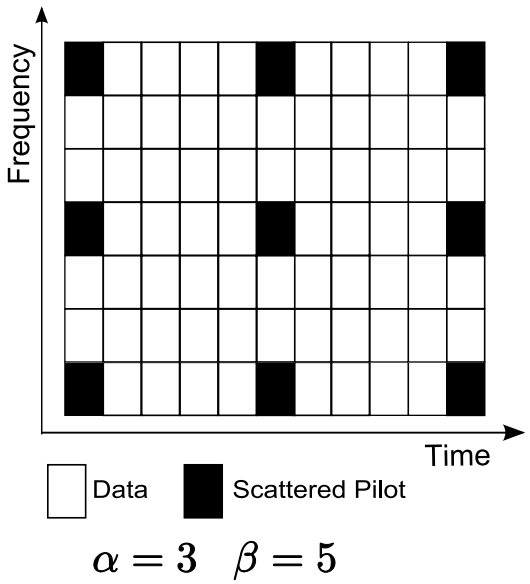

Figure 5: An example of rectangular pilot pattern scattered in time and frequency. α and β are pilot separations in frequency and time, respectively.

An example of scattered pilot pattern in OFDM systems is depicted in Fig. 5. This is known as rectangular pilot pattern where pilots appear in specific intervals, both in time and frequency. Furthermore, the pilots associated with different OFDM symbols appear exactly on the same tones. On the other hand, the scattered pilots do not necessarily need to appear on the same tones in each pilot carrying OFDM symbol. In other words, the pilots of a specific pilot-carrying OFDM symbol may experience a distinct frequency shift. This is known as skewed pilot pattern. If the pilot carrying OFDM symbols are arranged such that the pilot frequency shift increases monotonically with respect to the symbol time index, a distinct skewed pilot pattern, demonstrated in Fig. 6, can be achieved. This is known as a primary skewed pilot pattern in this thesis.

The scattered pilots can be viewed as a 2-D sampling of a time-frequency grid. Thus, Nyquist's sampling criteria, in time and frequency, needs to be met if a proper reconstruction of the original channel is desired. Thus, the sampling can not fall below a certain threshold set by the Nyquist's sampling criteria as well as certain system dynamics such as the presence of AWGN. On the other hand, the pilots introduce spectral inefficiency in communications systems since a portion of the BW needs to be allocated to pilots rather than data transmission. Besides, although increasing the number of pilots results in better estimation performance, the overall SNR scales down proportionally since more energy is allocated to the pilots rather than useful data transmission.

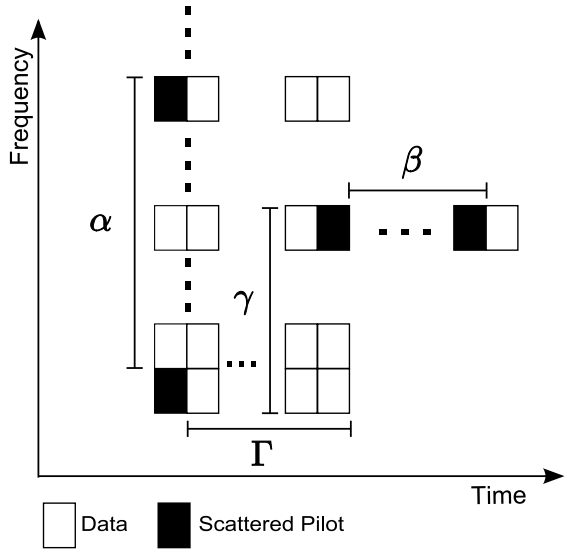

Figure 6: A primary skewed pilot pattern. The pilot frequency offset increases monotonically with respect to the symbol index time. α and β are the distances between pilots in frequency and time respectively. γ is the pilot frequency offset and Γ is the distance between two consecutive pilot-carrying OFDM symbols. The above mentioned parameters are related through $\beta = \Gamma(\frac{\alpha}{\gamma})$.

3.2 Minimum mean square error (MMSE) channel estimation

Being a linear algorithm, a full linear MMSE (LMMSE) estimator provides the ultimate performance in terms of MSE among its linear counterparts. The LMMSE estimators make use of several parameters such as SNR as well as 2nd-order statistics of the channel. In the following, the mathematical derivations for LMMSE channel estimation in the event of rectangular pilot pattern is derived. The results can be easily extended to skewed pilot scheme with minor mathematical manipulations.

Suppose in the system exemplified by Fig. 4, L consecutive OFDM symbols are collected for channel estimation purposes. As a result, compared to (2.15), $\mathbf{h}$ corresponds to a vector of size $LN \times 1$ encompassing the channel tones associated with L consecutive OFDM symbols stacked on top of each other. Besides, the pilot spacing in terms of the number of subcarriers in time and frequency are α and β respectively, see Fig. 5. If the variables associated with pilots are identified by $(\cdot)_{\mathrm{p}}$, the linear channel estimation for the above mentioned grid can be written as

$$\hat{\mathbf{h}} = \mathbf{W}\hat{\mathbf{y}}_{\mathrm{p}}, \tag{3.2}$$

where $\hat{\mathbf{y}}_{\mathrm{p}}$ is a $N_{\mathrm{p}} \times 1$ column vector containing the observations of transmitted pilots at the receiver. In other words, for an observation interval of $N \times L$ tones,

$\mathbf{y}_\mathrm{p}$ is the column vector of collected pilots from the pilot carrying OFDM symbols stacked on top of each other. In minimum mean square error (MMSE) estimators, the $LN \times N_\mathrm{p}$ matrix $\mathbf{W}$ is designed to minimize the MSE between the actual and estimated channel. In other words, the intention is to find

$$\min\left(\mathbb{E}\left[\left|\mathbf{h}-\hat{\mathbf{h}}\right|^2\right]\right). \tag{3.3}$$

It can be shown that the solution to the above optimization problem is

$$\mathbf{W} = \mathbf{R}_{\mathrm{hy_p}}\mathbf{R}_{\mathrm{y_p}}^{-1}, \tag{3.4}$$

where $\mathbf{R}_{\mathrm{hy_p}} = \mathbb{E}\left[\mathbf{h}\mathbf{y}_\mathrm{p}^H\right]$ is the $LN \times N_p$ matrix of cross correlation values between the channel and the received pilots, $\mathbf{R}_{\mathrm{y_p}} = \mathbb{E}\left[\mathbf{y}_\mathrm{p}\mathbf{y}_\mathrm{p}^H\right]$ is the $N_\mathrm{p} \times N_\mathrm{p}$ matrix of autocorrelation associated with the received data on the pilot positions. Throughout this thesis $(\cdot)^H$ denotes Hermitian transpose operation.

After some mathematical manipulations and simplifications of (3.4), (3.2) becomes

$$\hat{\mathbf{h}}_\mathrm{mmse} = \mathbf{R}_{\mathrm{hh_p}}\left(\mathbf{R}_{\mathrm{h_p}} + {\sigma_\eta}^2\left(\mathbf{X}_\mathrm{p}^H\mathbf{X}_\mathrm{p}\right)^{-1}\right)^{-1}\hat{\mathbf{h}}_\mathrm{p,ls}, \tag{3.5}$$

where $\hat{\mathbf{h}}_\mathrm{mmse}$ is a column vector of estimated tones, ${\sigma_\eta}^2$ is the AWGN power and $\mathbf{X}_\mathrm{p}$ is a diagonal matrix containing the transmitted pilots stacked on its main diagonal. Furthermore, $\hat{\mathbf{h}}_\mathrm{p,ls} = \mathbf{X}_\mathrm{p}^{-1}\mathbf{y}_\mathrm{p}$ is the least squares (LS) estimation of the pilots at the receiver. Moreover, if the pilots are selected in a way that they all constitute constant envelope, then $\mathbf{X}_\mathrm{p}^H\mathbf{X}_\mathrm{p}$ may be replaced by an identity matrix scaled by the energy of the pilots which can be further incorporated into the SNR. As a result, (3.5) can be written as

$$\hat{\mathbf{h}}_\mathrm{mmse} = \mathbf{R}_{\mathrm{hh_p}}\left(\mathbf{R}_{\mathrm{h_p}} + \frac{\mathbf{I}}{\mathrm{SNR}}\right)^{-1}\hat{\mathbf{h}}_\mathrm{p,ls}, \tag{3.6}$$

where SNR is the signal-to-noise ratio, $\mathbf{R}_{\mathrm{hh_p}}$ is the cross-correlation matrix between the pilot and data tones, and $\mathbf{R}_{\mathrm{h_ph_p}}$ is the autocorrelation matrix of the pilot tones.

For the above mentioned 2-D filtering operation, the MSE performance associated with tone k in OFDM symbol l is

$$J(l,k) = \sigma_\mathrm{h}^2 - \mathbf{r}_{\mathrm{hy_p}}\mathbf{R}_{\mathrm{y_p}}^{-1}\mathbf{r}_{\mathrm{hy_p}}^H, \tag{3.7}$$

where $\mathbf{r}_{\mathrm{hy_p}}$ is the $N(l-1)+k$ row in $\mathbf{R}_{\mathrm{hy_p}}$.

To tackle the computational complexity of the ideal 2-D filter, the filter can be designed for a presumed 2nd-order channel statistics as well as SNR. For instance, (3.4) can be designed for the worst-case PDP and Doppler spectrum. Thus, if filter $\mathbf{W}$ is designed for a presumed 2nd-order statistics other than the actual values, the MSE associated with the design mismatch equals

$$J(l,k) = \sigma_\mathrm{h}^2 - \mathbf{r}_{\mathrm{hy_p}}\mathbf{w}^H - \mathbf{w}\mathbf{r}_{\mathrm{hy_p}}^H + \mathbf{w}\mathbf{R}_{\mathrm{y_p}}\mathbf{w}^H, \tag{3.8}$$

where $\mathbf{w}$ is the $N(l-1)+k$ row in $\mathbf{W}$.

On the other hand, it has been shown that 2-D Wiener filters may be broken into two 1-D Wiener filters [28, 29]. Although suboptimal, the performance of the filters can be close to the performance of the 2-D filter while the computational complexity is considerably reduced. For the purposes of channel estimation, the ideal 2-D filter may be broken into $\mathbf{W}_\mathrm{t}$ and $\mathbf{W}_\mathrm{f}$, i.e., filtering in time and frequency respectively.[1] If filtering is first done in time domain, then

$$\hat{\mathbf{h}}_1 = \mathbf{W}_\mathrm{t}\mathbf{y}_{\mathrm{t,p}}, \tag{3.9}$$

where $\hat{\mathbf{h}}_1$ is the column vector of estimated tones on the pilot positions, $\mathbf{y}_{\mathrm{t,p}}$ is the vector of observed pilot tones in time direction, and $\mathbf{W}_\mathrm{t} = \mathbf{R}_{\mathrm{hy_{t,p}}}\mathbf{R}^{-1}_{\mathrm{y_{t,p}}}$.

Meanwhile, the estimated tone $\hat{h}_1(l,k)$ can be written as

$$\hat{h}_1(l,k) = h_1(l,k) + \eta'(l,k), \tag{3.10}$$

where $\eta'(l,k)$ is a zero mean noise process with variance $\mathbb{E}\left[|\eta'(l,k)|^2\right] = J_1(l,k)$. Moreover, $J_1(l,k)$ is the MSE due to the first filtering operation, i.e., filtering in time and can be expressed as

$$J_1(l,k) = \sigma^2_\mathrm{h} - \mathbf{r}_{\mathrm{h_t y_{t,p}}}\mathbf{w}^H_\mathrm{t} - \mathbf{w}_\mathrm{t}\mathbf{r}^H_{\mathrm{h_t y_{t,p}}} + \mathbf{w}_\mathrm{t}\mathbf{R}_{\mathrm{y_{t,p}}}\mathbf{w}^H_\mathrm{t}, \tag{3.11}$$

where the effects of model mismatch are included. Besides, $\mathbf{w}_\mathrm{t}$ is the kth row in matrix $\mathbf{W}_\mathrm{t}$. Following the time-domain filter, the 2nd filtering operation, i.e., filtering in frequency is performed. As a result, the estimated tones in frequency for one OFDM symbol may be written as

$$\hat{\mathbf{h}}_2 = \mathbf{W}_\mathrm{f}\hat{\mathbf{h}}_1, \tag{3.12}$$

where

$$\mathbf{W}_\mathrm{f} = \mathbf{R}_{\mathrm{h_f h_{f,p}}}\left(\mathbf{R}_{\mathrm{h_{f,p}}} + \mathbf{J}_1\mathbf{I}\right)^{-1}, \tag{3.13}$$

and $\mathbf{J}_1$ is a diagonal matrix of MSE values from the time-domain filtering.

3.3 Low-complexity MMSE channel estimation

If the 1-D estimators in (3.9) and (3.12) are designed for actual channel statistics, a formidable computational complexity still hits the system. On one hand, the channel statistics should be tracked and evaluated at each moment. On the other hand, even if the statistics do not change fast and stay rather constant over a number of OFDM symbols, the real-time matrix inversion consumes a lot of hardware resources. Thus, it is but inevitable to design and pre-compute the 1-D filters for a fixed set of variables in the wireless channel scenario to reduce the computational complexity. For instance, the covariance matrices in $\mathbf{W}_\mathrm{f}$ can be designed for a rectangular PDP whose length is equal to the maximum expected delay spread of the

[1] Due to the linearity of the filters, the ordering can be done arbitrarily. This holds for a rectangular pilot pattern and may not be true for a skewed pilot pattern. Besides, one should be careful about changing the order of the filters when the calculations are carried out in block matrices. Matrices do not generally commute.

wireless channel. Similarly, the covariance matrices in $\mathbf{W}_{\mathrm{t}}$ may be designed for a 3-D scattering environment [10], i.e., a rectangular Doppler spectrum whose length is equal to the maximum expected Doppler spread, D_{p}, in the channel. Throughout this thesis, such estimators are called robust MMSE (RMMSE) estimators.

To further reduce the computational complexity as well as on-chip memory requirements, one may alleviate the 1-D filtering in time domain. For instance, in piece-wise constant approach, the channel estimation is performed for each pilot-carrying OFDM symbol in frequency and the same estimation is used for equalization purposes of the subsequent OFDM symbols until the next pilot carrying OFDM symbol is received. In the event of skewed pilot pattern, another low-complexity estimation strategy, called merged-pilot channel estimation, can be used. This strategy usually outperforms the piece-wise alternative both in slow as well as moderately fast fading environments and is elaborated in the following sections.

3.4 Merged-pilot channel estimation strategy

Imagine a primary skewed scattered pilot pattern illustrated in Fig. 6, where α is the pilot tone separation in frequency, β is the pilot tone separation in time, γ is the pilot frequency shift and Γ is the distance between two consecutive pilot-carrying OFDM symbols. Besides, the pilots have been designed such that the Nyquist sampling criteria, both in time and frequency, are met with an acceptable margin.[2] For such systems the pilots from a number of pilot carrying OFDM symbols can be collected and merged into a pilot vector (PV) which is later fed into the frequency domain channel estimator. The pilot spacing in PV depends on the merging pattern. The estimated channel is further used for the equalization of the region encompassed by the pilot contributing OFDM symbols. Fig. 7 illustrates an instance of a primary skewed pilot pattern where pilot merging has been practiced.

The constructed PV in Fig. 7 (on the left) is one of the many ways pilot merging can be practiced. For instance, if the pilots from alternate OFDM symbols are collected into a PV (as seen on the right hand side in Fig. 7), the virtual pilot spacing associated with the PV becomes 4 rather than 2. Furthermore, if the pilots from OFDM symbols 1 and 4 are merged into a PV, an uneven virtual spacing is attained. In this thesis, due to the discrimination of certain tones against others, the merging schemes resulting in uneven spacing are not taken into consideration. Thus, by convention, pilot merging is referred to the family of merging schemes where the attained virtual pilot spacing remains constant throughout the constructed PV.

The pilot merging practice has a certain number of pros and cons attached to it. However, depending on the merging pattern, it outperforms piece-wise constant alternatives for the majority of merging scenarios. The merits are especially more emphasized for slow as well as moderately fast fading environments. One could attribute the performance gain to the higher number of available pilots for channel estimation. In other words, the effective number of available pilots for channel estimation in frequency direction is, at least, doubled in the event of merging. Thus,

[2] Due to a limited signal observation interval, twice as fast as Nyquist criteria has been adopted as a rule of thumb for proper sampling [29, 30].

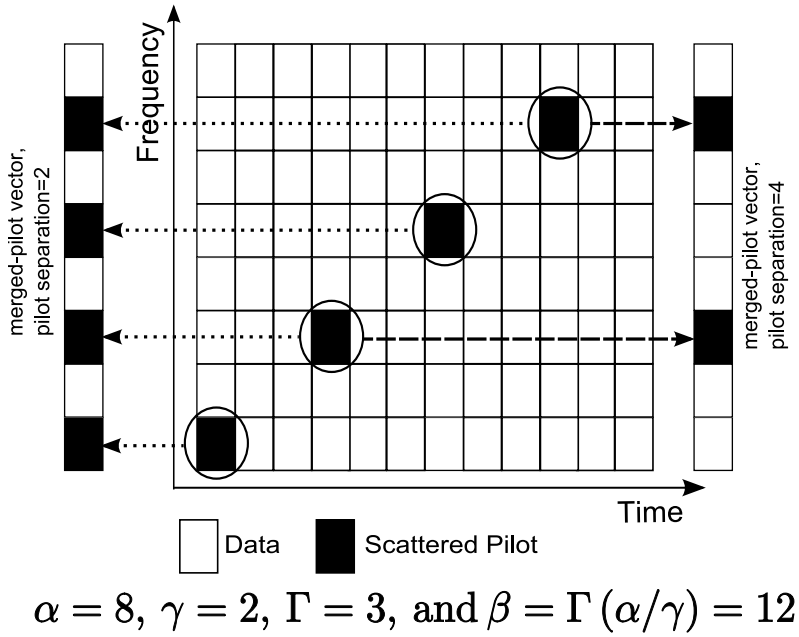

Figure 7: An example of pilot-merging practiced for a primary skewed pilot pattern.

a two-fold estimation performance increase in frequency direction is expected once merging is done provided that the channel remains stationary. Meanwhile, the estimation indirectly captures the time-variations of the wireless channel in fading environments. In other words, merging can be imagined as a robust 2-D filtering where the correlation coefficients in time domain associated with the pilots collected from the pilot-carrying OFDM symbols all equal 1. Thus, it is expected that it exhibits an acceptable performance up to a certain amount of fading, characterized by a certain Doppler spectrum where the channel estimation error due to mismatch surpasses a tolerable error threshold.

There are many ways to characterize the performance of the estimators. A simple and convenient way is to quantify that through MSE. Thus, The performance of pilot merging in various fading environments can be measured by MSE. Suppose $\mathbf{W}$ denotes the robust 2-D filter designed for a certain fixed PDP and a stationary channel in time, i.e., the channel is presumed to be time-invariant. In other words, the effect of pilot merging can be modeled by setting $r_{\mathrm{h,t}}\,[m - m']$ in (2.6) equal to 1. As a result, (2.6) can be written as

$$r_{\mathrm{h}}[k - k', m - m'] = \sum_{l=0}^{M-1} \theta(\tau_{l\mathrm{n}}) \exp(-2\pi j (k - k')\tau_{l\mathrm{n}}/N). \tag{3.14}$$

Furthermore, the MSE of the estimation operation can be measured by (3.11). Thus, depending on the tolerable MSE, one may use the merging scheme in slowly as well as moderately fast fading environments. In the event of bad MSE performance, an additional Wiener filtering in time may kick in to reduce the error due to mismatch.

The merits of pilot merging are not limited to the above mentioned facts. In skewed pilot patterns, one could attain several different virtual pilot separations through merging or time-domain filtering. As will be discussed in the following section, the possibility to vary the virtual pilot spacing, in the event of skewed pilot pattern, allows filter tap memory optimization. Moreover, the same filter coefficients may be re-used for channel estimation purposes in other OFDM systems, provided that certain requirements are met. However, before moving on to the next sections where the details are further elaborated, this section deserves one more discussion before being wrapped up.

The number of available pilots in a pilot-carrying OFDM symbol equals N/α. Thus, if the estimation is carried out in frequency domain only, while no merging is practiced, N/α pilots can be used for channel estimation of each tone. However, exploiting all pilots for estimation of one tone turns out to be unnecessary due to the considerable correlation loss among the tones and pilots which are located far apart, see Fig. 2. Thus, only a subset of pilots in the vicinity of each tone may be used for channel estimation purposes. Furthermore, the pilots can be selected symmetrically with respect to each tone. The combination of RMMSE estimators as well as selecting a subset of pilots results in a new low-complexity channel estimator called modified RMMSE (MRMMSE) estimator. The only problem with this approach is the inability of symmetric pilot selection at the edge subcarriers where a larger number of pilots may be used to compensate for the loss in estimation performance. Meanwhile, the number of selected pilots can be optimized for a certain metric, e.g., MSE. The proposed strategy in this thesis for channel estimation in low-power terminals can be briefly described as,

- Choose an appropriate number of pilots in the vicinity of each tone for estimation purposes. The selection criteria may be based on a certain tolerable MSE, i.e., SNR degradation with respect to stationary environments,
- Pilot-merging should be practiced unless the performance degradation due to mismatch surpasses a certain threshold. The threshold can be again based on, e.g., a certain acceptable MSE. As soon as the performance criteria is not met, additional 1-D time-domain filtering may be invoked to improve the mismatch due to fading.

The above principle has been proposed for channel estimation in Multi-base [31] where a number of high-speed standards need to be integrated into the same platform. One may observe that due to selecting a subset of pilots, the amount of on-chip memory for robust-filter tap storage decreases. In channels with high frequency selectivity the size difference between the available pilots and the proposed pilot subset may increase substantially. The combination of pilot-merging as well as employing a subset of pilots for robust channel estimation is known as merged-pilot modified robust MMSE (merged-pilot MRMMSE) channel estimation throughout this thesis unless otherwise stated.

3.5 Filter-tap memory optimization

In section 3.4, it was discussed how robust channel estimators can be pre-computed and stored in memory. The coefficients are later fetched during the estimation process. Besides, it was shown how the computational complexity can be further reduced if only a subset of pilots in the vicinity of each subcarrier is used for channel estimation purposes while introducing a small loss in the estimation performance. The loss can be quantified and optimized through calculations and Monte Carlo simulations so that a desired number of pilots can be selected for a specific system configuration.

For instance, imagine an OFDM system with N tones in one OFDM symbol where zero-padding of the edge subcarriers has been ruled out for simplicity. Besides, a pilot separation of α' is achieved in the constructed PV where the number of available pilots is $N_{\mathrm{p,merg}}$. Furthermore, it is decided that only a subset of the available pilots, i.e., $N'_{\mathrm{p,merg}}$, where $N'_{\mathrm{p,merg}}$ is a power of 2 and $N'_{\mathrm{p,merg}} \ll N_{\mathrm{p,merg}}$, may be used for estimation of each tone with an acceptable performance. As a result, it is easy to conclude that the number of required filter taps for estimation of one tone equals $N'_{\mathrm{p,merg}}$. A collection of such filter coefficients is called a filter set. Thus, except $2 \times \left(\frac{N'_{\mathrm{p,merg.}} \times \alpha'}{2} - 1\right)$ edge subcarriers, a few filter sets can be shared among all subcarriers for estimation purposes. More precisely, α' filter sets are needed to carry out the channel estimation for all tones other than the edge subcarriers.

Although the above discussed facts enable one to reduce the number of required filter coefficients, the intension is to reuse a portion of these coefficients for channel estimation purposes in other modes associated with the OFDM system of choice or even in other compatible OFDM systems. OFDM system mode in here means the one that is characterized by the employed CP.

Imagine the 1-D robust estimators designed for a rectangular PDP, i.e., the worst-case frequency selectivity for a given delay spread. It can be observed from (2.7) that the correlation coefficients are a function of N, L, and Δk. Thus, as long as the same ratio in $L\Delta k/N$ is held, the same filter coefficient can be used for different system configurations. In fact, it is desired to force

$$r_{\mathrm{h,f}_1}[\Delta k] = r_{\mathrm{h,f}_2}[\Delta k], \ \forall k, \tag{3.15}$$

where index 1 refers to system configuration 1 and index 2 refers to system configuration 2. As a result, the estimators will be identical for similar values of SNR.

For example, imagine the OFDM system in Fig. 4. Suppose the system has two different design CPs, $L1$ and $L2$, due to two different wireless channel environments. Furthermore, suppose $L_2 = 2L_1$. To address the channel estimation needs two different RMMSE filters are designed, each corresponding to one mode of operation, i.e., one CP. If the robust design strategy as mentioned above is followed, the correlation coefficients become,

$$\begin{aligned} r_{\mathrm{h,f}_1}[\Delta k_1] &= f_1(L_1\Delta k_1/N), \\ r_{\mathrm{h,f}_2}[\Delta k_2] &= f_1(L_2\Delta k_2/N), \end{aligned} \tag{3.16}$$

where $f_1(L\Delta k/N) = \dfrac{1-\exp(-2j\pi L\Delta k/N)}{2j\pi L\Delta k/N}$. Thus, to force

$$r_{\mathrm{h,f}_1}[\Delta k_1] = r_{\mathrm{h,f}_2}[\Delta k_2] \Rightarrow f_1(L_1\Delta k_1/N) = f_1(2L_1\Delta k_2/N), \tag{3.17}$$

the following relation between the pilot separations should hold,

$$\Delta k_1 = 2\Delta k_2. \tag{3.18}$$

As a result, the constructed PVs should have different virtual pilot spacing for each case, i.e., the pilot spacing in the event of L_2 should be twice the spacing in the event of L_1. Thus, one may use the merging scheme proposed in this thesis or use additional 1-D filtering, at the expense of more computational complexity. For the above example, where the pilot pattern is similar to Fig. 7, the constructed PV is fed into the designed MRMMSE filter when the system is configured to operate in mode 1. However, to insure a pilot spacing twice as much, pilots from alternate pilot-carrying OFDM symbols should be collected into the PV.

The application of the above strategy is not restricted to on-chip filter memory optimization associated with one OFDM system, with different modes of operation, only. As it will be discussed in the following sections, the same principle may be extended such that a family of filters can be reused across different OFDM systems. For instance, it will be shown how a novel selection of filter design parameters provides a maximum memory optimization when LTE and DVB-H coexist on the same platform. Finally, the examples will be used as the basis for a pilot design strategy where the goal is to maximize the number of system configurations which can employ the same filters for channel estimation purposes.

4 Channel estimation in LTE and DVB-H

4.1 LTE physical layer specifications

LTE has been proposed as the system of choice for high-speed wireless communications in the next generation of mobile terminals. The standardization was initiated and pursued by the 3rd Generation Partnership Project (3GPP) [32] where groups of telecommunications associations collaborate and contribute to the project development. Being a complicated system with various building blocks, a detailed analysis of LTE is well beyond the scope of this thesis. However, the following provides a brief introduction to some of the physical layer characteristics and specifications which are crucial from a channel estimation view point.

LTE is an OFDM system with a number of operation modes supporting different BWs. The supported BW ranges from 2 MHz to 20 MHz and corresponds to DFT sizes of 128 to 2048 points. One of the fundamental characteristics of LTE across its different configurations is the tendency to keep a fixed subcarrier spacing of 15 kHz,[3]

[3]The only exception is when LTE is used for multicast/broadcast over single frequency network (MBSFN) where $\Delta f = 7.5$ kHz. In this thesis, MBSFN associated with LTE has not been covered.

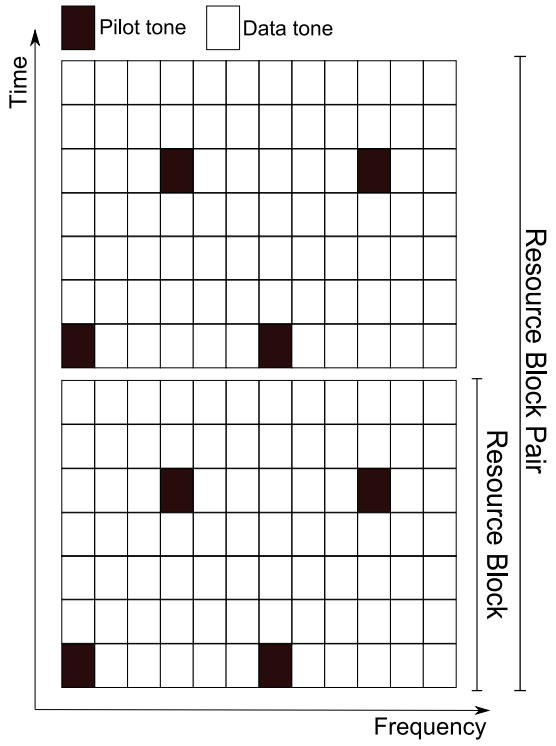

Figure 8: An example of time-frequency grid corresponding to one RBP for LTE. The scattered pilots are identified by the black boxes.

i.e., $\Delta f = 15$ kHz. As a result, the system's sampling frequency scales according to $f_{\mathrm{s}} = N\Delta f$ samples/s. Besides, two different CPs are defined in LTE, called normal and extended CPs. The normal CP, L_{normal}, is 4.69 μs long while the extended CP, L_{extended}, has a length of 16.67 μs. Depending on the operating environment, the system is configured for one of the above GIs. For instance, in larger cells where the delay spread of the channel is extensively longer, the extended CP can be used. Please note that the actual OFDM symbol duration, without CP, is $T_{\mathrm{u}} = 66.7\,\mu$s.

LTE is an example of orthogonal frequency division multiple access where user data in downlink is multiplexed for different users. As a result, data needs to be encapsulated in specific units. There are various data encapsulations in LTE. For example, an RB is the collection of 12 tones in 7 consecutive OFDM symbols if the normal CP is employed. If the extended CP is used, the number of constituting OFDM symbols reduces to 6 consecutive ones. Moreover, two consecutive RBs, encompassing the same tones, constitute a RB pair (RBP). Fig. 8 illustrates an example of RB and RBP. Although more coarse data encapsulations are also defined in LTE, an RBP is the smallest block which may be allocated to a single user during data transmission. Being properly encoded in the first few OFDM symbols in each RBP, each terminal needs to actively receive and decode the control signaling associated with each RBP. In the event of no data allocation, the terminal can enter a stand-by state, to save energy, until a new RBP is scheduled for reception.

To assist channel estimation, a scattered pilot pattern has been designed and

proposed in LTE. Being a MIMO system, the pilots transmitted between a pair of transmit/receive antennas have been designed to be orthogonal to the pilots associated with other antenna pairs. As a result, MIMO channel estimation in LTE reduces to several SISO estimations. For simplicity, the calculations are derived for a single antenna port, i.e., antenna port 0. Fig. 8 shows the scattered pilot pattern for antenna port 0 where pilot spacing in frequency is a constant value of 6 tones. Moreover, the pilot frequency shift is 3 tones. In other words, compared to the primary skewed pilot pattern in Fig. 6, $\alpha = 6$, $\gamma = 3$ and $\beta = 7$. On the contrary, the spacing between two consecutive pilot-carrying OFDM symbols associated with a single RBP is not a constant value, i.e., $\Gamma \in \{3, 4\}$. The pilots in each RBP appear in OFDM symbols 1, 5, 8 and 12 respectively.

Although the above described configuration is limited to a subset of antenna ports, it provides an acceptable basis for the derivation of channel estimation algorithms. Besides, the results can be easily extended to other antenna ports where the pilot patterns slightly vary to accommodate pilot orthogonality across multiple antennas. Meanwhile, in practical system implementations, certain OFDM symbols are discriminated against others due to the sensitivity of the information they carry. For instance, the first few OFDM symbols may undergo a different data modulation, e.g., BPSK or QPSK, compared to the rest of symbols where up to 64 QAM may be used for data modulation. However, for simplicity and without loss of generality similar parameters across all OFDM symbols in an RBP have been used, when applicable.

4.2 DVB-H physical layer specifications

Being a SISO OFDM system, DVB-H is an extension of digital video broadcast-terrestrial (DVB-T) for transmission of multimedia content to wireless mobile terminals. On top of various modifications to DVB-T, such as using different interleaving schemes, the fundamental difference, at least from a physical layer perspective, is the addition of 4K mode of operation in DVB-H. 4K mode provides a compromise between data rate , hardware complexity, and overhead during implementation when compared to the conventional 2K and 8K modes in DVB-T. Similar to LTE, an elaborate description of DVB-H is not the intention of this thesis and the interested reader may refer to [5] for further information. However, a short overview of DVB-H's physical layer parameters fundamental to derivation of channel estimation is provided as follows.

DVB-H supports three different BWs corresponding to each mode of operation, i.e., 2k, 4k, and 8k. The size of each BW is simply controlled by scaling the sampling frequency of the system. For a given BW, the sampling frequency remains constant throughout various modes of operation. As a result, contrary to LTE, the subcarrier spacing in DVB-H is not a constant value and varies inversely proportional to BW. Moreover, four different GIs have been designed for DVB-H. The GIs are expressed in terms of their length with respect to the useful OFDM symbol duration. As a result, the GIs are known as $\frac{1}{4}$, $\frac{1}{8}$, $\frac{1}{16}$, and $\frac{1}{32}$.

Scattered pilots are also employed in DVB-H to address the channel estimation

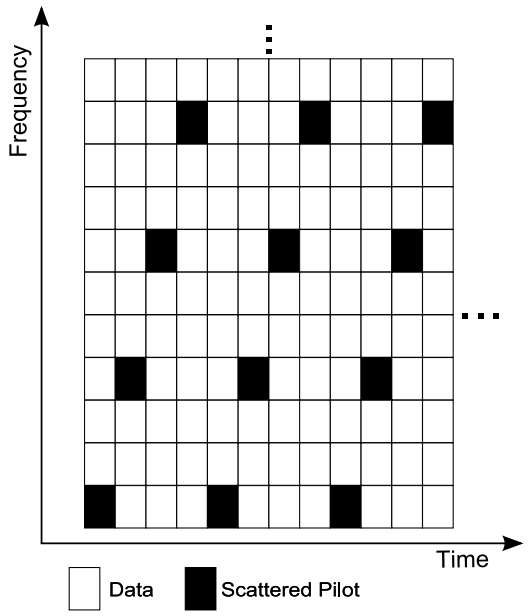

Figure 9: An example of time-frequency grid corresponding to DVB-H. The scattered pilots are identified by the black boxes.

needs. The pilots are evenly distributed in all OFDM symbols. Fig. 9 shows the pilot pattern in an exemplary time-frequency grid for DVB-H. Moreover, mapping the pilot scheme in DVB-H to the primary skewed pilot pattern in Fig. 6, $\alpha = 12$, $\beta = 4$, $\gamma = 3$ and $\Gamma = 1$ can be deduced. Meanwhile, to increase the channel estimation performance at the expense of a reduced effective SNR, the pilots can be transmitted with boosted power when compared to data symbols.[4]

4.3 Multi-mode filter-tap memory optimization in LTE

Following the discussion in Sec. 3 many different approaches can be pursued for channel estimation in LTE. However, we will focus on the low-complexity robust estimators, i.e., MRMMSE applied to antenna port 0. Doing so reduces MIMO LTE channel estimation to a simpler SISO counterpart. The results can be easily extended to MIMO LTE due to orthogonality of the pilots, though.

As already discussed, our general strategy is to alleviate the additional 1-D filtering in time while achieving acceptable performance in moderately fast fading environments. As a result, we have resorted to pilot-merging scheme to capture the time variations of the wireless channel to a certain extent. Fig. 10 shows the proposed methodology for pilot merging when an individual RBP has been selected for channel estimation as well as the equalization. It can be seen from the figure that we have relied not only on the pilot-carrying OFDM symbols within the specified RBP but also on the 1st pilot-carrying OFDM symbol associated with the next

[4]The boosted power option has not been employed for the deductions of the results in this thesis.

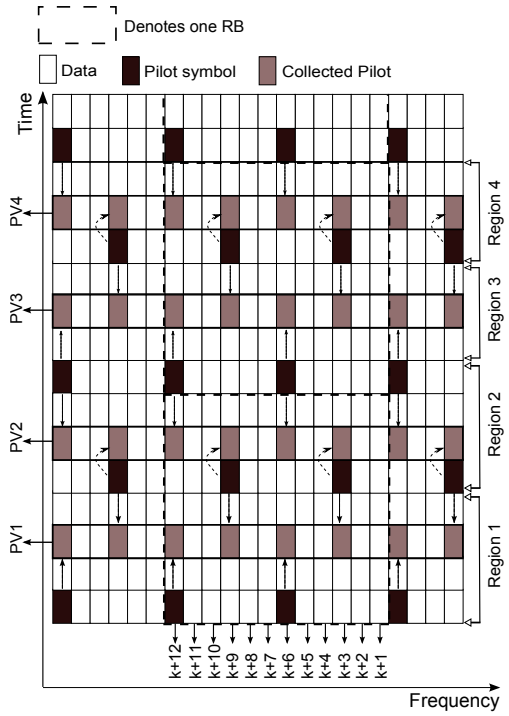

Figure 10: Pilot-merging strategy for channel estimation and equalization associated with LTE.

adjacent RBP. Although one may argue that there is no guarantee two consecutive RBPs are allocated to the same user, the terminal needs to receive and decode the first few symbols in each RBP to extract the scheduling information.

The constructed PV associated with channel estimation of each region is identified by brown tiles in Fig. 10. Considering PVs as such, the 1-D filter in frequency, i.e., (3.12) needs to be designed. As discussed in Sec. 3.3, a robust MMSE filter designed for the worst-case expected channel environment can be employed for channel estimation purposes in LTE. Thus, the filters are designed for rectangular GIs with delay spreads equal to the normal as well as the extended CPs. Besides, following the discussion in Sec. 3.4, only a subset of pilots in the vicinity of each tone is used for estimation purposes. Application of merged-pilot MRMMSE estimators introduces a certain design mismatch compared to the full 2-D MMSE filter. The amount of mismatch can be quantified and derived mathematically from (3.8) or through Monte Carlo simulations.

Due to pilot merging, the mismatch in the event of high Doppler shifts becomes more severe and dominates the PDP mismatch in fast-fading environments. As a result, the merged-pilot MRMMSE channel estimation's performance degrades for high terminal speeds as a result of which higher SNR is needed to sustain the design MSE. However, it can be shown in Sec. 5.2 that the BER performance degradation due to Doppler is not as severe when various coding and interleaving are applied in the practical system implementation. A thorough analysis of the performance for various fading environments is discussed in Secs. 5.1, 5.2, and 5.3.

Designing the MRMMSE estimators for LTE system alone, one might need two separate estimators, i.e., two estimators associated with the normal CP and extended CP respectively. However, the memory optimization strategy discussed in Sec. 3.5 can be practiced to reduce the amount of on-chip memory. As a result, it is required that

$$L_1 \Delta k_1 / N_1 = 2 L_1 \Delta k_2 / N_2 \tag{4.1}$$

for the filter coefficients associated with the different modes to be identical. Here, index 1 and 2 refer to filter design in the event of normal and extended CPs, respectively. However, it can be observed that $\frac{\Delta k_1}{\Delta k_2} = \frac{L_2}{N_2}\frac{N_1}{L_1} \approx 3.5$, when $N_1 = N_2$, is not an integer. A compromise in design CP has been proposed in Sec. 5.3, where the design PDP, called $L_{1,\text{trunc.}}$, is a truncation of normal GI such that

$$\frac{\Delta k_1}{\Delta k_2} = \frac{L_2}{N_2}\frac{N_1}{L_{1,\text{trunc.}}} = 4, \tag{4.2}$$

for $N_1 = N_2$.

In other words, the robust filters in the event of normal CP may be designed for a truncated GI such that (4.1) holds. Thus, to guarantee filter coefficient reuse, the only possibility is to use pilot merging in the event of extended CP and ignore alternate pilots in frequency for normal CP. By doing so the pilot spacing for normal CP becomes 12 tones. However, the maximum distance for pilot spacing in frequency is 14 tones if the Nyquist sampling criteria in frequency is to be met for LTE in normal mode of operation. But Nyquist sampling criteria holds where theres is an infinite (sufficiently large) signal observation interval in the absence of AWGN. Thus, a pilot spacing of 12, just below the Nyquist threshold, results in degraded channel estimation performance.

Had the pilot pattern for one RBP in LTE been designed according to Fig. 11, more flexibility in terms of filter memory optimization would be provided. In fact, three different merging schemes could be achieved either through merging or time-domain filtering while the pilot overhead would decrease by 25%. However, due to the longer separation between pilots in time, almost twice as long compared to the standardized pattern, the maximum supported mobility associated with the system would scale by 1/2. Besides, the performance deterioration would be more emphezised in the event of high mobility when pilot merging is practiced.

Alternatively, the robust estimator in the event of normal CP can be designed for an extended normal GI.[5] In other words, if the filter is designed for a rectangular PDP with a delay spread of 8.3 μs rather than 4.7 μs,

$$\frac{\Delta k_1}{\Delta k_2} = \frac{L_2}{N_2}\frac{N_1}{L_{1,\text{norm.,exten.}}} = 2, \tag{4.3}$$

where $L_{1,\text{norm.,exten.}}$ is the design PDP for an extended normal CP.

Thus, the same filter coefficients may be shared between the two modes provided that pilot merging in the event of extended CP is practiced while for operation in

[5]Here the extended normal GI refers to the adopted design CP used in MRMMSE estimators and should not be confused with the standardized extended CP in LTE, i.e., L_{extended}

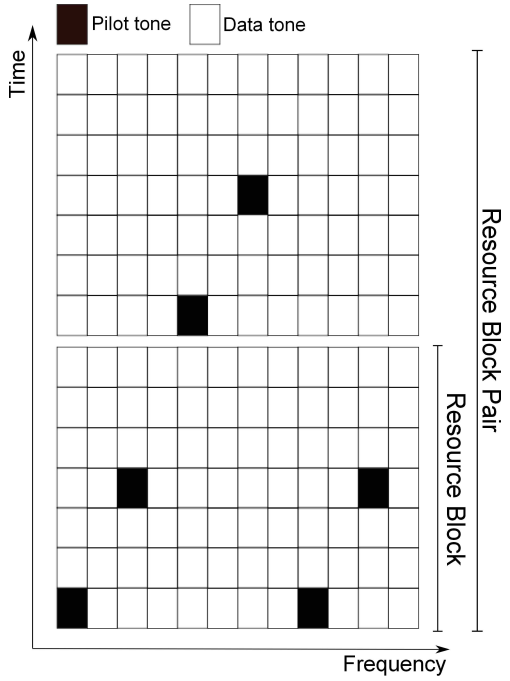

Figure 11: An example of hypothetical pilot pattern for LTE to optimize the filter-tap memory.

normal mode the pilot separation ought to remain 6, i.e., no pilot merging should be sought.

Designing the filters for an extended normal GI is considered a safer approach when compared to its truncated counterpart. Although, it introduces a considerable amount of mismatch in connection with the majority of practical cases, it does not discard the signal energy if the wireless channel constitutes high energy taps located in the discarded region. Moreover, it allows reuse of the same filter coefficients across the two modes of operation. On the contrary, if the estimator is viewed as a filter, more noise passes through the filter designed for an extended normal CP, when compared to the truncated normal CP, due to a wider filter BW.

4.4 Multi-mode filter-tap memory optimization in DVB-H

Due to a higher pilot density, merged-pilot MRMMSE channel estimation in DVB-H can exhibit better performance in high terminal mobilities when compared to LTE. Besides, more pilot merging patterns can be practiced. More precisely, 4 different pilot merging schemes can be done with pilot separations of 3, 6, 9 and 12 tones. Thus, for maximum filter memory optimization, one may use the same filter coefficients provided that pilot separations of 3, 6, 12, and 24 corresponding to 1/4, 1/8, 1/16, and 1/32 CPs, are forced in the constructed PVs. The drawback, however, is a poor channel estimation performance in the event of 1/32 CP because a pilot separation of 24 means ignoring alternate pilots in frequency.

4.5 Multi-standard filter-tap memory optimization across LTE and DVB-H

Following the discussion in Secs. 4.3 and 4.4, it can be observed that one family of filters may be used for channel estimation needs of both LTE and DVB-H provided that LTE channel estimators are designed for an extended delay spread in the event of normal CP. This is due to the fact that

$$\frac{L_{\text{design}}\Delta k}{N} = \frac{3}{4}, \tag{4.4}$$

for all possible configurations in LTE and DVB-H, provided that the parameters are selected from Table 1. Besides, L_{design} corresponds to the presumed delay spread of the wireless channel for which the estimators are designed. Table 1 shows the different configurations for which channel estimation filter tap memory optimization can be done for LTE and DVB-H.

Table 1: The configurations for which coefficient co-optimization is feasible according to our proposed scheme.

LTE			DVB-H			
N_{DFT}	Operation mode	Pilot Sep.	BW (MHz)	Mode (k)	CP len.	Pilot Sep.
128-2048 (except 1536)	Normal CP	6	6-8	2-8	$\frac{1}{32}$	24
					$\frac{1}{16}$	12
	Extended CP	3			$\frac{1}{8}$	6
					$\frac{1}{4}$	3

However, if the design criteria imposes the filters to be designed for a truncated CP when LTE operates in the normal mode, then two separate filters need to be designed and stored in memory to handle the channel estimation requirements when the two standards coexist. Please refer to Sec. 5.3 for further discussion of the technical details associated with such strategy.

5 Summary of included papers and technical reports

5.1 Paper I - Channel estimation for a mobile terminal in a multi-standard environment (LTE and DVB-H)

Being two different OFDM systems, LTE and DVB-H have their own distinct specifications and operation modes. For instance, DVB-H is a broadcast standard where multimedia content is simultaneously broadcasted to a large number of users. As a result, users have to receive and decode all the available data tones associated with the transmitted OFDM symbols. However, in LTE, data can be encapsulated in different data units bounded by a certain number of subcarriers in a given OFDM symbol. Thus, the receiver does not necessarily need to estimate and decode all the data associated with all the available data tones in a given OFDM symbol.

In this paper, two different approaches have been probed for channel estimation when applied to LTE and DVB-H. One approach is the application of MRMMSE algorithms as elaborated in this thesis. Contrary to the proposed MRMMSE algorithm, time domain estimation through the application of DFT and IDFT has also been probed. In other words, the performance of the above mentioned approaches to LTE and DVB-H have been partly evaluated. Besides, the hardware complexity in terms of the number of multiplications as well as memory requirements have been evaluated.

Taking the fact that the terminal in LTE does not necessarily need to decoded all the available data tones associated with an OFDM symbol into account, MRMMSE best suits LTE in terms of hardware resources. On the other hand, DFT-based algorithms exhibit much lower complexity when compared to the MRMMSE counterpart. However, there is one big hurdle when using the DFT-based algorithms. The majority of practical OFDM systems, including LTE and DVB-H, have spectral masks through nulling the edge subcarriers. As a result, mixed-radix FFT and IFFT algorithms need to be employed if DFT-based approach is to be applied.

Hardware implementation of mixed-radix FFT/IFFT algorithms seems to be far more complicated when compared to radix 2 algorithms. On the other hand, terminals usually have access to a radix-2 FFT for OFDM demodulation. As a result, using mixed-radix FFT/IFFT blocks increases the power and hardware resource requirements in a receiver. Thus, having separate MRMMSE and DFT-based estimators may not be motivated in a multi-standard environment unless it is dictated by the performance requirements. Meanwhile, MRMMSE algorithms provide a good alternative with respect to DVB-H when both performance and hardware requirements are taken into account. As a result, the MRMMSE estimators can efficiently address the channel estimation needs of the terminals both for LTE and DVB-H.

5.2 Paper II - Low-complexity channel estimation for LTE in fast fading environments for implementation on multi-standard platforms

The application of MRMMSE algorithms, when pilot merging is practiced, is an efficient approach to low-complexity estimators in mobile terminals. The merits of pilot merging in the event of fading environments are two-fold. First, nearly a 3-dB improvement in slowly-fading environments is achieved due to the fact that the number of pilots for estimation purposes is doubled. Second, the pilot merging partly captures the time-variations in fading environments. However, the introduced errors due to mismatch in fast fading environments start to surpass the improvements resulting from a larger number of available pilots for estimation. As a result, it is necessary to characterize the fading environments where pilot merging would provide an acceptable performance.

To reduce the complexity of the estimators, one needs to lower the number of estimation operations. One way to achieve this is to widen the equalization regions where the same estimated channel can be employed. However, in fast fading environments the regions need to be divided into smaller subset for equalization purposes. In this paper, it is shown that by using the available pilot pattern in LTE, pilot merging may be practiced for different equalization regions. The merits of such approach are observed in fast fading environments where a terminal speeds up to 120 km/h are expected. Beyond that, one may need to employ additional time-domain filtering to capture the time variations of the channel.

Meanwhile, it is shown that an additional simple filter in the direction of time can be employed in the event of fast fading environments where pilot merging cannot be practiced. The time-domain filter is designed for a worst-case Doppler spectrum, i.e., a rectangular Doppler spectrum where the Doppler spread is at its maximum value. The simulation results, show that the estimator exhibits a good performance when the above mentioned additional filter kicks in. Although, the adopted standard for investigation in this paper is LTE only, the proposed approaches can be easily extended to DVB-H.

5.3 Paper III - On coefficient memory co-optimization for channel estimation in a multi-standard environment (LTE and DVB-H)

In Sec. 5.1, 5.2, and 5.3 the merits of MRMMSE channel estimation algorithms were discussed when applied to LTE and DVB-H. Meanwhile, the main emphasis has been on reducing the computational complexity of such algorithms. Although, computational complexity accounts for a large portion of the required hardware resources, including power consumption, little attention was given to on-chip memory for the storage of the channel estimation filter taps.

MRMMSE estimators alleviates the requirement for real-time calculation of filter taps so they can be calculated off-line. However, the filter taps need to be stored in memory such that the estimation block can efficiently fetch them during the estimation operation. On the other hand, the number of filter taps increases as more standards need to be integrated in the same platform. Even different modes of operation associated with one standard may require additional filter memory.

In this paper, it is shown that by exploiting the similarities in pilot pattern in LTE and DVB-H, one could design the MRMMSE estimators such that similar filter taps could be employed for estimation purposes across LTE and DVB-H. Moreover, the robust estimators may need to be designed for delay spreads other than what is suggested by the standardized CPs so that similar filters can be shared among the standards. As a result, the performance of the filters in such cases has been evaluated in this paper. Specifically, the performance of the estimators in the event of designing the estimators for a truncated normal CP in LTE has been discussed.

On the other hand, the pilot separation plays an important role if similar filter taps need to be used. As a result, one may need to exercise pilot merging or additional time filtering to assure the compatibility among filter taps. Using different pilot merging for different modes of operation in each standard might impose certain performance degradation in fading environments. This is more emphasized in DVB-H where a number of different pilot merging schemes need to be practiced. Thus, the channel estimator's performance for various merging schemes has been characterized with respect to different fading environments.

5.4 Technical Report - Channel estimation filter-tap memory-optimized pilot pattern design for OFDM systems in multi-mode and multi-standard environments

The possibility to optimize the on-chip memory may provide a 6-fold optimization for the storage of channel estimation filter taps in a multi-standard environment where LTE and DVB-H co-exist. The above mentioned optimization could not be achieved if the divisor of the pilot separations in LTE and DVB-H was not the same prime number, i.e., 3. Thus, one might ask if there is a possibility to integrate more OFDM standards in the same platform while benefiting from similar channel estimation filter taps. In a broader perspective, is it possible to maximize the number of OFDM standards which can be integrated in the same platform, constrained to the availability of a finite set of channel estimation filters, when designing the pilot pattern.

In this paper, it is shown that by following a specific strategy in scattered pilot pattern design for OFDM systems, the number of required filter taps upon integration of several systems in a multi-standard environment is minimized. The designed pattern would still provide the possibility for channel estimation in the event of applying linear estimators other than the proposed MRMMSE estimators. A pilot pattern as such provides a maximum number of different frequency pilot spacings when pilot merging or time filtering is practiced. As a result, the proposed approach provides the flexibility for employing the MRMMSE channel estimators. Furthermore, it guarantees the proximity of the pilot carrying OFDM symbols such that upon merging the shortest distance exists between the pilot contributing OFDM symbols. This is especially important for equalization purposes in fast fading environments.

On the other hand, there are situations where one OFDM system is already standardized. So, how are the pilot patterns for new OFDM systems designed such that they remain compatible with an existing system in a multi-standard environment? A strategy has also been suggested in this paper which addresses compatible pilot pattern design for emerging OFDM systems with respect to an existing system. Meanwhile, LTE is expected to remain a prominent OFDM standard for voice and data communications in the foreseeable future. Thus, the report is wrapped up through an example which elaborates the application of the above strategy to pilot pattern design for the emerging OFDM systems which remain compatible with LTE.

6 Concluding remarks

Channel estimation and pilot pattern design for OFDM systems is a well-established area of research to which many researchers have contributed. However, as mobile terminals tend to integrate more high speed OFDM standards there is still a lot to do in terms of optimized signal processing algorithm design for such systems. Although the optimization might be performed at the expense of some performance degradation, a considerable reduction in the amount of hardware resources could motivate their application in low-power terminals. In this thesis, it is shown how the above principle can be applied to the channel estimation block in a multi-standard receiver. By adopting some of the already existing standards such as LTE and DVB-H, approaches to reduced complexity estimation algorithms are probed and solutions are suggested.

Furthermore, the lessons learnt from such an approach provided the opportunity to pursue a strategy for pilot pattern design for OFDM systems in multi-standard environments. The above mentioned strategy not only maximizes the performance of the receivers in the presence of merged-pilot MRMMSE channel estimators, but also enables sharing the same filters among a maximum number of compatible OFDM systems. Moreover, it is possible to design the pilot pattern in emerging OFDM systems such that they are compatible, in terms of employing similar channel estimation filters, with existing OFDM systems in a multi-standard platform.

To further explore the capabilities of such pilot pattern design, one could evaluate the performance of the proposed estimators in the presence of correlation mismatch. In other words, how much correlation deviation can be tolerated if the proposed optimization schemes does not guarantee the similarity among channel estimation filter taps. Last but not least, one may explore the potentials of the proposed digital signal processing optimization techniques to other baseband digital signal processing blocks. For instance, the possibilities for low-complexity digital signal processing algorithms for estimation of I/Q imbalance, probably combined with channel estimation, may be probed in multi-standard receivers.

7 References

References

[1] "IEEE Standard for Information technology–Telecommunications and information exchange between systems–Local and metropolitan area networks–Specific requirements Part 11: Wireless LAN Medium Access Control (MAC) and Physical Layer (PHY) Specifications Amendment 5: Enhancements for Higher Throughput," *IEEE Std 802.11n-2009*, pp. c1–502, Sep. 2009.

[2] "Evolved Universal Terrestrial Radio Access (E-UTRA); LTE physical layer; General description," 3rd Generation Partnership Project, Tech. Specifications, 3GPP TS 36.201, Dec. 2009. Available: http://www.3gpp.org/ftp/Specs/html-info/36201.htm.

[3] M. Gertsman and J. Lodge, "Symbol-by-symbol MAP demodulation of CPM and PSK signals on Rayleigh flat-fading channels," *IEEE Trans. Commun.*, vol. 45, pp. 788–799, July 1997.

[4] C. Knievel et al., "2-D graph-based soft channel estimation for MIMO-OFDM," in *Proc. IEEE Int. Conf. Commun.,* Cape Town, pp. 1–5, 2010.

[5] "Digital Video Broadcasting (DVB); Framing structure, channel coding and modulation for digital terrestrial television," European Telecommunications Standards Institute (ETSI), Tech. Specifications Final Draft, 2004.

[6] J. McKown and R. Hamilton, "Ray tracing as a design tool for radio networks," *IEEE Trans. Netw.*, vol. 5, pp. 27–30, Nov. 1991.

[7] M. Sandell and O. Edfors, "A comparative study of pilot-based channel estimators for wireless OFDM," Tech. Rep., Div. of Signal Process., Luleå Univ. of Technology, Luleå, Sweden, 1996.

[8] O. Edfors et al., "OFDM channel estimation by singular value decomposition," *IEEE Trans. Commun.*, vol. 46, pp. 931–939, July 1998.

[9] M. Gertsman and J. Lodge, "A statistical theory of mobile radio reception," *Bell Syst. Tech. J.*, pp. 957–1000, July 1968.

[10] M. Gans, "A power-spectral theory of propagation in the mobile-radio environment," *IEEE Trans. Veh. Technol.*, vol. 21, pp. 27–38, Feb. 1972.

[11] A. Goldsmith, *Wireless communications.* New York, NY: Cambridge University Press, 2005.

[12] R. W. Chang, "Synthesis of band-limited orthogonal signals for multichannel data transmission," *Bell Syst. Tech. J., 45*, pp. 1775–1796, 1996.

[13] R. Chang and R. Gibby, "A theoretical study of performance of an orthogonal multiplexing data transmission scheme," *IEEE Trans. Commun.*, vol. 16, pp. 529–540, Aug. 1968.

[14] Y. Li et al., "MIMO-OFDM for wireless communications: signal detection with enhanced channel estimation," *IEEE Trans. Commun.*, vol. 50, pp. 1471–1477, Sep. 2002.

[15] M. Engels, *Wireless OFDM systems: How to make them work?* Norwell, MA: Kluwer Academic Publishers, 2002.

[16] G. Stuber et al., "Broadband MIMO-OFDM wireless communications," *Proc. IEEE*, vol. 92, pp. 271–294, Feb. 2004.

[17] M. Windisch, *Estimation and Compensation of I/Q imbalance in Broadband Communications Receivers*. Dresden, Germany: Jorg Vogt Verlag, 2007.

[18] G. Strang, *LINEAR ALGEBRA AND ITS APPLICATIONS*. Belmont, CA: Thomson Brooks/Coles, 2006.

[19] Y. Li et al., "Channel estimation for OFDM systems with transmitter diversity in mobile wireless channels," *IEEE J. Sel. Areas Commun.*, vol. 17, pp. 461–471, Mar. 1999.

[20] M. Ozdemir and H. Arslan, "Channel estimation for wireless OFDM systems," *Commun. Surveys Tuts., IEEE*, vol. 9, pp. 18–48, July 2007.

[21] M. Morelli and U. Mengali, "A comparison of pilot-aided channel estimation methods for OFDM systems," *IEEE Trans. Signal Process.*, vol. 49, pp. 3065–3073, Dec. 2001.

[22] V. Srivastava et al., "Robust MMSE channel estimation in OFDM systems with practical timing synchronization," in *Proc. IEEE Wireless Commun. and Netw. Conf.,* Atlanta, GA, pp. 711–716, 2004.

[23] W. Tianbin et al., "Graph-based soft channel and data estimation for MIMO systems with asymmetric LDPC Codes," in *Proc. IEEE Int. Conf. Commun.,* Beijing, pp. 620–624, 2008.

[24] L. Tong et al., "Blind identification and equalization of multipath channels," in *Proc. IEEE Int. Conf. Commun.,* Chicago, IL, pp. 1513–1517, 1992.

[25] L. Baccala and S. Roy, "A new blind time-domain channel identification method based on cyclostationarity," *IEEE Signal Process. Lett.*, vol. 1, pp. 89–91, June 1994.

[26] H. Zeng and L. Tong, "Blind channel estimation using the second-order statistics: Algorithms," *IEEE Trans. Signal Process.*, vol. 45, pp. 1919–1930, Aug. 1997.

[27] W. Songping and Y. Bar-Ness, "OFDM channel estimation in the presence of frequency offset and phase noise," in *Proc. IEEE Int. Conf. Commun.,* Anchorage, AK, pp. 3366–3370, 2003.

[28] O. Edfors, *Low-complexity algorithms in digital receivers.* PhD thesis, Div. of Signal Process., Luleå Univ. of Technology, Luleå, Sweden, 1996.

[29] P. Hoeher et al., "Two-dimensional pilot-symbol-aided channel estimation by Wiener filtering," in *Proc. IEEE Int. Conf. Acous., Speech and Signal Process.,* Munich, pp. 1845–1848, 1997.

[30] R. Nilsson et al., "An analysis of two-dimensional pilot-symbol assisted modulation for OFDM," in *Proc. IEEE Int. Conf. Personal Wireless Commun.,* Mumbai, pp. 71–74, 1997.

[31] Ericsson AB et al., "System Requirements Specification (2nd version), incl. scope and time plan," Scalable Multi-tasking Baseband for Mobile Communications, Tech. Rep. D1.2, Jan. 2008. Available: http://www.multibase-project.eu.

[32] "Third generation partnership project (3GPP)."
Available: http://www.3gpp.org.

Channel estimation for a mobile terminal in a multi-standard environment (LTE and DVB-H)

Farzad Foroughi Abari, Johan Löfgren, and Ove Edfors

Paper I

Abstract

In this paper, we present an analysis of different channel estimator structures that can be used and efficiently implemented with minor configuration changes of a common hardware for both LTE and DVB-H. Such common estimator structures for LTE and DVB-H allow algorithm and hardware reuse when both standards are implemented on the same platform. In this approach, a core estimator will be utilized to address parameter estimation for the two standards. The estimators exploit similarities in pilot patterns between LTE and DVB-H. The estimation techniques are discussed taking both algorithm and complexity issues into account.

1 Introduction

Orthogonal Frequency Division Multiplexing (OFDM) is a special case of multi-carrier transmission and it can accommodate high data rate requirement of multimedia based wireless systems [1]. Due to its inherent structure, it is feasible to achieve a multiple-access format while benefiting from various coding and frequency hopping schemes. This will provide a high degree of diversity and inter-cellular interference suppression, etc. Another way of increasing the wireless system throughput is the employment of multiple antennas both on transmitter and receiver sides. Since parallel channels are established over the same time and frequency grid, high data rates without the need of extra bandwidth are achieved [1].This is known as Multiple Input Multiple Output (MIMO) in literature and has been the integral part of some recent state of the art wireless systems such as IEEE 802.11n and LTE.

In OFDM, the bandwidth is divided into a number of orthogonal narrow band subcarriers. The orthogonality of subcarriers is essential to OFDM which imposes some constraints on their spacing. The spacing should be smaller than the coherence bandwidth of the communications channel. An OFDM system is also prone to time variations of the channel. The system, however, is simple to implement and enjoys application of low complexity equalization techniques. Although equalization is rather simple especially when compared to non-OFDM communications systems, appropriate channel parameter estimation is still required to obtain the Channel State Information (CSI). Accurate CSI is crucial for resource allocation, adaptive modulation and coherent detection [2].

LTE is one of the evolved standards which promises a high consistent data rate over the wireless channels. It has already been adapted as the next generation standard for mobile communications. Similarly, DVB-H addresses the need for high multimedia data rates over the wireless communications channels. Operating in a multi-standard environment mobile terminals are soon expected to be able to receive and decode data streams related to these two standards. Thus, it is desirable for them to accommodate the essential hardware/software to handle the requirements of the above mentioned standards. It is also envisaged that a typical terminal will have to decode and process multiple parallel streams corresponding to concurrent handling of LTE and DVB-H data at the same time. As a result, an increased amount of processing power needs to be provided while keeping the power efficiency

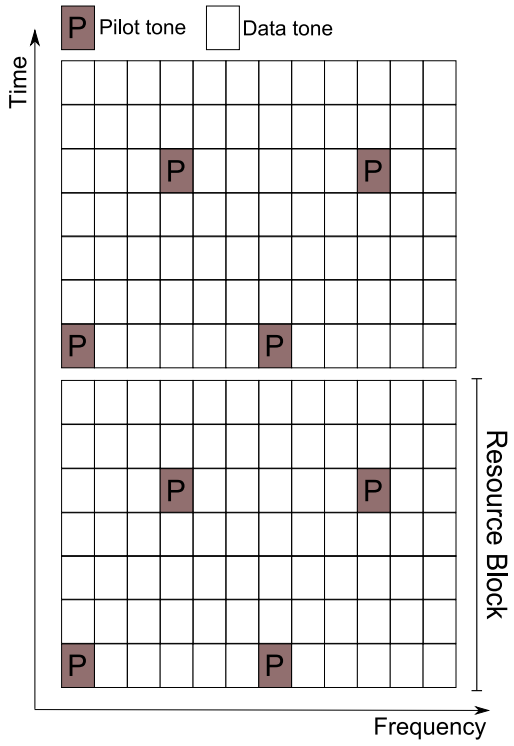

Figure 1: LTE, time-frequnecy grid. Each box corresponds to one Resource Element(RE). A typical Resource Block is composed of 7 OFDM symbols in time and 12 subcarriers.

as much as possible. Since the processing power cannot be surged indefinitely, novel low complexity algorithms need to be investigated in connection with the hardware design. We have probed the channel estimation issues in the scope of this paper. More elaborately, new low complexity methods have been suggested which take both LTE and DVB-H standard requirements into consideration. Although the topic of channel estimation is both well-known and well-investigated to the communications community, the authors have not found many works which address designing flexible estimators that can be tailored to multi-standard processing specifically to support coexisting of both LTE and DVB-H.

To assist channel estimation in DVB-H and LTE, scattered pilots have been allocated throughout the time-frequency grid as defined in the following sections. The pilot pattern is specific to each standard and largely depends on the typical environment the terminal experiences in practice. Although there are differences in the way pilots are scattered for LTE or DVB-H, there are many similarities among them which can be exploited to develop a core estimator. Making good use of the similarities which arise from the inherent nature of the standards, common channel estimators can be developed. The proposed methods in this paper will rearrange the pilots in LTE and DVB-H in such a way they will look similar in structure. As a result, a number of flexible core estimators can be developed which can be equally applied to both standards with minor modifications in some parameters such as FFT

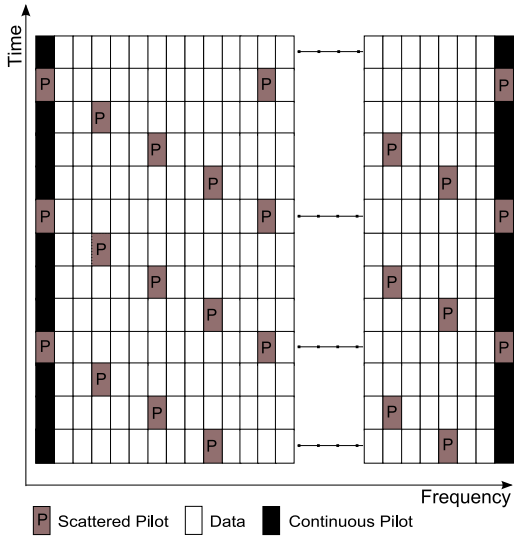

Figure 2: DVB-H time-frequency structure.

size, number of pilots, etc.

2 Standards

The two different standards mentioned in the introduction have individually been designed based on the specific requirements of the environment they are to operate. Even though the standards are both based on OFDM, they embody major differences that need to be independently analyzed. In this section similarities and differences among the standards are highlighted from a channel estimation perspective. Important parameters of interest in this paper are the pilot patterns as well as resource allocations.

2.1 LTE (Long Term Evolution)

Mobile broadband encouraged the specification of LTE which became the basis for the next generation of UMTS Mobile standards [3]. The standard is intended for high data rates of at least 100Mbps in the downlink and 50Mbps in the uplink. It also constitutes flexible carrier bandwidth allocations from below 5MHz up to 20MHz [4] .

The entire downlink chain has been designed to decrease the receiver complexity. Several modes of operation have been designed to adapt to various channel environments. The downlink chain in LTE has the following properties which are of considerable importance when it comes to channel estimation.

2.1.1 Downlink Frame Structure

A time-frequency representation of the available spectrum is called a resource grid [5], where the minimum unit is composed of one subcarrier in one symbol, named

Resource Element (RE). Another important definition is physical Resource Block denoted as RB for simplicity. An RB is a measurement in time and frequency corresponding to 6 or 7 OFDM symbols and 12 subcarriers, refer to Fig. 1.

2.1.2 Resource Allocations

LTE has a channel dependent scheduling [4]. This technique is specially tailored to the needs of low speed terminals. The specific resources are allocated to a terminal in relation to a channel condition measurement reported to the base station. There are three different formats for downlink scheduling assignments but only one of them supports frequency-contiguous allocation [4]. Generally, each terminal is guaranteed at least two consecutive RBs once the access to downlink data is granted. Fig. 1 shows the structure of two RBs and their relative location in the defined time frequency grid.

2.1.3 Pilot Pattern

LTE enjoys application of scattered pilots in the whole time-frequency grid. Being a MIMO system, LTE standardization has specified independent pilot patterns for each antenna port to facilitate parameter estimation. The LTE radio-access specifications refers to antenna ports rather than antennas to emphasize that what is referred to does not necessarily correspond to a single physical antenna [4]. Fig. 1 shows the pilot pattern for antenna port0 [4]. Since scattered pilots do not cover the whole time-frequency grid interpolation/extrapolation techniques should be practiced to derive a good channel estimate. The pilot patterns have been designed to address the need for a maximum attainable spectrum efficiency while satisfying the basic requirements for deriving a consistent channel estimate.

2.2 DVB-H (Digital Video Broadcasting-Handheld)

The Digital Video Broadcasting project (DVB) is an international industry-led consortium committed to the development of technical standards related to Multimedia broadcast. Being an evolution of DVB-T, DVB-H was specifically developed to address the needs of a low power mobile terminal. Some of the characteristics of DVB-H are as follows.

2.2.1 Frame Structure

DVB-H may operate in different modes, e.g., 2K, 4K, 8K. Irrespective of the mode of operation, one frame in DVB-H is defined to constitute 68 OFDM symbols [6]. DVB-H is in fact a broadcast standard and in contrast to LTE, all subcarriers in a symbol carry the information for all User Equipments (UEs). As stated earlier, in LTE data is individually allocated to UEs. Besides, each UE is guaranteed as few as 12 subcarriers in a given symbol.

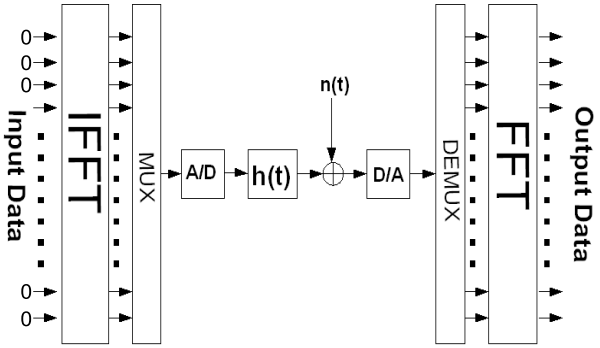

Figure 3: The proposed system model. Zero padding is performed on both sides of input data vector on the subcarriers corresponding to the guard bands.

2.2.2 Pilot Pattern

The pilots are intended to be used for time synchronization, frame synchronization, channel estimation, transmission mode identification and phase noise tracking. Both scattered as well as continuous pilots are transmitted in each symbol. While continuous pilots are primarily used for synchronization, scattered pilots are alloted for channel estimation purposes. Scattered and continual pilot structure are shown in Fig. 2

3 System model

Fig.3 demonstrates a simple baseband OFDM system model. This general description of system fits any of the two standards being investigated in this paper without loss of generality. The uncoded data is modulated through one of the standardized modulation schemes (e.g., 4QAM) and placed on N_c parallel streams where N_c denotes the number of used subcarriers (excluding guard band). The combination of data and pilot subcarriers is fed into an IFFT block to finalize the OFDM modulation. The modulated data is passed through a fading channel with AWGN and OFDM demodulated through a FFT block at the other end. Demodulated data is further processed to decode the transmitted bit stream. To preserve the orthogonality of the subcarriers a Cyclic Prefix (not shown in this system model) with a length equal to the maximum expected delay spread is attached to the OFDM modulated data on the transmitter and discarded before the demodulator on the receiver. We assume perfect synchronization at the receiving side. The data is fed to a channel estimator where data subcarriers indicated by white boxes in Fig.1 and 2 need to be estimated using the available scattered pilots.

4 Channel estimation

Depending on the designated pilot pattern there are many approaches towards channel estimation for OFDM-based systems. Taking the fact that scattered pilots are

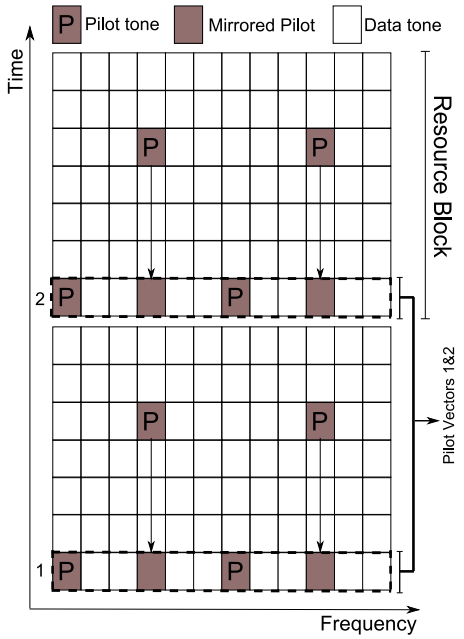

Figure 4: LTE, time-frequency grid. Mirrored pilots are collected from other symbols to create the pilot vectors used in the estimators. Pilot vector 1 is used for estimation over all subcarriers in RB1 while pilot vector 2 is used for estimation over all subcarriers in RB2. The arrows indicate how the pilots from future symbols are reflected into the pilot vectors.

standardized for the channel estimation in LTE as well as DVB-H into account, a number of estimation/interpolation techniques can be applied for channel estimation purposes in these systems. As already discussed in the previous section, Fig.1 and 2 illustrate how the pilots are placed in the time-frequency grid for these two standards. Probably the best as well as the most complicated linear approach is the application of a 2-D Wiener filtering [7]. Yet, the mentioned estimator can be broken into two 1-D filters [7] to reduce the complexity. The 1-D filters correspond to separate MMSE estimations one in time and the other in frequency directions. The estimation in time is a function of channel variations in time. The variations of channel taps over time can be described by the Doppler spread, D_{s}. Meanwhile the Doppler spread shapes the spectrum [8] and affects the correlation properties of the channel taps over time. Thus, the coherence time (T_{c}) of a wireless channel can be defined as the interval over which the channel taps don't change significantly [9] given as,

$$T_{\mathrm{c}} = \frac{1}{4D_{\mathrm{s}}} \tag{4.1}$$

where D_{s} is the Doppler spread in the channel. This definition is a somewhat imprecise definition since the significant changes might belong to those taps which have lower energy [9] or vice versa. It is expected that the correlation between two realizations of a typical tap almost disappears beyond the coherence time.

Considering the restrictions wrapped around the coherence time, only the pilots

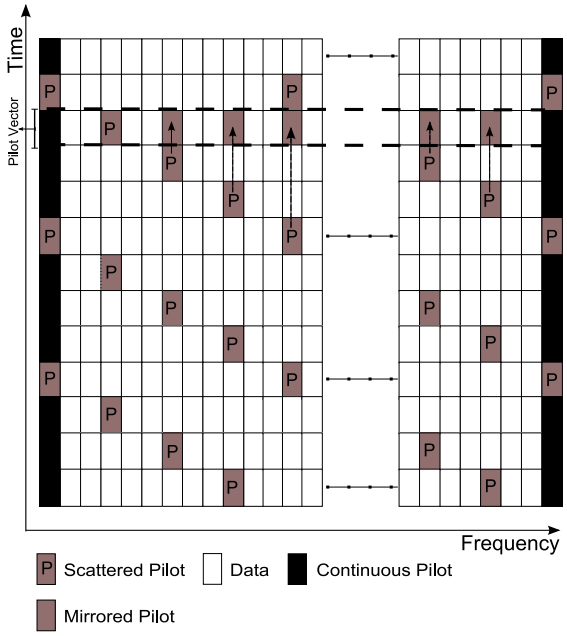

Figure 5: DVB-H time-frequency structure. Mirrored pilots are collected from the past three symbols to create the pilot vectors used in the estimators. Contrary to LTE, each pilot vector in DVB-H is used to estimate only one OFDM symbol (the current symbol).

in the vicinity of the estimated channel attenuations should be used. The time window in which the above mentioned method works shrinks as the Doppler spread increases. The Doppler spread can be described by the equivalent terminal speed relative to the transmitter (base-station). As the equivalent speed increases, the coherence time decreases which results in lower correlation among subsequent channel realizations. There are a number of proposed approaches to exploit the time correlation of various channel realizations. If the second-order channel statistics are known, MMSE methods can be used to estimate/interpolate the pilots in time. For instance, a robust MMSE estimator similar to the one applied for estimation in frequency (as described in the following sections) can be used in time as well.

In our proposed approach, however, we have resorted to a simple method which does not involve any estimations/interpolations in time. In fact, pilots from a number of neighboring symbols are collected and used to improve the channel estimation. This has been done presuming stationary channel environment and as a result works well in scenarios with low Doppler spreads. We have used the term mirrored pilots referring to the ones collected from the neighboring symbols and inserted to the pilot vectors used in the estimators. The mentioned pilot vectors as depicted in Fig. 4 and Fig. 5 also contain the existing pilots in each symbol.

To carry out the estimation in LTE the pilots from symbols 1 and 5 in each RB are combined into a single pilot vector as depicted in Fig. 4. This pilot vector is subsequently fed into the proposed channel estimators. The derived estimation will be used for the whole OFDM symbols corresponding to that RB. Considering

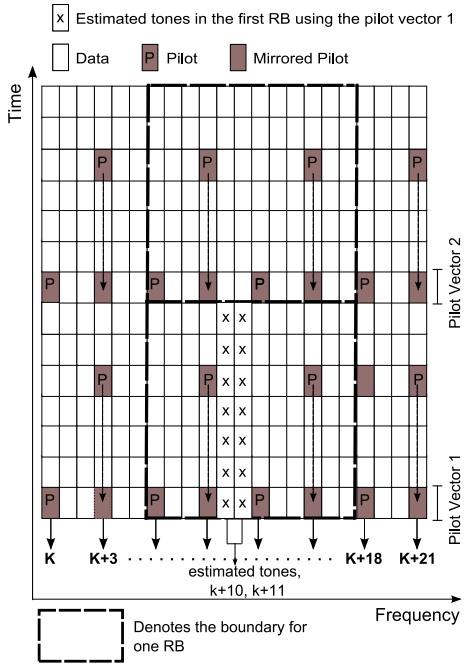

Figure 6: Subcarrier estimation in LTE using only 8 pilots. Pilots from future symbols are mirrored to the current symbol to assist the channel estimation. The UE has access to all the pilots in each symbol irrespective of its allocated RBs. MRMMSE with 8 pilots can be used to carry out the estimation.

the definition of the coherence time as explained previously, it is expected that this method works for slow fading channels or in other words in channels characterized with low Doppler. Furthermore, the farther the pilots are located from a target symbol for estimation the lowest the cross-correlation they exhibit. As a result, the largest Mean Squared Error (MSE) is expected for OFDM symbol 7 in each RB, as it is furthest away from the pilots used in the estimation. Being the worst-case scenario, the derived Mean Squared Error as well as uncoded BER have been derived for symbol 7 as demonstrated in the simulations section.

The proposed approach is characterized with some drawbacks. For instance, data decoding for each symbol cannot initiate until the 5th symbol in each RB has been received and its pilots collected (mirrored). Thus, decoding has to be postponed until the pilot-assisted channel estimation is carried out using the pilots collected from symbols 1 and 5 in each RB. The associated memory overhead is expected to be acceptable specially for the noncontiguous resource allocation in LTE.

Similarly, to estimate a symbol in DVB-H, the pilots from other symbols are mirrored to facilitate the channel estimation. In other words, the pilots from the past three OFDM symbols are saved in memory and consequently mirrored to the current symbol for the estimation purposes. Thus, the largest distance between the mirrored pilots and the current symbol is three OFDM symbols. Fig. 5 shows how the symbol identified by the dashed line is estimated through collection of pilots from the current as well as the past three symbols. It can be seen from the figure that the

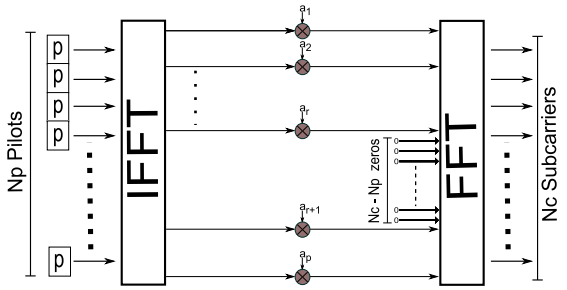

Figure 7: The DFT-based estimator structure for the proposed estimators DFT-A, DFT-B, DFT-C. The elements in **a** will be all ones in case of DFT-A.

resulting pilot spacing in frequency will be three subcarriers after the appropriate pilots have been mirrored. This is quite similar to the witnessed pilot pattern in the attained pilot vector in LTE. Refer to Fig. 4 and Fig. 5 to see how the derived pilot vectors compare. In comparison to LTE, it is expected that application of this method to DVB-H does not affect the quality of the estimators as adversely in high Doppler scenarios. Besides, decoding of received symbols can immediately start (provided that the UE has already collected the pilots from the past three symbols) and the terminal does not need to wait for the additional pilots from the future symbols.

Having collected the desired pilots in time, data subcarriers need to be estimated in the frequency direction. Among the various investigated methods ML, MMSE [10] and DFT-based [11] estimators are examples of estimation algorithms. Our approach in this paper is the application of modified variants of MMSE and DFT-based estimators. There are benefits to simplified estimators for a low power mobile terminal due to the restricted amount of available processing power. If the estimators can benefit from the commonly available hardware on the platform, like FFT blocks or baseband processors, allocation of extra resources dedicated to channel estimation becomes minimal.

4.1 MMSE estimator

The best linear estimator in terms of Mean Squared Error is the Linear Minimum Mean Squared Error Estimator (LMMSE) [7]. Given the transmitted symbols $\mathbf{X}$ and recieved symbols $\mathbf{Y}$, under certain conditions the simplified MMSE estimation of the channel $\mathbf{h}$ can be expressed as [12],

$$\hat{\mathbf{h}}_{\text{mmse}} = \mathbf{R}_{\text{hh}}(\mathbf{R}_{\text{hh}} + \frac{\beta}{\text{SNR}}\mathbf{I})^{-1}\hat{\mathbf{h}}_{\text{ls}} \tag{4.2}$$

where

$$\hat{\mathbf{h}}_{\text{ls}} = \mathbf{X}^{-1}\mathbf{Y} \tag{4.3}$$

is the Least Squares estimate of the channel attenuations $\mathbf{h}$, $\mathbf{R}_{\text{hh}}$ is the autocorrelation of the channel, $\text{SNR} = E|x_k|^2/\sigma^2$ is the signal-to-noise ratio and β is a constant

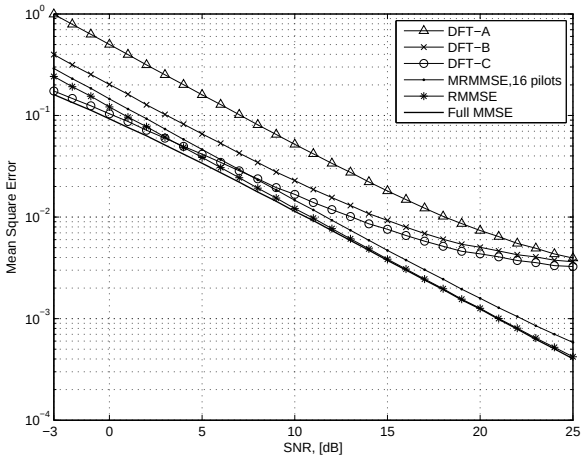

Figure 8: LTE, MSE performance in a stationary environment.

which depends on the signal constellation of transmitted symbols, $\mathbf{X}$. For a 4QAM modulation scheme β equals 1.

In systems where scattered pilots are used to assist channel estimation the above equation may be rewritten as,

$$\hat{\mathbf{h}}_{\text{mmse}} = \mathbf{R}_{\text{h}_\text{m}\text{h}_\text{p}}(\mathbf{R}_{\text{h}_\text{p}\text{h}_\text{p}} + \frac{\beta}{\text{SNR}}\mathbf{I})^{-1}\hat{\mathbf{h}}_{\text{p,ls}} \tag{4.4}$$

where $\mathbf{X}_\text{p}$ and $\mathbf{Y}_\text{p}$ are the transmitted and received data sampled on the pilot positions and,

$$\hat{\mathbf{h}}_{\text{p,ls}} = \mathbf{X}_\text{p}^{-1}\mathbf{Y}_\text{p} \tag{4.5}$$

is the Least Squares estimate of the channel attenuations $\mathbf{h}_\text{p}$ on the pilot tones, $\mathbf{R}_{\text{h}_\text{p}\text{h}_\text{p}}$ is the autocorrelation of the sampled channel $\mathbf{h}_\text{p}$ on pilot positions and $\mathbf{R}_{\text{h}_\text{m}\text{h}_\text{p}}$ is the cross correlation matrix between the pilot tones and the data subcarriers.

The above equation system shows that for a channel containing N_p scattered pilots we need to have access to the second order channel statistics as well as the noise variance at any given time. Moreover, a matrix inversion of $N_\text{p} \times N_\text{p}$ should be carried out for any given SNR and a matrix calculation of $N_\text{m} \times N_\text{p}$ is required to the interpolation over N_m data subcarriers. Thus, this estimator exhibits considerable complexity [12].

4.2 Robust MMSE (RMMSE) estimator

As its name implies, RMMSE is designed to provide robustness of estimation for various channel realizations. It should provide an acceptable performance irrespective of the environment in which the UE is about to operate. For this purpose, the estimator could be designed for a worst-case scenario and its performance compared to the full MMSE. It can be shown [13] that this estimator preforms well under certain conditions. In this paper, we have chosen a uniform Power Delay Profile

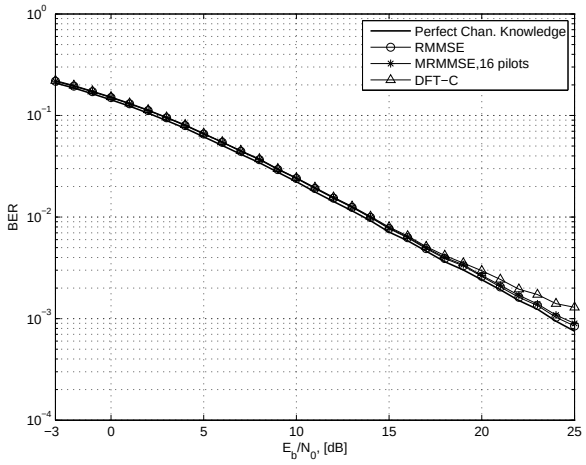

Figure 9: LTE, uncoded BER performance for 4QAM in a stationary environment.

(PDP) where all the channel taps are equally strong. The length of the channel has been set to the length of the Cyclic Prefix. Consequently, the required correlation matrices , $\mathbf{R}_{\mathrm{h_m h_p}}$ and $\mathbf{R}_{\mathrm{h_p h_p}}$ can be precalculated. Meanwhile, it has been shown [12] that the performance loss is relatively acceptable for the lower SNRs if the estimator is designed for the maximum SNR the system is expected to experience in practice. Our simulation results also prove this point. Having fixed SNR in equation 4.4 the required matrices can be precalculated and stored in memory. Since large matrix inversions in 4.4 can be avoided the terminal can save a lot of processing as well as battery power. In fact, the RMMSE estimator reduces the complexity to a mere matrix multiplication of size $N_{\mathrm{m}} \times N_{\mathrm{p}}$.

4.3 Modified Robust MMSE (MRMMSE) estimator

Channel estimation using a RMMSE estimator makes use of all the pilot tones allocated to an OFDM symbol and is still a rather costly approach when it comes to hardware implementations. The implementation cost becomes even more crucial when the number of pilots grows like in 8K DVB-H mode of operation where each symbol constitutes at least 568 pilots. As a result, we have investigated alternative approaches to the RMMSE estimator. To estimate each subcarrier only a few pilots in the vicinity of that subcarrier might be used. Fig. 6 illustrates how, e.g., 8 pilots in the vicinity of two subcarriers k+10 and k+11, can be used and fed into the MRMMSE to carry out the channel estimation. In other words, exploiting the correlation for the full extent of the frequency axis might be of little use specially when the estimator is designed for a worst-case PDP. The autocorrelation of a system having a uniform PDP illustrates low correlation among subcarriers which are located far apart. We have exploited this feature to develop an estimator which uses only 16 neighboring pilots for estimation of each tone. As a result, in the proposed MRMMSE, $R_{\mathrm{h_p h_p}}$ is a matrix of size 16×16. The pilots are preferably

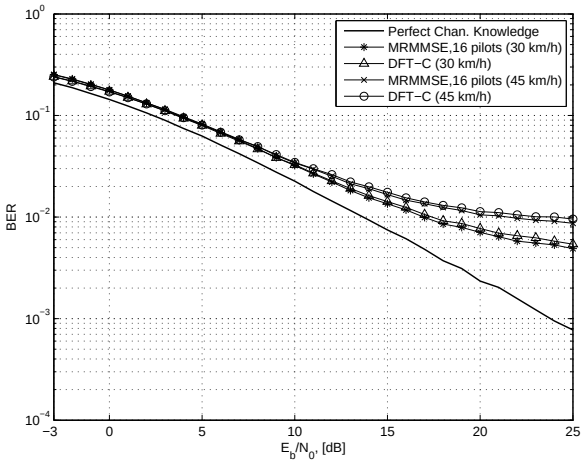

Figure 10: LTE, uncoded BER performance for 4QAM corresponding to two different terminal speeds. Simulations have been done for OFDM symbol 7 in a typical RB which represents the worst-case scenario due to its low correlation with the constructed pilot vector.

selected symmetrical with respect to the estimated tone. As stated earlier, not only the pilots in the present symbol are used for estimation but also the pilots from other symbols as depicted in Fig. 4 and Fig. 5 are mirrored to improve the performance. This novel rearrangement of pilots proves to be performing well for low and medium terminal speeds. This has been proved through simulations as illustrated in the following sections. [1]

4.4 DFT-based estimators

In OFDM systems where scattered pilots are used for channel estimation IDFT/DFT interpolation is one of the alternative approaches towards channel estimation. In these estimators the interpolation over all used subcarriers is obtained by [14],

$$\hat{\mathbf{h}}_{\mathrm{IDFT}} = \frac{1}{N_{\mathrm{p}}} \mathbf{F}_{\mathrm{L}} \mathbf{F}_{\mathrm{P}}^{H} \hat{\mathbf{h}}_{\mathrm{p,ls}} \tag{4.6}$$

where N_{p} is the number of pilots $\mathbf{F}_{\mathrm{L}}$ is a $N \times L$ matrix constructed by taking the first L columns of the full $N \times N$ Fourier transform matrix and $\mathbf{F}_{\mathrm{P}}$ is a subset of the Fourier transform matrix on the pilot positions where N is the FFT size of the system.

Since the Least Squares approach is applied to obtain noisy estimations of the pilot subcarriers denoted as $\hat{\mathbf{h}}_{\mathrm{p,ls}}$, the interpolation over all subcarriers will produce

[1] In this paper we have dropped the merged-pilot for MRMMSE and RMMSE estimators simply because all the simulations have been carried out while merging the pilots. Thus, RMMSE and MRMMSE estimators mentioned in this paper correspond to merged-pilot RMMSE and merged-pilot MRMMSE estimators respectively.

noisy estimates of the channel subbands. This will result in a relatively high noise floor which will end up in high Bit Error Rate after equalization. The associated error covariance matrix can be derived as [14],

$$\hat{\mathbf{C}}_{\mathrm{H_{IDFT}}} \approx \frac{1}{N_{\mathrm{p}}} {\sigma_{H_{\mathrm{p}}}}^2 \mathbf{F}_{\mathrm{L}} {\mathbf{F}_{\mathrm{L}}}^H \tag{4.7}$$

where ${\sigma_{H_{\mathrm{p}}}}^2$ is the variance of the AWGN on the pilot subcarriers. The above equation indicates that the error covariance is a function of noise variance which will be reflected into the estimation results if no measures are taken to reduce its effect. Referred to as DFT-A estimator this method has been used in the context of channel estimation in this paper.

Table 1: LTE,simulated system parameters

FFT size	512	$\delta f, [kHz]$	15
CP length,[n]	36	Used tones	300
Pilots/Symbol	50	PDP	$exp(-t/\tau_{\mathrm{rms}})$
Carrier Freq.,[GHz]	2.6	Doppler Spec.	Two-dimensional, Jake's

There are a handful of methods to remove the noise and decrease its variance in the system. One simple low complex way (we call that DFT-B estimator) is to capture the high energy taps of the channel after the IDFT and zero out the rest [11]. This is equivalent to a simple vector multiplication. The time-domain representation of noisy pilots fed into an IDFT of size N_{p} is,

$$\hat{\mathbf{g}}_{\mathrm{ls}} = \mathrm{IDFT}(\hat{\mathbf{h}}_{\mathrm{p,ls}}) \tag{4.8}$$

Furthermore, the estimated channel can be described as,

$$\hat{\mathbf{h}}_{\mathrm{IDFT}} = \mathrm{DFT}(\hat{\mathbf{g}}_{\mathrm{ls}} \times \mathbf{a}) \tag{4.9}$$

where vector $\mathbf{a} = [a_1 a_2 ... a_p]$ is a smoothing vector and the DFT size is equal to the number of used subbands, N_c as depicted in Fig. 7. Due to the nature of wireless channels the energy is usually concentrated in the first few taps. In case of sample-spaced channels the energy is perfectly confined in a limited area in the beginning of the CIR. In case of the nonsample-spaced channels, part of this energy is leaked outside this area [11]. If the energy is confined to an area corresponding to the first r taps and the last q taps(which is due to cyclic nature of the DFT), the elements in vector $\mathbf{a}$ will be modified as follows,

$$\mathbf{a} = [a_1\ a_2 ... a_r\ 0\ 0 ... 0\ a_{p-q} ... a_p] \tag{4.10}$$

where all nonzero elements in the above vector will be equal to 1. Fig. 7 shows the general estimator structure we are using for our DFT-based estimators. The amount of time-domain processing after IDFT in DFT-B method is minor since it is limited to discarding the low energy channel taps and keeping the high energy ones [11].

Another low complexity DFT-based estimator (denoted as DFT-C estimator) is to weight each channel tap by the following factor [11],

$$\frac{{\gamma_i}^2}{{\gamma_i}^2 + {\sigma_{H_\mathrm{p}}}^2} \tag{4.11}$$

where ${\gamma_i}^2$ is the tap energy and ${\sigma_{H_\mathrm{p}}}^2$ is the noise variance. Thus, vector $\mathbf{a}$ will have N_p nonzero elements each corresponding to a weighting factor. This factor suppresses the noise energy on the channel taps and gives higher weight to useful signal energy. This estimator has a higher complexity compared to DFT-B which is proportional to the number of pilots. Weighting the taps in time-domain will introduce $3 \times N_\mathrm{P}$ additional real multiplications compared to DFT-A and DFT-B. The performance/complexity trade-off, however, proves worthy specially when operating in lower SNR range as illustrated in the simulations section.

5 Hardware implementation issues

Due to the availability of FFT/IFFT blocks on an OFDM-based UE, it is beneficial to apply methods which might use the available hardware provided that it does not jeopardize its accessibility to more critical system components (e.g., OFDM demodulator, etc.). Since the focus of this paper is on algorithmic design, we will leave the detailed analysis of hardware implementation issues to future work. The nature of typical OFDM systems like LTE and DVB-H requires FFT transforms of sizes other than radix 2. Thus, the mixed-radix FFT blocks have to be used instead. A number of these FFT blocks have been proposed in literature [15]. In this paper we have suggested application of a well-known mixed-radix Cooley-Tuckey algorithm which has the radices 2,3 and 5. This suffices the requirements of our proposed implementation for LTE and DVB-H. The block involves the following computations for an FFT size of N [15],

$$N = 2^p \times 3^q \times 5^r \tag{5.1}$$

$$A(N) = 2N(\frac{3}{2}p + \frac{8}{3}q + 4r - 1) + 2 \tag{5.2}$$

$$M(N) = 2N(p + 2q + \frac{14}{5}r - 2) + 4 \tag{5.3}$$

$$A(N) + M(N) = 2N(\frac{5}{2}p + \frac{14}{3}q + \frac{34}{5}r - 1) + 2 \tag{5.4}$$

where $M(N)$ and $A(N)$ denote the number of real multiplications and additions. To measure the complexity of the proposed algorithms we have resorted to the corresponding number of required multiplications. The above mentioned mixed-radix FFT suits the LTE DFT-based estimators without any further modifications. The number of pilots in different modes of LTE can be always broken into $N_\mathrm{p} = 2^p \times 5^r$. Moreover, using the proposed pilot rearrangement in this paper the number of subcarriers will always be 3 times as many as the number of pilots which brings about the resulting number fed to the IFFT block being factorized into radices 2,3

Table 2: LTE, estimator complexity, number of real multiplications per OFDM symbol. N_{RB} refers to the number of allocated RBs

Estimator	Total Complexity	Complexity Per RB
RMMSE	75,000	3,000
MRMMSE	12,000	480
DFT-B	5,688	$\frac{5,688}{N_{\mathrm{RB}}}$
DFT-C	5,988	$\frac{5,988}{N_{\mathrm{RB}}}$

Table 3: LTE, required SNR to maintain a constant uncoded BER = 10^{-2} for a number of terminal speeds. Simulations are associated with OFDM symbol 7 in a typical RB. The figures have been derived from MRMMSE simulation results.

Speed, [km/h]	Doppler spread, [Hz]	SNR, [dB]
10	48	14.8
20	96	15
30	144	17
40	192	20
45	217	21
48	231	30
50	241	N.A.

and 5. Quite contrary to LTE, the standard number of pilots in DVB-H does not allow a mixed-radix FFT as mentioned above. For instance in 2K mode, the number of pilots in each symbol is 142 which after rearrangement (mirroring) the collected number of pilots in the pilot vector will be 568 that cannot be factorized into the desired radices (2,3 and 5). Thus, it is not possible to directly apply the desired FFT block in this paper for DFT-based channel estimation in DVB-H. To overcome this obstacle, we have extrapolated a minimum number of pilots outside the used band such that the resulting number of total pilots can be factorized into the desired radices. As a result, 8, 16 and 32 pilots (distributed symmetrically on each side of the used band) need to be extrapolated corresponding to 2K, 4K and 8K modes of operation in DVB-H. For the purposes of simulations in this paper we have resorted to the proposed MMSE channel estimation methods (MRMMSE) to extrapolate 8 pilots in the unused subband of DVB-H which makes the total number of pilots in the pilot vector be factorized as follows,

$$576 = 2^6 \times 3^2 \tag{5.5}$$

From a complexity overhead view point, the required additional processing for extrapolation is negligible compared to the whole. A comparison among the complexity requirements of the algorithms has been provided in the simulation section. We are, however, aware that to extrapolate the desired pilots, estimators with a better MSE performance exist compared to what we have applied here. These estimators can

be precalculated and fetched from memory when needed. Yet, we have resorted to the estimators proposed in this paper since they provide acceptable performance as evidenced in the simulations section and eliminate the need for added complexity.

To address the computational needs of the MMSE-based algorithms, a pool of fast multipliers can be harnessed. In an efficient implementation each complex multiplication is carried out by 3 real multiplications. Similarly, a baseband processor can provide the necessary processing power. The mentioned resources are usually available as standard components on a typical OFDM-based UE and can be exploited for the purposes of channel estimation.

Table 4: DVB-H, simulated system parameters

FFT size	2048	$\delta f, [kHz]$	4.464
CP length,[n]	63	Used tones	1704
Pilots/Symbol	142	PDP	$exp(-t/\tau_{\text{rms}})$
Carrier Freq.,[MHz]	500	Doppler Spec.	Jake's Spectrum

6 Simulation results

6.1 LTE

The LTE simulation system parameters were chosen according to Table 1. To illustrate the performance of the estimators, the widely used Mean Square Error as well as the Bit Error Rate measures have been used. Furthermore, no coding or interleaving schemes have been adopted. Thus, illustrated BERs correspond to uncoded data. Besides, the BER simulations have been carried out for a SISO system so that a fair comparison can be done among the performance of the estimators for both LTE and DVB-H. Fig. 8 shows how our estimators perform in a Mean Square Error sense for LTE.

As mentioned earlier, full MMSE estimator is the best existing linear estimator. As a result, it has been selected as the reference against which other estimators are compared. As expected, DFT-A estimator has the worst performance amongst our proposed estimators due to its redundant noise variance both in low and high SNRs. DFT-C performs best in low SNRs due to its capability to remove the additive noise and capture the useful energy of the channel taps. The RMMSE as well as the MRMMSE estimators display an acceptable performance in the MSE sense over the whole SNR range.

Having discarded DFT-A and DFT-B, Fig. 9 depicts the performance of DFT-C, RMMSE and MRMMSE estimators from a BER view point. It can be seen that the vivid MSE differences occurring in the high SNR region shrink from a BER point of view when the simulations are done for 4QAM data modulation. The estimators have comparable performances for a stationary environment (no Doppler). Having a relatively equal performance, the RMMSE can be also eliminated due to its complexity as elaborated in Table 2. Figure 10 displays the BER performance of DFT-C and MRMMSE for two different environments. The environments have

Table 5: DVB-H, required SNR to maintain a constant uncoded BER = 10^{-2} for a number of terminal speeds. The figures have been derived from MRMMSE simulation results.

Speed, [km/h]	Doppler spread, [Hz]	SNR, [dB]
10	9	14
50	46	14.8
100	92	15.4
150	139	17
190	176	22
200	185	24
210	194	N.A.

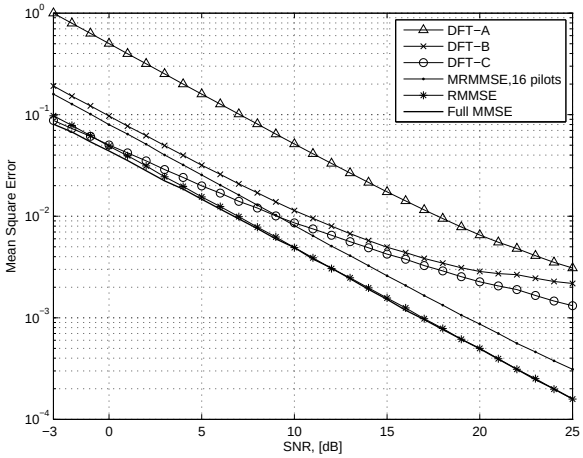

Figure 11: DVB-H, MSE performance in a stationary environment.

been simulated using the classical Jake's model [8] [16] as a reference. The variations in this environment are simulated as an equivalent terminal speed. It can be seen that the decreased coherence in time can be partially compensated by increasing the Signal-to-Noise-Ratio. A quick look at Table 3 reveals the fact that it is not possible to maintain a target uncoded BER = 10^{-2} when the terminal speed reaches a breaking threshold value.

The result of our simulations suggest a terminal speed of around 50 km/h as the breaking value. Any attempts to sustain the uncoded BER above this speed fails even if the SNR is increased indefinitely. As discussed previously, the above mentioned effect is mainly the result of the correlation loss among realizations of channel taps due to the Doppler spread.

One should, however, consider the fact that the simulations have been done for the worst-case scenario (OFDM symbol 7) and it is expected that on average the breaking value for the terminal speed increases. For instance, our uncoded BER simulations for OFDM symbol 1 indicates a speed of 90km/h as the breaking threshold. We also know from experience that a mobile UE rarely operates in fast fading channels characterized by high terminal speeds and as a result a top speed of

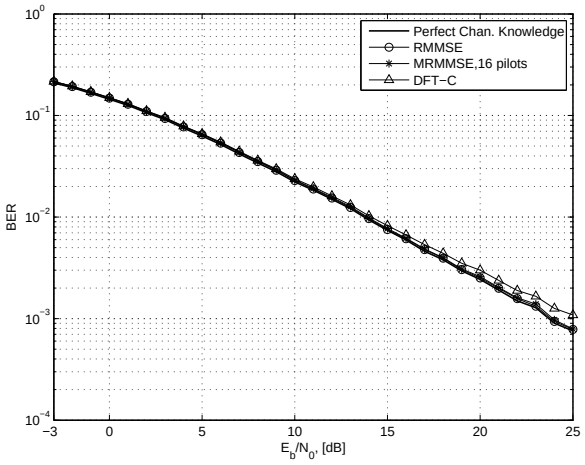

Figure 12: DVB-H, uncoded BER performance for 4QAM in a stationary environment.

around 50 km/h satisfies the user needs in a majority of situations. It should also be pointed out that no coding/interleaving schemes have been used in the simulations and the system might perform better if the complete chain as standardized in LTE and DVB-H is implemented.

The complexity of DFT-based methods depend on the total number of available pilots corresponding to the LTE mode of operation. For the system simulated in this paper 100 scattered pilots have been used. Table 2 shows the required number of multiplications to estimate the channel for the complete set of subcarriers corresponding to each OFDM symbol. The figures suggest that these estimators have a lower complexity compared to their MMSE counterparts. However, the overall cost of these estimators increases in the mean sense for LTE. The underlying reason can be described by the fact that the resource allocation in LTE is not always contiguous. As stated earlier, as few as two consecutive Resource Blocks (RB) -one RB in each symbol- can be allocated to each terminal. That alone implies the redundancy of using the proposed DFT-based methods since they do the estimation over all subccariers in each symbol. On the other hand, MRMMSE estimator proves to provide a lower complexity in the mean sense since the complexity is a function of the number of estimated subcarriers (allocated RBs). The estimation complexity can be described and quantized on the basis of per Resource Block (RB). While the complexity of DFT-based estimator remains the same irrespective of the allocated number of subcarriers, the MRMMSE estimator's complexity can range from 480 to 12,000 multiplications per RB.

6.2 DVB-H

The DVB-H simulation system parameters were according to Table 4. The simulation environment has been modeled similar to LTE except for the parameters which are specific to DVB-H like PDP length, etc. Furthermore, MSE as well as

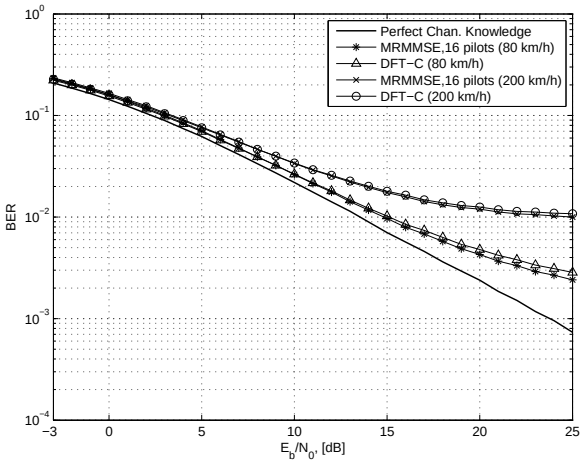

Figure 13: DVB-H, uncoded BER performance for 4QAM corresponding to two different terminal speeds.

BER have been used as measures of estimator performance. Fig. 11 shows the MSE performance while Fig. 12 displays the BER results for the proposed estimators in a stationary environment. Similarly, we can witness the quality of these estimators under varying channel conditions as depicted in Fig. 13. Analogous to LTE, we have investigated the BER breaking terminal speed for the proposed algorithms.

Table 6: DVB-H, estimator complexity, number of real multiplications per OFDM symbol

Estimator	Complexity
RMMSE	2,661,648
MRMMSE	74,976
DFT-B	44,168
DFT-C	45,896

The results in Table 5 expose us to the fact that these algorithms perform well for a larger range of terminal speeds when applied to DVB-H. This can be partly described by the lower carrier frequency in DVB-H as well as the used pilot structure. Contrary to LTE, DFT-based estimators provide lower complexity when compared to MRMMSE for DVB-H systems. This is largely due to the fact that DVB-H is a broadcast scheme in which each terminal needs to decode the entire subcarriers in each OFDM at a time. Thus, the terminal needs to estimate all the data subccariers to decode the received data. Table 6 reveals the required complexity for each estimator. Hence, the DFT estimators provide a lower complexity in contrast with MRMMSE.

7 Conclusion

In this paper, a number of novel methods have been proposed to address the channel estimation needs for a mobile terminal operating in a multi-standard environment. Exploiting pilots in past/future symbols makes a core estimator plausible. The resultant pilot spacing for both LTE and DVB-H provides the opportunity to design a single estimator. These estimators have a relatively low computational complexity when compared to other investigated methods. The coexistence of these two low complexity estimators can provide the reliability and flexibility needed for the LTE as well as DVB-H systems. These estimators, however, lose their performance when significant changes in the environment (as a function of Doppler spread) occur specially for LTE. Considering the fact that UEs on average operate in a low terminal speed range as well as the reduced complexity which is gained by applying these estimation methods, the performance loss due to Doppler spread becomes acceptable in many situations. Meanwhile, these estimators perform well for relatively high terminal speeds when implemented for DVB-H which is mainly the result of the standardized pilot pattern as well as lower carrier frequency. Thus, the overall performance of these estimators when applied to fast fading channels becomes acceptable when both LTE and DVB-H are taken into consideration.

To improve the performance of these estimators for higher Doppler spreads in LTE, low complexity estimation techniques need to be applied to track the channel variations in time. Designing new estimators as such does not void the application of the proposed estimators in this paper. They will appear as added computational overhead which is due to time-domain filtering for LTE.

References

[1] M. Ozdemir and H. Arslan, "Channel estimation for wireless OFDM systems," *Commun. Surveys Tuts., IEEE*, vol. 9, pp. 18–48, July 2007.

[2] P. Fertl and G. Matz, "Multi-user channel estimation in OFDMA uplink systems based on irregular sampling and reduced pilot overhead," in *Proc. IEEE Int. Conf. Acous., Speech and Signal Process.,* Honolulu, HI, pp. III.297–III.300, 2007.

[3] "LTE: An introduction [Online]," Ericsson AB, 2011. Available: http://www.ericsson.com/res/docs/2011/lte-an-introduction.pdf.

[4] E. Dahlman et al., *3G Evolution, Second Edition: HSPA and LTE for Mobile Broadband*. Burlington, MA: Academic Press, 2008.

[5] "Evolved Universal Terrestrial Radio Access (E-UTRA); Physical layer procedures (Release 8)," 3rd Generation Partnership Project, Tech. Specifications 3GPP TS 36.213, May 2008. Available: http://www.3gpp.org/ftp/Specs/html-info/36213.htm.

[6] "Digital Video Broadcasting (DVB); Framing structure, channel coding and modulation for digital terrestrial television," European Telecommunications Standards Institute (ETSI), Tech. Specifications Final Draft, 2004.

[7] O. Edfors, *Low-complexity algorithms in digital receivers*. PhD thesis, Div. of Signal Process., Luleå Univ. of Technology, Luleå, Sweden, 1996.

[8] M. Gans, "A power-spectral theory of propagation in the mobile-radio environment," *IEEE Trans. Veh. Technol.*, vol. 21, pp. 27–38, Feb. 1972.

[9] A. Goldsmith, *Wireless communications*. New York, NY: Cambridge University Press, 2005.

[10] M. Morelli and U. Mengali, "A comparison of pilot-aided channel estimation methods for OFDM systems," *IEEE Trans. Signal Process.*, vol. 49, pp. 3065–3073, Dec. 2001.

[11] O. Edfors, M. Sandell, J.-J. van de Beek, S. K. Wilson, and P. O. Börjesson, "Analysis of DFT-based channel estimators for OFDM," *Wireless Personal Communications*, vol. 12, no. 1, pp. 55–70, 2000.

[12] O. Edfors et al., "OFDM channel estimation by singular value decomposition," *IEEE Trans. Commun.*, vol. 46, pp. 931–939, July 1998.

[13] V. Srivastava et al., "Robust MMSE channel estimation in OFDM systems with practical timing synchronization," in *Proc. IEEE Wireless Commun. and Netw. Conf.,* Atlanta, GA, pp. 711–716, 2004.

[14] S. Omar, A. Ancora, and D. Slock, "Performance analysis of general pilot-aided linear channel estimation in LTE OFDMA systems with application to simplified MMSE schemes," in *Proc. IEEE 19th Int. Symp. Personal, Indoor and Mobile Commun.,* Cannes, pp. 1–6, 2008.

[15] D. Takahashi and Y. Kanada, "High-performance radix-2, 3 and 5 parallel 1-D complex FFT algorithms for distributed-memory parallel computers," *The J. of Supercomputing*, vol. 15, pp. 207–228, Feb. 2000.

[16] D. Young and N. Beaulieu, "The generation of correlated rayleigh random variates by inverse discrete Fourier transform," *IEEE Trans. Commun.*, vol. 48, no. 7, pp. 1114–1127, 2000.

Low-complexity channel estimation for LTE in fast fading environments for implementation on multi-standard platforms

Farzad Foroughi Abari, Farnaz Sharifabad, and Ove Edfors

Paper II

Abstract

In this paper a number of low-complexity channel estimator structures tailored to the needs of LTE terminals have been investigated. The focus has been on the algorithms exhibiting reduced complexity while providing an acceptable level of performance. To design these estimators other factors such as interoperability with another OFDM-based standard, DVB-H, in a multi-standard environment have been taken into account. The key underlying parameter has been exploiting the pilot pattern in LTE providing the possibility of minimal filtering in time domain while exhibiting an acceptable level of performance in fast fading environments.

1 Introduction

Providing a multiple-access scheme, Orthogonal Frequency Division Multiplexing (OFDM) has replaced many of the traditional single carrier alternatives where data is encapsulated in symbols which are usually shorter than the time span of the physical channel. As a result, the communication over single carrier systems is usually prone to Inter Symbol Interference (ISI) and needs complicated equalization structures to reliably retrieve and decode the data on the receiver side.

In an OFDM based systems, however, data is modulated on a number of subcarriers which occupy a predefined BandWidth (BW). The system is designed in such a way that subcarrier spacing is chosen to be smaller than the coherence bandwidth of the channel. As a result, simple equalization techniques can be carried out on the receiver side. The system, however, can suffer from Inter Carrier Interference (ICI) which results from the fast fading channel environments. To counter this problem, the symbol time in OFDM systems is designed to be shorter than the coherence time of the physical channel. Contrary to single carrier systems, parallel data multiplexing in the downlink for a number of User Equipments (UE) is rather simple in OFDM. The original idea of OFDM dates back to 1966 [1] but implementing the system was cumbersome due to technology shortcomings. The advances in digital signal processing and circuit design, however, have enabled practical realization of OFDM systems in recent years.

Initially, OFDM systems were used in combination with Single-Input-Single-Output systems (SISO) such as Digital Audio Broadcast (DAB). With the introduction of Multiple-Input-Multiple-Output (MIMO), opening a new horizon in the area of digital communications, new standards benefiting from the combination of both OFDM and MIMO emerged into the telecommunications world. The application of multiple antennas on both transmitter and receiver enables the system to enjoy various diversity, multiplexing and beam forming schemes.

Long Term Evolution (LTE) has been opted as the 4th generation standard for mobile wireless communications. LTE combines both OFDM and MIMO in downlink to materialize the desired data rates of up to 100 Mbits/Sec in fading environments. Channel estimation in LTE is a complex but nonetheless important. To enable proper channel estimation, scattered pilots have been employed in the LTE downlink channel.

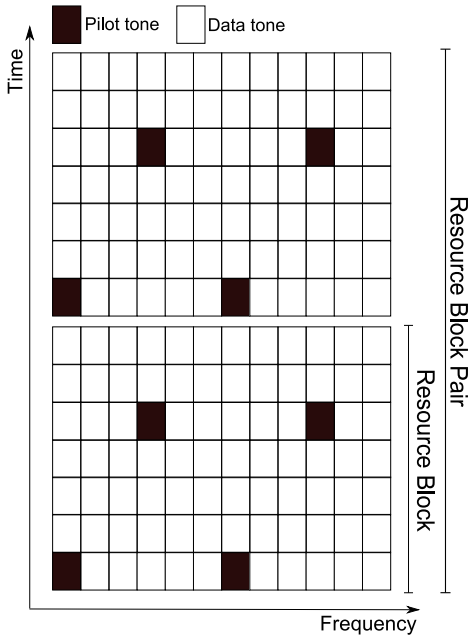

Figure 1: LTE, scattered pilot structure. Each RBP consists of two consecutive RBs and covers 12 subcarriers over 14 OFDM symbols.

Channel estimation based on scattered pilots is considered a challenging task when limited processing power restricts the scope of the applied algorithms. The estimator usually needs to interpolate the unknown subcarriers in two dimensions (time and frequency) which adds to the inherent complexity. The computational complexity becomes even more detrimental when the estimation needs to be carried out for a multitude of channels when the system is configured with MIMO.

In this paper we, in addition to a comparative analysis between previously known estimation techniques, also introduce a new channel estimation technique which exhibits both very low complexity as well as satisfactory performance up to terminal speeds of 120 km/h, as specified for LTE. The new estimation technique is designed with multi-standard processing on a single terminal platform in mind, like in [2] where common channel estimation structures for both LTE and Digital Video Broadcasting-Handheld (DVB-H) are addressed. Comparisons are provided in terms of the required number of multiplications as well as memory usage.

2 LTE (Long Term Evolution)

Mobile broadband encouraged the specification of LTE which became the basis for the next generation of UMTS Mobile standards [3]. One of the motivations behind LTE system design is to break the limitations of high data rates in wireless channels. The standardization not only demands LTE to provide high data rates in stationary channel environments but also demands that LTE based terminals provide a peak data rate of 100 Mbits/Sec in fading environments characterized with an equivalent terminal speed of up to 50 km/h while maintaining a moderate performance when

the terminal speed increases up to 120 km/h [4]. While many of the system components in LTE have already been standardized, some of the intermediate components, e.g., the channel estimator, have been left for the individual system designers and manufacturers to contemplate. As a result, each vendor has the opportunity to integrate its own designated algorithms into their products.

To assist channel estimation, pilot data known to both the transmitter and receiver are sent over the wireless channel. The pilots are either continual (e.g., in IEEE 802.11n) or scattered (e.g., LTE). Depending on the expected behavior of the wireless channel, one or a combination of both schemes will be employed for channel estimation purposes. LTE standardization has utilized scattered pilots in the downlink to assist the channel estimation. Fig. 1 illustrates how pilots have been scattered in time and frequency grid for a single antenna, i.e., antenna port 0. In the LTE standard, the term antenna port is preferred over physical antenna to emphasize the fact that multiple physical antennas can transmit the same data and as a result the combination can be considered as one antenna port using the same pilot pattern. Considering the fact that channel estimation for MIMO systems can be more cumbersome, as compared to SISO systems, LTE has defined different pilot patterns for the different antenna ports. To reduce the channel estimation complexity at the expense of spectral efficiency, the subcarriers corresponding to the pilot locations in one antenna port remain silent during data transmission on the other antenna ports. As a result, the estimator blocks don't need to take interference among the antenna ports into consideration when using pilot assisted channel estimation methods.

In contrast to some of the contemporary wireless communications systems such as DVB-H, data can be multiplexed for different users in each OFDM symbol in LTE. In other words, the Band Width (BW) of the system can be broken into a number of units each carrying data for one single UE. In LTE a Resource Block (RB) consists of twelve consecutive subcarriers in frequency and seven OFDM symbols in time as depicted in Fig. 1. Meanwhile, resource allocation for each UE consists of at least two consecutive RBs in time. Thus, the smallest allocable data unit to a typical UE is 12 subcarriers in 14 consecutive OFDM symbols known as one RB Pair (RBP). Fig. 1 shows how RB and RBP are defined over time-frequency grid in LTE. Having mentioned that, the UE needs to receive the first three OFDM symbols in each RBP to decode the control signaling. Among other things, control signals carry information about data scheduling [5] for each UE. If no data has been allocated for a certain UE, it can enter a standby mode for the next eleven OFDM symbols to save power.

The pilots associated with one RBP in LTE are distributed in OFDM symbols 1, 5, 8 and 12 for a 2×2 MIMO scheme. The pilot spacing in frequency domain for the pilot carrying OFDM symbols is 6 subcarriers. Fig. 1 displays an example of pilot structure for antenna port 0. The same pattern is shifted in frequency for antenna port 1. These pilots provide possibility of employing various channel estimation techniques, depending on the accuracy/complexity requirements of the system, to acquire the proper Channel State Information (CSI).

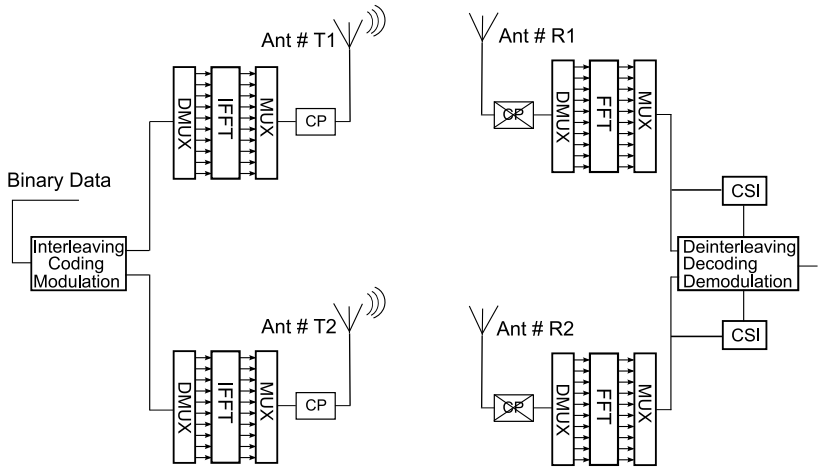

Figure 2: LTE, simplified MIMO system model.

3 System model

Fig. 2 shows a simple MIMO OFDM system model which can be used as a reference for a simplified LTE system. For the purposes of simulation in this paper a 2×2 MIMO scheme with optional turbo coding, similar to the one standardized for LTE, has been used. LTE benefits from two different Cyclic Prefixes (CPs) known as normal and extended CPs [5] to prevent ISI. In this paper, we have resorted to the application of the normal CP. The same analysis can, of course, be done with the extended CP. This is, however, beyond the scope of this paper. Similar to a typical OFDM-based system, information is modulated through one of the standardized modulation schemes for LTE, e.g., 4QAM. The modulated data as well as the pilots are placed on the corresponding subcarriers and after zero padding, as standardized in LTE providing the necessary Guard Band (GB), the result is fed into an IFFT. The IFFT output is then CP extended, A/D converted and transmitted over a time dispersive wireless channel with AWGN. The wireless channel length does not exceed the CP length. The received signal in the form of added multi-path components is received on each receiving antenna and passed through a D/A. After CP removal, the result is OFDM demodulated through an FFT block. It is assumed that the channel does not vary during each OFDM symbol transmission and hence the there is no ICI in the system. Besides, we have assumed perfect synchronization in the system.

We assume that the wireless channels between each pair of transmit/receive antennas have the same properties and each can be mathematically described as [6],

$$h(t,\tau) = \sum_{l=0}^{L-1} \alpha_l(t)\delta(\tau - \tau_l) \tag{3.1}$$

where L is the number of taps, α_l is the complex path gain and τ_l is the path delay corresponding to each tap. The above equation is the description of a time-varying linear system in which the path gains, α_l, are WSS complex Gaussian random pro-

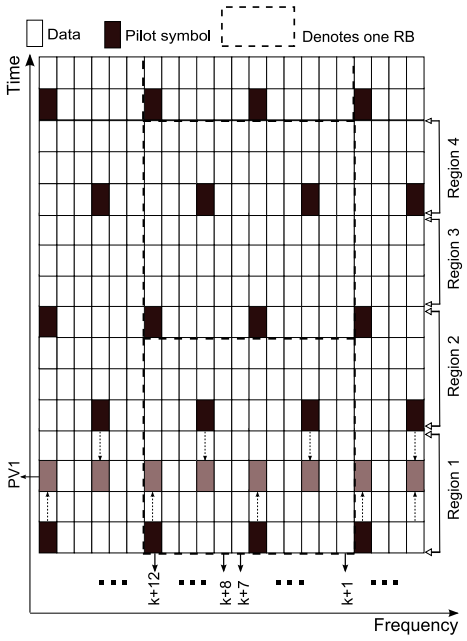

Figure 3: Merged-pilot estimation technique, merging (collecting) the pilots into Pilot Vectors (PVs). This picture shows how pilots from the 1st and 5th OFDM symbols are collected to create PV1. For estimation of subcarriers in each region, the pilots from the two closest pilot carrying OFDM symbols are collected and fed into the MRMMSE estimator. Hence, four PVs are constructed and channel estimation is done four times per RBP each corresponding to one region for equalization purposes. The depicted PV in this figure consists of eight pilots chosen symmetrically with respect to subcarriers $k+7$ and $k+8$ and is used to estimate them in region 1. The proposed estimator in this paper, however, uses sixteen pilots instead.

cesses. The Channel Frequency Response (CFR) of the wireless channel at time t can be written as,

$$H(t,f) = \int_{-\infty}^{+\infty} h(t,\tau)\exp(-2j\pi\tau)d\tau. \tag{3.2}$$

Assuming WSS channel taps, the time-frequency correlation function of a channel can be described as,

$$R(\Delta f, \Delta t) = E[H(f_1,t_1)H(f_2,t_2)]. \tag{3.3}$$

It can be shown that the frequency correlation function, which is obtained by setting $\Delta_{\mathrm{t}} = 0$ in $R(\Delta f, \Delta t)$ is the Fourier transform of the Power Delay Profile (PDP) of the channel, while the time correlation function, which is obtained by setting $\Delta_{\mathrm{f}} = 0$ in $R(\Delta f, \Delta t)$ can be described by the inverse Fourier transform of the Doppler spectrum of the channel. The inverse Fourier transform of the Doppler spectrum for a two dimensional isotropic uncorrelated scattering environment is [7]

$$R(\Delta t) = J_0(2\pi\phi_{\max}\Delta t), \tag{3.4}$$

where $J_0(.)$ is the zeroth-order Bessel function of the first kind, $\phi_{\max}$ is the maximum Doppler in Hertz and Δt is the time difference between two observations of the channel at two different time instances. Equivalently, the coherence time of the channel, T_{coh}, can be defined as the time interval over which the autocorrelation falls 3 dB from its maximum value [8]. According to equation (3.4), T_{coh} decreases inversely with the maximum Doppler frequency.

4 Channel estimation

The scattered pilot structure in LTE enables the application of various channel estimation techniques. The proper choice of the estimators depends on many factors among which the quality and the complexity of the estimators are the dominant criteria. Meanwhile, a lot of research has been done in the area of channel estimation for the wireless systems employing scattered pilots [6]. In one work [2], a number of DFT based estimators have been analyzed when applied to both LTE and DVB-H for a multi-standard terminal. The best linear estimator in terms of Mean Square Error (MSE) is the well-known 2-D LMMSE which exploits the second order channel statistics in time and frequency to estimate/interpolate the unknown subcarriers. However, real time processing of such a 2-D filter is intensive and due to its inherent complexity it is rarely used in practical systems. Meanwhile, it has been shown that the 2-D filter, under certain conditions, can be broken into two 1-D filters one in time and one in frequency with negligible performance loss [9]. The 1-D filter in frequency can be mathematically described as [10],

$$\hat{\mathbf{h}}_{\mathrm{mmse}} = \mathbf{R}_{\mathrm{h_m h_p}}(\mathbf{R}_{\mathrm{h_p h_p}} + \frac{\beta}{\mathrm{SNR}}\mathbf{I})^{-1}\hat{\mathbf{h}}_{\mathrm{p,ls}} \tag{4.1}$$

where $\mathbf{X}_{\mathrm{p}}$ and $\mathbf{Y}_{\mathrm{p}}$ are the transmitted and received data sampled on the pilot positions and,

$$\hat{\mathbf{h}}_{\mathrm{p,ls}} = \mathbf{X}_{\mathrm{p}}^{-1}\mathbf{Y}_{\mathrm{p}} \tag{4.2}$$

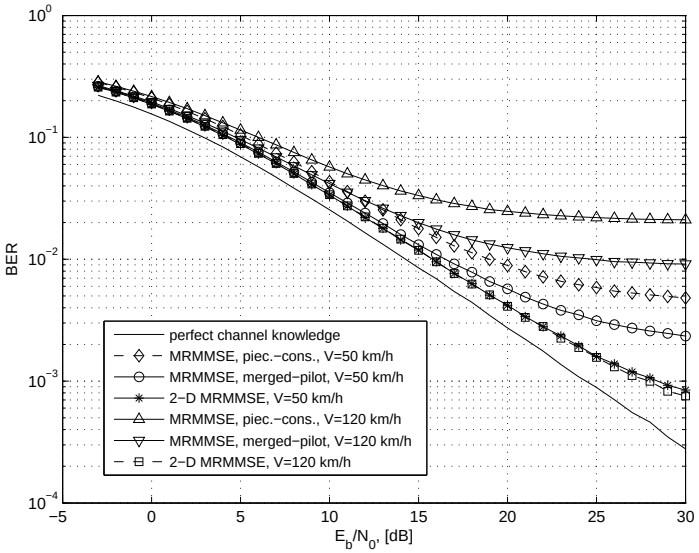

Figure 4: LTE, uncoded BER. The simulations have been done for a 2×2 $MIMO$ system configured for spatial multiplexing using a ZF receiver.

is the Least Squares estimate of the channel attenuations $\mathbf{h}_\mathrm{p}$ on the pilot tones, $\mathbf{R}_{\mathrm{h_p h_p}}$ is the autocorrelation of the sampled channel $\mathbf{h}_\mathrm{p}$ on pilot positions, $\mathbf{R}_{\mathrm{h_m h_p}}$ is the cross correlation matrix between the pilot tones and the data subcarriers, $\mathrm{SNR} = E|x_k|^2/\sigma^2$ is the signal-to-noise ratio and β is a constant which depends on the signal constellation of transmitted pilot symbols, $\mathbf{X}$. For a 4QAM modulation scheme β equals 1.

According to (4.1), a matrix inversion of $N_\mathrm{p} \times N_\mathrm{p}$, where N_p is the number of available pilots, needs to be done each time the second order channel statistics or the SNR value change. Thus, the complexity of the above estimator is still formidable. Due to the fact that the processing power on the mobile terminal is usually limited, a number of low complexity variants of the above estimator need to be derived. Reducing the complexity of the above estimator has been investigated in a number of previous works [6]. A simple method to overcome the matrix inversion problem, is to use a robust variant of the above estimator, robust MMSE [6], designed for a fixed SNR and a fixed PDP. Despite its performance loss, its reduced complexity makes this estimator more attractive for practical applications. In this paper, we have chosen a uniform design PDP where the worst case channel condition has been presumed. Although the robust MMSE estimator is more computationally efficient than the full MMSE, N_p complex multiplications need to be done to estimate each subcarrier in frequency. To counter the complexity problem even more, it has been shown [2] [11] that not all the available pilots in one OFDM symbol need to be used to estimate/interpolate each subcarrier. Acceptable performance can be achieved by only using the pilots in the vicinity of each subcarrier due to the correlation loss between subcarriers and pilots which are located far apart, especially in highly frequency selective channels. It has been shown [2] that for the

LTE system configuration simulated in this paper, as few as 16 pilots will provide satisfactory performance in terms of BER. We call this estimator Modified Robust MMSE (MRMMSE) as originally proposed in [2].

Table 1: LTE,simulated system parameters

FFT size	512	$\Delta f, [kHz]$	15
CP length,[n]	36	Used tones	300
Pilots/Symbol	50	PDP	$exp(-t/9)$
Carrier Freq.,[GHz]	2.6	Doppler Spec.	Jake's

Similarly, a robust MMSE in time direction can be used to estimate/interpolate the unknown subcarriers in time. The applied 1-D robust MMSE is designed based on the second order channel statistics in (3.4). Thus, the simplified 2-D MMSE (2-D MRMMSE) can be performed through two separate 1-D filtering first in time or frequency, followed by the filtering in the other domain [6]. In order to lower the complexity of the algorithm even further, we have adapted two more time domain strategies which waive the 1-D filtering in time. One approach is based on the well-known piecewise constant interpolation where the channel is estimated for each pilot carrying OFDM symbol in frequency and used for all the other subsequent nonpilot carrying symbols. As soon as the next pilot carrying symbol is received, a new frequency domain estimation is done and used likewise. The third method, merged-pilot [1], uses the mutual correlation existing between two consecutive pilot carrying OFDM symbols through merging (collecting) the pilots into a single Pilot Vector (PV) as depicted in Fig. 3. The constructed PV is then fed into a channel estimator and the corresponding CSI is estimated. The same CSI is used for equalization of all symbols exhibiting the shortest distance from the pilot contributing symbols. In other words, four CSIs corresponding to four PVs are obtained. CSI1 is used for equalization of OFDM symbols 1-4 (region 1), CSI2 is used for OFDM symbols 5-8 (region 2), CSI3 is used for OFDM symbols 9-11 (region 3) and CSI4 is used for OFDM symbols 11-14 (region 4). To achieve optimal results for region 4, the pilots from the first OFDM symbol corresponding to the next consecutive RBP are used to construct PV4 which is a valid assumption because the terminal always needs to listen to the first three OFDM symbols of each RBP. The feasibility of the above approach arises from a rather strong correlation between consecutive OFDM symbols in LTE. For the presumed system parameters in this paper, the T_{coh} derived from equation (3.4) covers as many as 6 OFDM symbols for an equivalent terminal speed of 120 km/h. However, the largest distance between any pilot carrying OFDM symbols in this approach is 4 which is associated with the PV1.

The above three approaches are characterized by their own pros and cons. The 2-D MRMMSE provides the best performance, esp. in high Doppler scenarios. Yet, it has a larger computational complexity and causes a delay in the equalization and decoding since all the pilot symbols in the entire RBP are used for the estimation.

[1]We have used the term mirrored-pilot in [2] which is literally the same as the merged-pilot. The notation has been changed to eliminate the probable ambiguity/confusion associated with the term, mirrored.

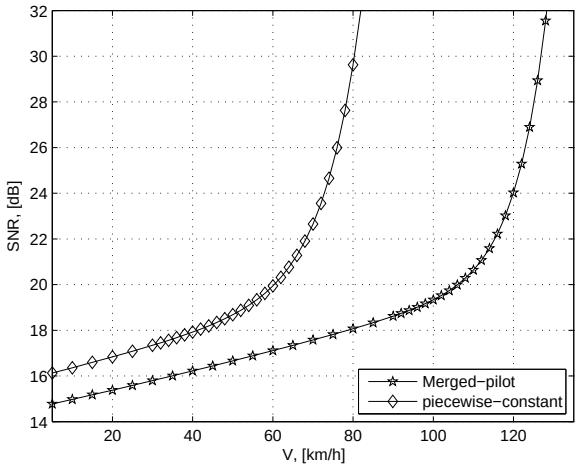

Figure 5: LTE, SNR vs. velocity to sustain an uncoded BER = 10^{-2} for a 2×2 MIMO system configured for multiplexing with ZF receiver. The figure shows the performance superiority of the merged-pilot over the piecewise constant for both slowly and fast fading wireless channels.

The piecewise constant approach does not need much memory to store symbols before the estimation initiates. Hence, it does not cause any considerable delay in the system. Besides, the complexity is only restricted to the MRMMSE applied in the frequency domain. The performance of this approach, however, is quite limited specially when used in fast fading environments. The last but not least approach, merged-pilot, provides a good compromise between hardware resources and performance as shown in the simulation section. This new approach has a considerably higher performance compared to the piecewise constant in environments characterized with high Doppler spreads. The performance gain can be described by two facts. First, the pilot spacing corresponding to the PV in the merged-pilot approach is half the spacing in the piecewise constant. Consequently, the cross correlation between the pilots and the estimated subcarriers is higher. Second, the mutual correlation provided by the pilots merged from two different OFDM symbols increases the reliability of the estimator in fading environments, esp. in areas located half way between the two pilot contributing symbols. Meanwhile, computational complexity of this estimator is identical to the piecewise constant's because both methods use the same MRMMSE (16 pilots) estimator in frequency. Yet, the merged-pilot approach has higher memory requirements since all the intermediate OFDM symbols need to be stored before the pilots from the target pilot carrying symbols are merged. Thus, an equalization lag hits the system which is still considerably lower than the simplified 2-D MRMMSE.

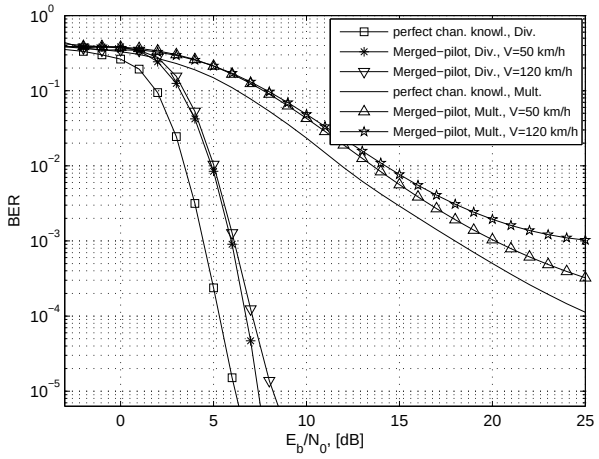

Figure 6: LTE, coded BER performance corresponding to the merged-pilot estimator for two different terminal speeds. Simulations have been done for a 2×2 MIMO system configured for both multiplexing and diversity using a ZF receiver. The diversity results have been simulated using Alamouti precoding scheme.

5 Simulation results

For the purposes of simulation in this paper, the LTE simulation system parameters were chosen according to Table 1. To illustrate the performance of the estimators, the widely used Bit Error Rate (BER) measure has been used. Although the choice of estimators has been based on the conventional uncoded BER, coded BER using the standardized turbo code in LTE [5] has also been simulated for the estimators of choice proposed in this paper. Besides, the simulations have been mainly performed for a 2×2 MIMO scheme configured for spatial multiplexing using a Zero Forcing (ZF) receiver. Since the possibility of diversity has also been provided in the LTE system design, some of the simulations have also been done for a 2×2 MIMO with diversity. Fig. 4 shows the performance of the estimators for a fading environment for three different terminal speeds from an uncoded BER view point. The BER performance reveals the advantage of collecting the pilots in the merged-pilot over the piecewise constant approach. The difference becomes even more significant when the terminal speed increases. The simplest method, piecewise constant, does not exhibit a good level of performance for the terminal speed of 120 km/h. The merged-pilot, however, offers a better performance as expected.

Table 2 contains the complexity and memory requirements of each technique per RBP. The complexity as well as memory requirements of the 2-D MRMMSE is much higher than the other two alternatives. The excessive complexity becomes prohibitive on mobile terminals especially in case of multi-standard platforms. On the other hand, our alternative approach, the merged-pilot estimator, provides an acceptable level of performance while exhibiting a moderate complexity. The piecewise constant estimator, however, has a significantly worse performance at high terminal speeds. Fig. 5 further describes the merits of the merged-pilot approach over the

piecewise constant. It can be seen from the figure that the uncoded BER = 10^{-2} breaking terminal speed is approximately 130 km/h for the merged-pilot approach

Table 2: LTE, complexity versus memory requirements for the three estimation techniques. The results are estimated per RBP.

Estimation technique	Complexity, [real Mul.]	Memory requirements, [byte]
piecewise-constant	2688	96
merged-pilot	2688	480
2-D MRMMSE	8424	1440

while that value drops to almost 80 km/h for the piecewise constant. Theoretically, it is possible to sustain an acceptable uncoded BER = 10^{-2} by having SNR = 24 dB for a terminal speed of 120 km/h in the merged-pilot case while the other estimator cannot sustain the BER = 10^{-2} for the same speed even if the SNR is increased indefinitely. Fig. 6 demonstrates the behavior of the merged-pilot estimator when coding is used. It can be witnessed that a coded BER = 10^{-2} can now be reached at SNR = 14 dB which is almost 10 dB lower compared to the uncoded BER when the system is configured for multiplexing. If the system is configured for diversity, on the other hand, the BER = 10^{-2} can be reached already at SNR = 5 dB which is almost 20 dB lower than for the uncoded case. Fig. 6 also reveals that for most SNRs the simulated LTE system using our proposed estimator is only a few dBs away from one with perfect channel knowledge. We also know from experience that it is possible to have as a high SNR as 25 dB in a mobile terminal. As a result, the performance of the estimator is well within the operational SNR region of the UE and can be reliably used in practical systems.

6 Conclusion

In this paper, the MRMMSE in frequency in conjunction with three time-domain strategies has been analyzed. The performance of the estimators for fast fading environments shows that the best trade-off between complexity and performance corresponds to the merged-pilot method as proposed in this paper. It has been shown that this low complexity estimator outperforms the conventional piecewise constant approach in fast fading environments while exhibiting the same complexity level and waives the need for computationally complex estimators which involve additional time-domain filtering. More importantly, the structure of this estimator enables its efficient application in a multi-standard environment where LTE and DVB-H coexist [2]. Having a core estimator as such, shared between LTE and DVB-H, enables efficient hardware design which results in reduced chip area, lower power consumption, etc.

7 Acknowledgments

The authors would like to thank MULTI-BASE, a 7th Framework Program funded by the European Commission, for supporting this work.

References

[1] R. W. Chang, "Synthesis of band-limited orthogonal signals for multichannel data transmission," *Bell Syst. Tech. J., 45*, pp. 1775–1796, 1996.

[2] F. Foroughi Abari et al., "Channel estimation for a mobile terminal in a multi-standard environment (LTE and DVB-H)," in *Proc. IEEE Int. Conf. Signal Process. and Commun. Syst.,* Omaha, NE, pp. 1–9, Sep. 2009.

[3] "LTE: An introduction [Online]," Ericsson AB, 2011. Available: http://www.ericsson.com/res/docs/2011/lte-an-introduction.pdf.

[4] "Evolved Universal Terrestrial Radio Access (E-UTRA); LTE physical layer; General description," 3rd Generation Partnership Project, Tech. Specifications, 3GPP TS 36.201, Dec. 2009. Available: http://www.3gpp.org/ftp/Specs/html-info/36201.htm.

[5] E. Dahlman et al., *3G Evolution, Second Edition: HSPA and LTE for Mobile Broadband*. Burlington, MA: Academic Press, 2008.

[6] M. Ozdemir and H. Arslan, "Channel estimation for wireless OFDM systems," *Commun. Surveys Tuts., IEEE*, vol. 9, pp. 18–48, July 2007.

[7] D. Young and N. Beaulieu, "The generation of correlated rayleigh random variates by inverse discrete Fourier transform," *IEEE Trans. Commun.*, vol. 48, no. 7, pp. 1114–1127, 2000.

[8] A. F. Molisch, *Wireless communications*. West Sussex, United Kingdom: John Wiley & Sons Ltd., 2007.

[9] M. Sandell and O. Edfors, "A comparative study of pilot-based channel estimators for wireless OFDM," Tech. Rep., Div. of Signal Process., Luleå Univ. of Technology, Luleå, Sweden, 1996.

[10] O. Edfors et al., "OFDM channel estimation by singular value decomposition," *IEEE Trans. Commun.*, vol. 46, pp. 931–939, July 1998.

[11] K. Manolakis et al., "Performance evaluation of a 3GPP LTE terminal receiver," in *Proc. 14th European Wireless Conf.,* Prague, pp. 1–5, 2008.

On coefficient memory co-optimization for channel estimation in a multi-standard environment (LTE and DVB-H)

Farzad Foroughi Abari, Fredrik Rusek, and Ove Edfors

Paper III

Abstract

This paper presents a novel memory optimization technique to exploit the analogy between correlation coefficients in MMSE-based channel estimators across multiple standards. The need for coefficient storage for robust MMSE channel estimators is expensive in terms of on-chip memory. Besides, the memory requirements grow linearly by integrating more standards onto one platform. Thus, it becomes inevitable to address the increased on-chip memory problem for such estimators. In this paper, we have shown that by exploiting the inherent similarities between LTE and DVB-H design parameters, a three-fold memory optimization may be achieved with minimal performance loss.

1 Introduction

Orthogonal frequency division multiplexing (OFDM) is a driving force behind the latest high speed standards in wired as well as wireless communications. The ability to break a wide spectrum into narrowband subchannels where data could possibly be multiplexed for different users has provided a number of different possibilities, including but not limited to, reducing or eliminating the inter symbol interference (ISI), using simple equalizers and employing flexible channel estimators.

Long Term Evolution (LTE) is the 4th generation standard for mobile wireless communications. It provides high spectrum efficiency with data rates of up to 100 Mbits/s. To facilitate channel estimation, scattered pilots are used in the downlink transmission. As a result, a variety of channel estimation algorithms may be used, as suggested in literature [1].

Similar to LTE, Digital Video Broadcast-Handheld (DVB-H) employs OFDM for data transmission. DVB-H is an evolution of Digital Video Broadcasting-Terrestrial (DVB-T) to address the needs of mobile terminals in time-varying wireless channels. To facilitate channel estimation, scattered pilots are also used in DVB-H. Although the pilot patterns in LTE and DVB-H are different, they both exhibit similarities which may be exploited for co-optimization.

This paper is the continuation of the work started in [2] and followed by [3]. Although the channel estimation techniques presented in this paper are similar to [2, 3], the presented memory optimization principle across LTE and DVB-H in this work binds the proposed estimators into a single channel estimation package. We will show that by exploiting the similarity between the 2nd-order wireless channel statistics across LTE and DVB-H a three-fold on-chip memory reduction associated with the channel estimator filter coefficients can be achieved.

The structure of the paper is as follows. After giving a short introduction to DVB-H and LTE standards in Sec. 2, the employed channel estimation approach is briefly discussed in Sec. 3. In Sec. 4 we show how designing the proposed estimator for specific system parameters allows us to reuse certain coefficients across LTE and DVB-H. Furthermore, it is shown that by designing the estimators for a truncated guard interval in LTE further memory optimization is achieved. Finally, in Sec. 5 simulation results for the proposed design methods in terms of channel estimation performance are discussed and conclusive remarks are given in Sec. 6.

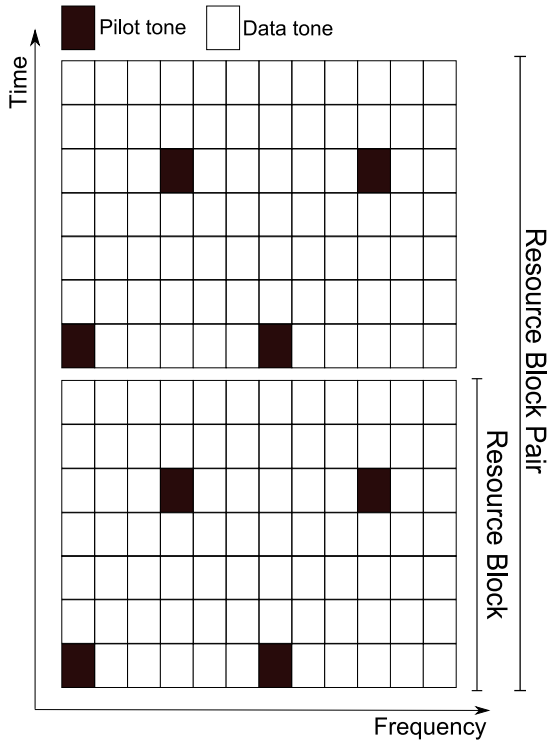

Figure 1: An example of time-frequency grid corresponding to one RBP for LTE. The scattered pilots are identified by the black boxes.

2 LTE and DVB-H

LTE exploits the spectrum efficiency provided by OFDM and promises high data rates in wireless communications systems which can be harnessed for various purposes, such as, wireless Internet, high-quality multimedia transmission, etc. It also provides the flexibility for various system implementations through different modes of operation, i.e., different bandwidths (BW). The supported BW range (2-20 MHz) corresponds to DFT sizes of $128 - 2048$ points.

To combat ISI two different cyclic prefixes (CP) are defined for LTE, i.e., *normal* and *extended* CPs each having a length equal to that of the maximum expected delay spread in the wireless channel. The normal CP has a fixed length of $4.69\,\mu$s and the extended CP's spread is equal to $16.67\,\mu$s.

To facilitate channel estimation for such a wide spectrum in a multi-path fading environment, scattered pilots are introduced in the physical layer of LTE. An example of scattered pilots for a resource block pair (RBP) [4] is depicted in Fig. 1. As can be seen the pilots are scattered in both time and frequency, which provides the opportunity to apply various channel estimation schemes.

DVB-H is also an OFDM based system. It is a refinement of DVB-T and is adapted for the needs of mobile communications. Among many different modifications, one can mention the addition of 4k operation mode which offers an additional trade-off between transmission cell size and mobile reception capabilities [5].

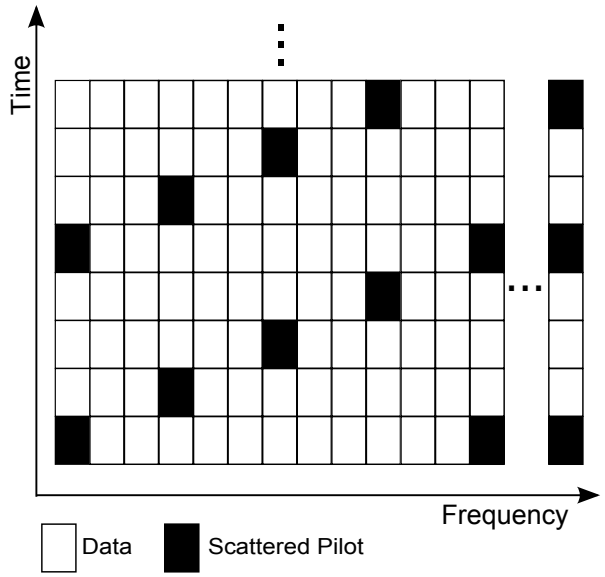

Figure 2: An example of time-frequency grid for DVB-H. The scattered pilots are identified by the black boxes.

Similar to many other OFDM-based systems different CPs are also standardized for DVB-H. More precisely, there are four different CPs adopted in DVB-H which are known as 1/4, 1/8, 1/16 and 1/32. The numbers correspond to the ratios of the CP duration and the useful symbol duration.

Scattered pilots are also employed in DVB-H for channel estimation purposes. Fig. 2 illustrates an example of scattered pilots distribution, in time and frequency, for a typical DVB-H system. It can be observed that the pilot density is higher in DVB-H when compared to LTE. This enables the possibility to adopt a wider set of channel estimation techniques, such as various merging schemes elaborated in this paper.

3 Channel estimation

A number of techniques can be used for pilot-assisted channel estimation in LTE and DVB-H. Depending on the estimators complexity-performance trade-off, several algorithms may be used in practice [6]. In [2, 3] the concept of a modified robust MMSE (MRMMSE) estimator is introduced. The MRMMSE enables low-complexity channel estimation with an acceptable performance in fading environments specified by LTE standard [4].

Considering a wide sense stationary uncorrelated scattering (WSSUS) environment our wireless channel, composed of M impulses with a certain power delay profile (PDP), $\Theta(\tau_l)$, is modeled as

$$h_{\text{cont.}}(\tau) = \sum_{l=0}^{M-1} \alpha_l \delta(\tau - \tau_l T_s), \tag{3.1}$$

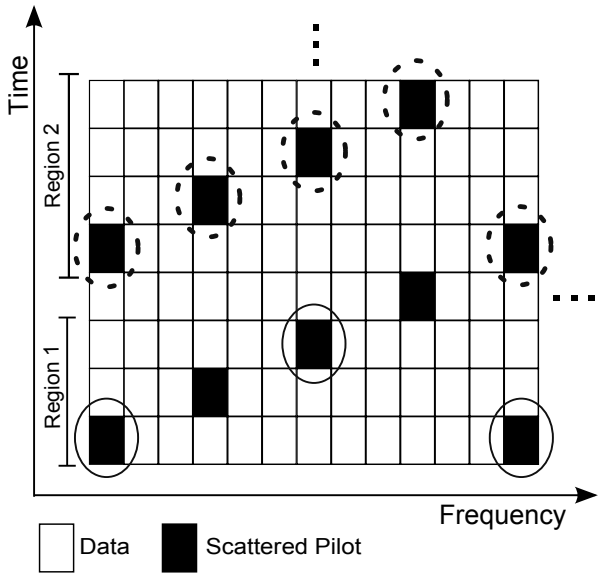

Figure 3: An example of time-frequency grid for DVB-H. The scattered pilots are identified by the black boxes. The solid circles show how pilots from three consecutive OFDM symbols are collected to construct a pilot vector with a pilot separation of 6. Similarly, the dotted circles identify the pilots collected from four consecutive OFDM symbols resulting in a pilot vector with a separation of 3.

where α_{l} are zero-mean complex Gaussian random variables and T_{s} is the system's sampling interval. Furthermore, the channel attenuation on tone k for the above channel model becomes,

$$h\left[k\right] = \sum_{l=0}^{M-1} \alpha_{\mathrm{l}} \exp(-2\pi j(k/N)\tau_{\mathrm{l}}). \tag{3.2}$$

If the subcarriers, including both pilots and data carrying tones, corresponding to one OFDM symbol are collected into a single column vector at the receiver, we can model the received vector as,

$$\mathbf{y} = \mathbf{X}\mathbf{h} + \mathbf{w} \tag{3.3}$$

where $\mathbf{y}$ is the received data column vector of size N, $\mathbf{X}$ is a diagonal matrix of size $N \times N$ encompassing the transmitted data, $\mathbf{h}$ and $\mathbf{w}$ are column vectors of size N containing the channel attenuations and the independent and identically distributed (IID) white Gaussian noise values respectively. Moreover, let $(.)^H$ denote the Hermitian transpose, then the 1-D MMSE-based channel estimation in frequency for the above model is given by the following equation,

$$\hat{\mathbf{h}}_{\mathrm{mmse}} = \mathbf{R}_{\mathrm{hh_p}} \left(\mathbf{R}_{\mathrm{h_p h_p}} + \frac{1}{\mathrm{SNR}} \mathbf{I} \right)^{-1} \hat{\mathbf{h}}_{\mathrm{p,ls}} \tag{3.4}$$

where $\hat{\mathbf{h}}_{\mathrm{mmse}}$ is a column vector of size N containing the estimated channel tones and $\mathbf{h}_{\mathrm{p}}$ is a column vector of size N_{p} encompassing the sampled channel at the

pilot positions. Moreover, $\mathbf{R}_{\mathrm{h_p h_p}} = \mathbb{E}[\mathbf{h}_\mathrm{p}\mathbf{h}_\mathrm{p}^H]$ is a matrix containing the autocorrelation values of the sampled channel on the pilot positions, $\mathbf{R}_{\mathrm{h h_p}} = \mathbb{E}\left[\mathbf{h}\mathbf{h}_\mathrm{p}^H\right]$ is the cross-correlation matrix between the pilot tones and subcarriers and SNR is the signal-to-noise ratio. Furthermore,

$$\hat{\mathbf{h}}_{\mathrm{p,ls}} = \mathbf{X}_\mathrm{p}^{-1}\mathbf{y}_\mathrm{p} \tag{3.5}$$

is the least squares (LS) estimate of the channel attenuations $\mathbf{h}_\mathrm{p}$ on the pilot tones, where $\mathbf{X}_\mathrm{p}$ is a matrix containing the transmitted pilot data on its diagonal and $\mathbf{y}_\mathrm{p}$ is the column vector of received pilot tones.

To avoid computationally expensive matrix inversions imposed by (3.4), a robust estimator may be used which has been shown to exhibit acceptable performance [2]. The robust estimators may be designed for a set of fixed channel estimation parameters, e.g., SNR and 2nd order channel statistics. For instance, the frequency correlation, corresponding to the channel model in (3.1), between two subcarriers, with a spacing of Δk, depends on the PDP, $\Theta(\tau_\mathrm{l})$, of the channel. Furthermore, for a uniformly distributed PDP the frequency correlation amounts to [7]

$$r_\mathrm{h}\left[\Delta k\right] = \frac{1 - \exp(-2j\pi L\Delta k/N)}{2j\pi L\Delta k/N}, \tag{3.6}$$

where L is the delay spread of the wireless channel in samples. It can be seen in (3.6) that the correlation among subcarriers in a single OFDM symbol depends only on the distance between the corresponding subcarriers (Δk), the PDP length (L), and the number of DFT points (N). As we will see in the following sections, the ratio between the above parameters facilitates co-optimization of filter coefficients across LTE and DVB-H.

It can be shown [2, 3] that due to correlation loss among the subcarriers located far apart, using only a few pilots in the vicinity of each subcarrier provides an acceptable performance in terms of channel estimation. Doing the estimation as such, not only lowers the computational complexity of the estimator but also reduces the coefficient memory requirements [3].

In [3] it has been shown that by combining the above mentioned strategy, i.e., using a subset of pilots, and the pilots merging scheme, low-complexity estimators, called merged-pilot modified robust MMSE (merged-pilot MRMMSE) can be developed. Moreover, these estimators exhibit an acceptable performance in moderately fast fading environments for LTE [3]. Likewise, the same principle may be applied to DVB-H [2] with different approaches to pilot merging. Fig. 3 shows how two different pilot merging schemes can be performed for channel estimation using (3.4). To construct a pilot vector similar in concept to the one in [3], where the pilot separation is 3, pilots from four consecutive OFDM symbols are collected and merged into a single pilot vector. This is illustrated by dotted circles in Fig. 3. The constructed pilot vector is further used for channel estimation as well as equalization of, say, region 2 in Fig. 3. Similarly, if a pilot separation of 6 is desired, pilots from alternate OFDM symbols, as shown by solid-line circles in Fig. 3, are collected into a pilot vector. The built pilot vector is further fed into the channel estimator whose

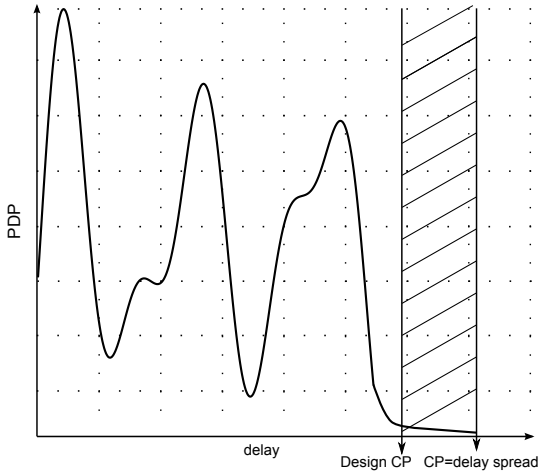

Figure 4: An example of a wireless channel's PDP. It is expected that the wireless channel's delay spread does not exceed the CP length. The dashed region shows how part of channel energy, though minimal, is ignored during estimator design.

Table 1: The configurations for which coefficient co-optimization is feasible according to our proposed scheme.

LTE				DVB-H			
N_{DFT}	$N_{\text{cp,trunc.}}$ (normal)	N_{cp} (Extended)	Pilot Sep.	BW (MHz)	Mode (k)	CP len.	Pilot Sep.
128-2048	8-128	N.A.	3	6-8	2-8	$\frac{1}{32}$	6
				6-8	2-8	$\frac{1}{16}$	3
128-2048	N.A.	32-512	3	6-8	2-8	$\frac{1}{8}$	6
				6-8	2-8	$\frac{1}{4}$	3

output is used for equalization of the region encompassed by the pilot contributing OFDM symbols, e.g., region 1 in Fig. 3.

Each pilots merging scheme has its own pros and cons in terms of performance and computational complexity. An elaborate analysis of the computational complexity versus performance is beyond the scope of this paper. However, manipulating the pilots spacing as such provides the opportunity for further coefficient memory optimization discussed in the following sections.

4 Coefficient memory co-optimization

As discussed in previous section and elaborated in [2, 3], using a subset of pilots in the vicinity of each subcarrier for estimation purposes already reduces the memory storage requirements for the RMMSE filter coefficients. This may be practiced for each standard, i.e., DVB-H and LTE in this paper, separately. In other words, using the above mentioned approach, 6 different MRMMSE filter coefficient sets should be generated each designed for one specific CP configuration in LTE and DVB-H, i.e., normal and extended CP in LTE as well as 1/4, 1/8, 1/16 and 1/32 CPs in

DVB-H.

To enable further memory optimization across the standards, however, one may use the innate similarity between LTE and DVB-H. In Sec. 2, it was shown that by fixing the variables in (3.4),(3.6) the robust estimator is a function of delay spread of the channel (L), subcarrier spacing (Δk) and DFT length (N). Let the robust estimators be designed for a uniform PDP with a length equal to that of the maximum expected delay spread in the wireless channel, i.e., the CP length, then (3.6) becomes

$$r_{\mathrm{h}}\left[\Delta k\right] = \frac{1-\exp(-2j\pi N_{\mathrm{CP}}\Delta k/N)}{2j\pi N_{\mathrm{CP}}\Delta k/N}, \tag{4.1}$$

where N_{cp} is the designated CP length.

Considering the fact that pilots from neighboring OFDM symbols, as discussed in previous sections, may be merged to address the channel estimation needs of the terminals, various merging patterns may be practiced in LTE and DVB-H to force the corresponding correlation matrices to be identical. In fact, our intention is to force

$$r_{\mathrm{h}_1}[\Delta k] = r_{\mathrm{h}_2}[\Delta k],\ \forall k, \tag{4.2}$$

where index 1 refers to LTE and index 2 refers to DVB-H. As a result, the estimators will be identical for similar values of SNR. By doing so, it is easy to show that it is required that

$$\frac{\Delta k_1 N_{\mathrm{CP}_1}}{N_1} = \frac{\Delta k_2 N_{\mathrm{CP}_2}}{N_2} \tag{4.3}$$

for the estimators in LTE and DVB-H to become identical.

Table 2: System simulation parameters.

Standard	N	F_c, [GHz]	V, [km/h]	Modulation	Channel model	Fading model
LTE	512	2.2	50	4QAM	3GPPTUx [8]	2-D, Jake's
DVB-H	2048	0.75	10-200	4QAM	TU-6 [5]	2-D, Jake's

One can see that by adjusting the three different variables in (4.3), i.e., N, N_{cp} and Δk, the same coefficients can be shared between the two standards. For instance, by designing the estimator based on the extended CP in LTE, when the pilot separation is 3, a certain ratio suggested by (4.3) is achieved which enables reusing the same estimator in DVB-H, across all different BWs and modes of operation, provided that the system is configured for 1/4 and 1/8 CP lengths. Moreover, constrained by (4.3), a pilot separation of 3 should be practiced for 1/16 CP while the pilot separation in case of 1/8 CP should be kept at 6, see Table 1. By doing so the required number of filter coefficient sets reduces to 4 rather than 6.

Nevertheless, to be able to maximize the coefficient co-optimization, even further, the normal CP length in LTE needs to be truncated to $N_{\mathrm{cp,trunc.}}$ where $N_{\mathrm{cp,trunc.}} = 2^i$ is the largest value that is smaller or equal to N_{cp} and is further used as the basis for the generation of the MRMMSE estimators. These estimators are identified as truncated MRMMSE (TMRMMSE) throughout this paper. Table 1 shows the different configurations for which the same coefficients across LTE and DVB-H may be reused. It can be seen that by designing the estimators for the truncated normal

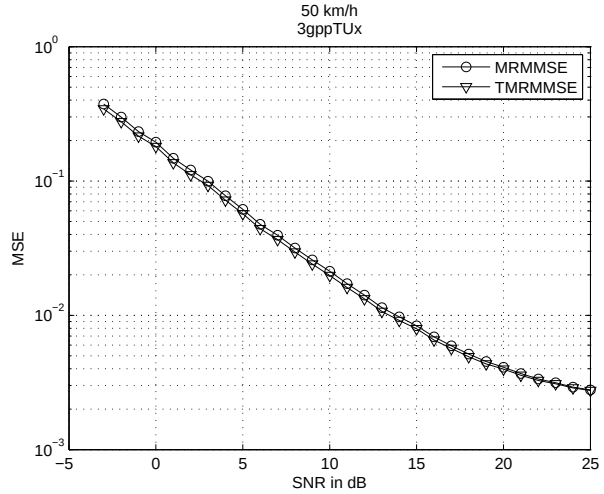

Figure 5: LTE channel estimator performance in terms of MSE. The difference in MSE between MRMMSE and TMRMMSE is minimal. The observed MSE floor in the high SNR region is because of the channel estimators mismatch with respect to both fading and PDP.

CP in LTE, the estimators can be shared with DVB-H provided that the system is set-up for 1/16 and 1/32 CP lengths. Furthermore, a pilot separation of 6 and 3 needs to be practiced for 1/32 and 1/16 respectively. One may practice other pilot merging schemes for LTE and DVB-H to force identical estimation coefficients. However, the suggested configuration in Table 1 not only is optimal in terms of maximum coefficient optimization but also is in-line with [3] in terms of the channel estimator's performance in fast fading environments.

Designing the robust estimator for a truncated CP provides a two-fold memory co-optimization. In other words, it further reduces the number of filter coefficient sets from 4 to 2. However, it may result in a loss in the channel estimator's performance if the delay spread of the wireless channel exceeds the length of the truncated CP. Fig. 4 illustrates how part of channel energy is ignored during estimator design for an exemplary continuous time wireless channel. However, we expect that the discarded channel energy is minimal for the majority of the wireless channels in practice, specially because the required truncation is minimal. On the contrary, the performance of the estimators may even improve if the root mean squared (rms) delay of the wireless channel is considerably smaller than the CP length. As a result, due to the mismatch reduction between the actual and design PDP the channel estimator's performance for such cases slightly improves.

5 Simulation results

Estimator performance results for LTE, when the pilot merging scheme with a separation of 3 is adapted, are discussed in [2, 3]. The provided simulations provide a good insight into the performance of such estimators when coefficients are generated

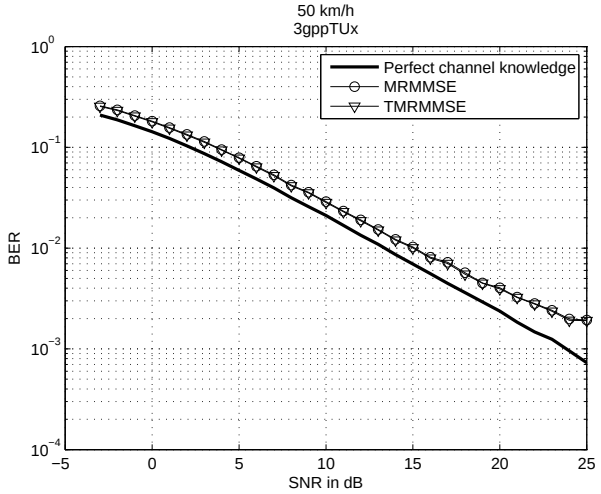

Figure 6: LTE channel estimator performance in terms of uncoded BER.

for a normal CP without truncation. They also depict a detailed picture of the estimator's performance, in different fading environments, when the proposed pilots merging schemes are practiced.

Fig. 5 shows the MSE performance of the two estimators designed based on the normal and truncated CP. It can be seen that the MSE difference between the two is quite small. This is in agreement with the discussion about the minimal mismatch introduced by truncation in section 4. In fact, TMRMMSE estimators exhibits a better performance for this specific simulation environment where one of the standard ITU-R 3G [8] channel models, i.e., 3GPPTUx has been adopted. This is mainly due to the fact that not only the rms delay spread of the channel is considerably smaller than the CP length but also there is no resolvable multi-path component in the discarded area, as in Fig. 4. As a result, the mismatch between the design and actual PDP is improved resulting in an slightly improved channel estimation performance.

Fig. 6 shows how the performance of the estimator in terms of uncoded bit error rate (BER) is affected. In fact, the TMRMMSE BER curve overlays the MRMMSE which supports the minimal MSE difference observed in Fig. 5. Furthermore, although not included in this paper, the performance of TMRMMSE for all the different standardized channel models, ITU-R 3G channel models [8], have been performed and the comparisons show similar behavior. On the whole, unless the wireless channel in practice has strong taps located in the to-be-discarded region, as depicted in Fig. 4, the TMRMMSE performance takes after the MRMMSE, i.e., without any CP truncation.

Although, no CP truncation is required during DVB-H estimator design, the estimator's performance results need to be discussed due to the application of various pilot merging schemes. As elaborated in [3] for LTE, pilots merging results in different performance and complexity trade-offs. The impact is specifically more visible in fast fading environments. In Fig. 7 the performance of the MRMMSE

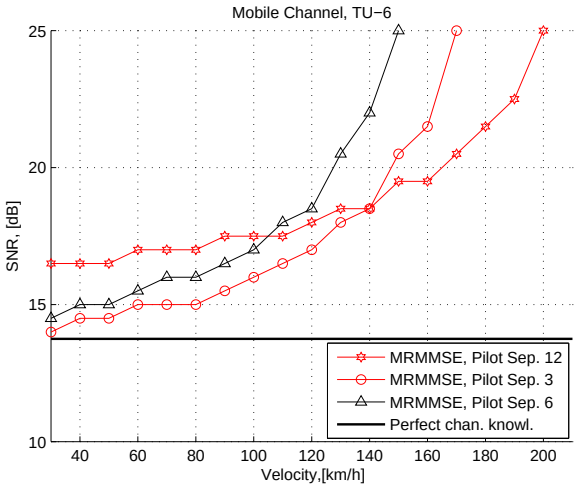

Figure 7: The required SNR to sustain an uncoded BER of 10^{-2} for a range of terminal speeds. The simulations have been done for a carrier frequency of 750 MHz and 4QAM modulation scheme in DVB-H.

estimators for two different pilots merging schemes, i.e., pilot separations of 3 and 6 are illustrated. Although, coefficient optimization for pilot separation of 12, i.e., with no merging, is not discussed in this paper, its performance result provides a valuable reference for comparison purposes.

It is evident from Fig. 7 that different merging schemes provide a certain gain/compromise in terms of the required SNR for various fading environments. Besides, there is a significant loss in the estimators performance when the terminal speed increases beyond a certain limit. However, if the performance constraints for the fast fading environments are arbitrarily based on the requirements set by LTE, i.e., an acceptable performance up to terminal speeds of 120 km/h [4], all the merging schemes proposed in this paper satisfy the requirements of the multi-standard platforms specified by [9]. On the other hand, the proposed practice in this paper, enables a three-fold coefficient memory reduction, 2 rather than 6 filter coefficient sets, when both LTE and DVB-H are co-implemented.

6 Conclusion

We have shown that by employing various pilots merging schemes in DVB-H while designing the MRMMSE estimators for a truncated normal CP in LTE, it is possible to optimally share the MRMMSE estimators between LTE and DVB-H. In other words, having the estimators designed for LTE enables the integration of DVB-H standard on the same platform without any additional filter coefficient memory cost. In effect, the on-chip memory requirement for the storage of the robust estimation coefficients in a multi-standard platform considerably decreases. For co-implementation of LTE and DVB-H the on-chip coefficient memory is reduced by a factor of three. Although, the above mentioned procedure forces specific pilot

merging patterns for a number of configurations in a given standard, the simulation results show that the performance loss is acceptable for slow as well as moderately fast fading environments.

7 Acknowledgments

This project was funded by Multi-base, a 7th Framework Program by the European Commission.

References

[1] M. Ozdemir and H. Arslan, "Channel estimation for wireless OFDM systems," *Commun. Surveys Tuts., IEEE*, vol. 9, pp. 18–48, July 2007.

[2] F. Foroughi Abari et al., "Channel estimation for a mobile terminal in a multi-standard environment (LTE and DVB-H)," in *Proc. IEEE Int. Conf. Signal Process. and Commun. Syst.,* Omaha, NE, pp. 1–9, Sep. 2009.

[3] F. Foroughi Abari et al., "Low complexity channel estimation for LTE in fast fading environments for implementation on Multi-Standard platforms," in *Proc. IEEE Veh. Tech. Conf.,* Ottawa, pp. 1–5, Sep. 2010.

[4] "Evolved Universal Terrestrial Radio Access (E-UTRA); LTE physical layer; General description," 3rd Generation Partnership Project, Tech. Specifications, 3GPP TS 36.201, Dec. 2009. Available: http://www.3gpp.org/ftp/Specs/html-info/36201.htm.

[5] "Digital Video Broadcasting (DVB); Framing structure, channel coding and modulation for digital terrestrial television," European Telecommunications Standards Institute (ETSI), Tech. Specifications Final Draft, 2004.

[6] M. Sandell and O. Edfors, "A comparative study of pilot-based channel estimators for wireless OFDM," Tech. Rep., Div. of Signal Process., Luleå Univ. of Technology, Luleå, Sweden, 1996.

[7] O. Edfors et al., "OFDM channel estimation by singular value decomposition," *IEEE Trans. Commun.*, vol. 46, pp. 931–939, July 1998.

[8] "Guidelines for Evaluation of Radio Transmission Technologies (RTTs) for IMT-2000," International Telecommunication Union, RECOMMENDATION ITU-R M.1225, 1997.

[9] Ericsson AB et al., "System Requirements Specification (2nd version), incl. scope and time plan," Scalable Multi-tasking Baseband for Mobile Communications, Tech. Rep. D1.2, Jan. 2008. Available: http://www.multibase-project.eu.

Channel estimation filter-tap memory optimized pilot pattern design for OFDM systems in multi-mode and multi-standard environments

Farzad Foroughi Abari, Fredrik Rusek, and Ove Edfors

Technical Report

Reprinted, with permission, from Farzad Foroughi Abari, Fredrik Rusek, and Ove Edfors, "Channel estimation filter-tap memory optimized pilot pattern design for OFDM systems in multi-mode and multi-standard environments," Tech. Rep., Dept. of Elect. and Inform. Tech. (EIT), Lund Univ., Lund, Sweden, 2011.

Abstract

As more and more OFDM standards are integrated in one single platform, there is a growing interest to adopt low-complexity signal processing algorithms to lower the hardware requirements. A challenging part of many transceivers is the channel estimation block. As a result, it is desired that the number of necessary channel estimators is minimized while addressing several OFDM standards in one platform. In this paper, we have shown that by following a specific strategy in pilot pattern design for OFDM systems in multi-standard environments the number of OFDM systems sharing a limited number of channel estimation filters can be maximized. Besides, we have shown that by pursuing a variant of the proposed strategy, pilot patterns compatible with an already existing standard of interest, can be designed. This is specially of significant importance where a number of OFDM systems need to be co-integrated with an existing/standardized one such as LTE.

1 Introduction

The wireless communications entered a new era when orthogonal frequency division multiplexing (OFDM) became practically feasible. Although the main concept was introduced in the 1960s [1, 2], its application was mostly limited to military applications due to the required sophisticated radio frequency electronics. However, as digital electronics matured, OFDM could be realized through fast and efficient digital circuits. OFDM provides many advantages over its single-carrier communication counter part. One of its main advantages is dividing the available band width (BW) into narrow band channels such that inter symbol interference (ISI) can be mitigated. It also provides the possibility for implementation of simple frequency equalization. Simple frequency equalization can also be realized through single carrier with frequency domain equalization (SC-FDE) [3]. However, OFDM and SC-FDE each have their own pros and cons making them suitable for specific applications. Besides, OFDM is mostly used in the downlink of a radio communication while SC-FDE is used in the uplink.

The opportunity for simple frequency equalization, provided by the OFDM, cannot be fulfilled unless channel state information (CSI) is available at the receiver. Taking the fact that it is usually cumbersome or even impossible to feed the CSI to the receiver, it needs to be estimated at the receiving side. As a result, channel estimation becomes an inevitable part of any OFDM transceiver architecture. There are many approaches to channel estimation. The methods cover a wide range from blind estimation methods [4–7] to low-complexity approaches suitable for low-power mobile terminals. Blind channel estimation, channel estimation in the presence of channel coding, and minimum mean square error (MMSE) pilot-aided channel estimation are examples of various existing approaches.

A common and widely acceptable way of performing channel estimation is to use data known to both the transmitter and the receiver, i.e., pilot data. The pilots are either contiguous, meaning they appear in the form of a preamble such as in IEEE 802.11n [8] or are distributed over the time-frequency grid in OFDM

systems. The distribution of the pilots is based on many different factors such as spectral efficiency and transmit power requirements. Moreover, the pilot pattern may depend on the channel estimation algorithm. For instance, in joint channel estimation and data detection the pilot density could be much lower than what is required by the conventional linear estimators [9].

A lot of research has been carried out in the area of pilot pattern design for OFDM systems [10–12]. One could refer to [13] where an intuitive description of 2-D pilot pattern design has been provided. The parameters of interest for pilot pattern design are are associated with the most encountered issues in single standard transceivers. Instances of such issues are the effect of pilots on spectral efficiency, the peak to average power ration (PAPR), and signal to noise ratio (SNR). Meanwhile, being a multi-variable optimization, the design should provide a proper balance between estimation performance and pilot overhead. Moreover, when designed for a practical implementation on systems with limited hardware resources, e.g., mobile terminals, it should provide the possibility for proper application of low complexity signal processing algorithms. Thus, depending on the target system requirements, a number of different patterns may be adopted.

However, little research has been carried out to probe the pilot pattern design for OFDM systems in multi-standard environments. As more OFDM systems are gradually standardized for wireless communications, this topic deserves a more in-depth investigation. Besides, the smart mobile terminals of today have to handle several streams associated with different standards simultaneously. For instance, a typical terminal could be hooked up to Long Term Evolution (LTE) network while streaming multimedia through Digital Video Broadcasting-Handheld (DVB-H). It is expected that more OFDM standards enter the wireless market in future. Thus, mobile terminals have to support them to be able to stay on the competing edge.

On the other hand, mobile terminals have their own restrictions in terms of hardware resources and power requirements. The hardware and battery technology have not been able to keep pace with the intensive signal processing algorithmic developments. As a result, it is but inevitable to dig into low-complexity alternatives for the demanding and greedy algorithms. This has motivated, e.g., the research results in [14–16] within Multi-base [17] project. The results indicate that there is a good chance of exploiting the similarities in the existing OFDM standards such as LTE and DVB-H so the available hardware resources can be shared among the channel estimation blocks. For instance, it has been shown in [16] that by using the similarity in the available pilot pattern in LTE and DVB-H a significant reduction, in terms of the required on-chip memory for the storage of channel estimator filter taps, can be done. In other words, a few filter sets can be reused in LTE and DVB-H across their different modes of operation.

However, we have observed that the low-complexity channel estimators proposed in [14, 15] could provide a higher performance in fading environments if the pilot pattern was designed differently. For instance, with some modifications to the available DVB-H pilot pattern as elaborated in Sec. 5.2, one could enhance the performance of the proposed channel estimators in fast fading environments. Besides, one may design the pilot pattern in future OFDM systems such that maximum compatibility

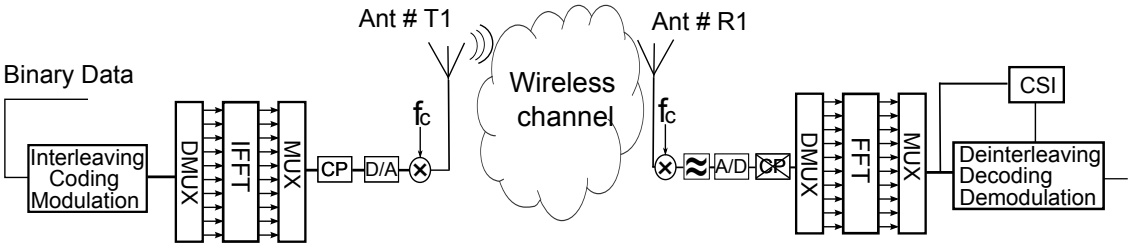

Figure 1: The adopted SISO OFDM system model.

in terms of the proposed low-complexity channel estimators [14, 15] may be achieved with respect to other OFDM standards. This is of significant importance in low-power multi-standard environments where the hardware resources should be utilized as efficiently as possible.

In this work, we will show a strategy for pilot pattern design in emerging OFDM standards. The main criteria for the proposed design strategy focuses on pilot pattern design for maximum compatibility with other OFDM standards, with respect to channel estimation, as elaborated above. Meanwhile, the suggested strategy does not restrict the estimation algorithms to the ones proposed in [14–16]. The proposed pilot pattern strategy does not confine the possible estimators to MMSE estimators only and other linear estimators can be invoked, if needed. In other words, it will follow the Nyquist sampling criteria with a sufficient margin [13] to sample the available signal space to create a pilot subset. Moreover, it is expected that some of the recently proposed OFDM standards such as LTE will prevail in the wireless market for the foreseeable future and may remain as an integral part of multi-standard platforms. Thus, we will also propose a pilot pattern design strategy for emerging OFDM systems provided that they remain compatible with an existing OFDM standard, e.g., LTE.

We have adopted the following structure in this report. First, an OFDM system model will be provided where our adopted transceiver structure, including the wireless channel, is characterized. Then, a brief introduction to the low-complexity MMSE channel estimation is given. This is the basis on which the pilot patterns will be designed. In Sec. 5, we will elaborate our design strategy for pilot pattern design in multi-standard OFDM environments. Finally, Sec. 6 will wrap up the report through some concluding remarks.

2 System model

Our adopted system model is a single-input single-output (SISO) OFDM system operating in a fading and frequency-selective wireless environment. We have chosen a SISO OFDM model because it provides a simple approach for description of the concepts discussed in this paper. However, the results may be easily extended to multiple-input multiple-output (MIMO) OFDM systems. Fig. 1 illustrates a simple transceiver structure for a typical OFDM system operating in a wireless environment.

Presuming the wireless channel to be composed of M resolvable paths in a wide sense stationary uncorrelated scattering (WSSUS) environment, it can be mathematically described as

$$h_{\text{cont.}}(\tau, t) = \sum_{l=0}^{M-1} \alpha_l(t)\delta(\tau - \tau_l), \tag{2.1}$$

where α_ls are independent zero-mean complex-valued Gaussian random variables, with Rayleigh distributed amplitudes, and τ_l is the arrival time associated with the lth component. Moreover, the 2nd-order channel statistics associated with (2.1) in discrete-time can be described through the following separable autocorrelation function

$$r_{\text{h}}[k - k', m - m'] = r_{\text{h,f}}[k - k']r_{\text{h,t}}[m - m'] \tag{2.2}$$

where $r_{\text{h,f}}$ is the frequency correlation and $r_{\text{h,t}}$ is the time correlation. Moreover, depending on the 2nd-order channel statistics in (2.2), the channel is characterized by a maximum Doppler spread, D_{p}, and delay spread, D_{s}.

Following the signal flow depicted in Fig. 1, data corresponding to one OFDM symbol are inserted on the designated tones at the transmitter and fed into an N-point IFFT. Then, the GI (CP) is inserted at the output of the IFFT block and after going through digital-to-analogue (D/A) conversion and modulation to the proper carrier frequency the outcome is transmitted over the wireless channel modeled by (2.1).

Upon reception at the receiver, the signal is picked up by the receiving antenna and after carrier demodulation, low-pass filtering, analogue-to-digital (A/D) conversion, and CP removal, the result is fed into an N-point FFT. If the signal samples after the FFT block are collected into the column vector $\mathbf{y}$ of size N, then

$$\mathbf{y} = \mathbf{X}\mathbf{h} + \boldsymbol{\eta}, \tag{2.3}$$

where $\mathbf{X}$ is a $N \times N$ diagonal matrix containing the transmitted symbols, $\mathbf{h}$ corresponds to the $N \times 1$ vector of subchannel attenuations, and $\boldsymbol{\eta}$ is the $N \times 1$ vector of additive white Gaussian noise (AWGN).

3 Pilot-pattern design in OFDM systems

To be able to capture the CSI in a communications system, one often needs to rely on the (noisy) observations of the received signal values. Moreover, the estimator, e.g., at the receiver, usually needs to know the transmitted signal values to estimate the channel. Yet, there are classes of estimators, known as blind estimators, which rely only on the received signal and its pseudo-stationary properties to carry out the estimation [4–7]. Their application, however, is prohibitive in low-power terminals with limited processing resources due to their high computational complexity.

In the majority of practical cases the transmitter and receiver should have a priori knowledge of the transmitted data for the purposes of channel estimation. Thus, the transmitter and receiver agree on a subset of data which is called pilot-data

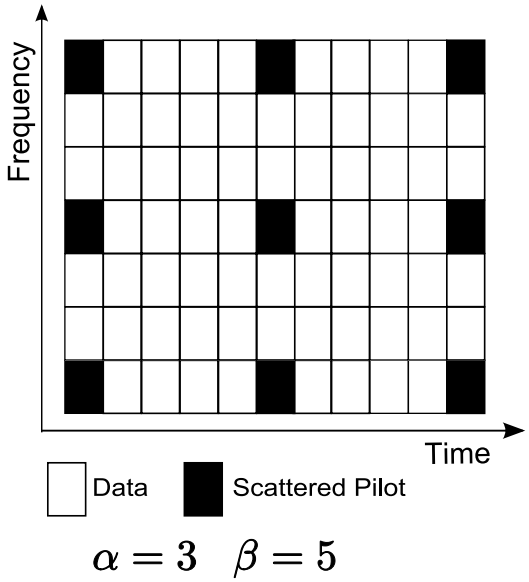

Figure 2: An example of rectangular pilot pattern scattered in time and frequency.

by convention. This approach is extensively used in practical system implementations. The pilots are inserted in specific locations in the transmitted signal. They appear either in continuous or scattered patterns. The contiguous scheme is usually employed in wireless systems where little fading is expected. For instance, IEEE 802.11n [8] uses continuous transmission of pilots for the purposes of channel estimation in its preamble. Contrary, if the wireless channel experiences a considerable amount of fading, e.g., movements in the environment, scattered pilots distributed both in time and frequency need to be used so that the channel variations over both time and frequency can be tracked.

An example of scattered pilot pattern in OFDM systems is depicted in Fig. 2. This is known as rectangular pilot pattern where pilots appear in specific intervals, both in time and frequency. Furthermore, the pilots associated with different OFDM symbols appear exactly on the same frequency tones. On the other hand, the scattered pilots do not necessarily need to appear on the same tones in each pilot carrying OFDM symbol. In other words, the pilots of a specific pilot-carrying OFDM symbol may experience a distinct frequency shift. This is known as skewed pilot pattern. If the pilot carrying OFDM symbols are arranged such that the pilot frequency shift increases monotonically with respect to the symbol time index, a distinct skewed pilot pattern, shown in Fig. 3, can be achieved. This is known as primary skewed pilot pattern in this report.

The scattered pilots can be viewed as a 2-D sampling of a time-frequency grid. Thus, Nyquist's sampling criteria, in time and frequency, needs to be met if a proper reconstruction of the original channel is desired. Thus, the sampling can not fall below a certain threshold set by the Nyquist's sampling criteria as well as certain system dynamics such as the presence of AWGN. On the other hand, the pilots

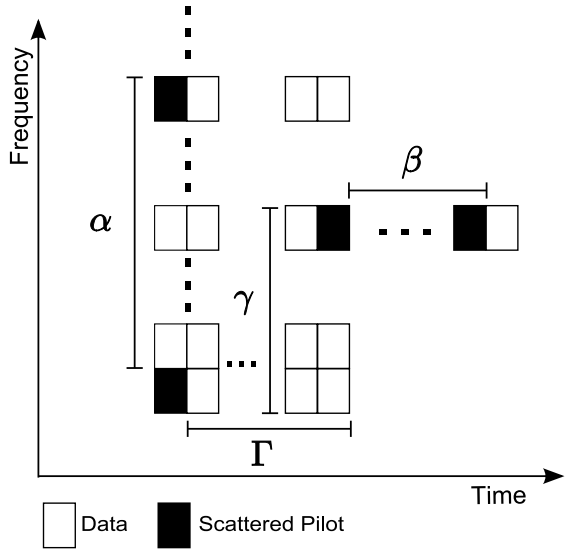

Figure 3: A primary skewed pilot pattern. The pilot frequency offset increases monotonically with respect to the symbol index time. α and β are the distances between pilots in frequency and time respectively. γ is the pilot frequency offset and Γ is the distance between two consecutive pilot-carrying OFDM symbols.

reduce the spectral efficiency in communication systems since a portion of the BW needs to be allocated to pilot rather than data transmission. Besides, although increasing the number of pilots results in better estimation performance, the overall SNR scales down proportionally. Thus, a pilot pattern should provide an acceptable balance among different optimization criteria.

4 Channel estimation

Although there are various approaches to channel estimation for OFDM systems, we have resorted to the application of low-complexity MMSE variants suggested in [14, 15]. A full MMSE estimator can be mathematically described as,

$$\hat{\mathbf{h}}_{\text{mmse}} = \mathbf{R}_{\text{hh}_\text{p}} \left(\mathbf{R}_{\text{h}_\text{p}} + \frac{\mathbf{I}}{\text{SNR}} \right)^{-1} \hat{\mathbf{h}}_{\text{p,ls}}, \tag{4.1}$$

where SNR is the signal-to-noise ratio, $\mathbf{R}_{\text{hh}_\text{p}}$ is the cross-correlation matrix between the pilot and data tones, $\mathbf{R}_{\text{h}_\text{p}\text{h}_\text{p}}$ is the autocorrelation matrix of the pilot tones, and $\hat{\mathbf{h}}_{\text{p,ls}}$ is the least squares (LS) estimation of the channel on the pilot tones. It has been shown in [14, 15] that the estimators can be designed for a worst-case channel environment, i.e., rectangular Doppler spectrum and power delay profile (PDP) where the Doppler and delay spreads are attributed to the maximum expected values.

Meanwhile, due to the correlation loss among the pilots and subcarriers which are located far apart, only a subset of pilots in the vicinity of each tone can be used for estimation purposes. This already results in a significant reduction in computational complexity. To avoid additional time-domain filtering, the estimation is primarily done in frequency direction. To capture the variations of the wireless channel in slow and moderately fast fading environments, a pilot merging practice, only available for skewed pilot patterns, has been suggested in [14–16]. In fast fading environments an additional filtering may kick in to compensate for the time variations of the channel. It can be observed that both alternatives provide a pilot vector which may have different pilot spacing, depending on the merging or time-domain filtering practice. For instance, Fig. 4 shows how a pilot separation of 3 can be attained if all the pilots from all the pilot-carrying OFDM symbols, shown in the figure, are merged or interpolated. A pilot spacing of 6 may be achieved if pilots from alternate pilot-carrying OFDM symbols are merged or interpolated.

On the other hand, it has been shown in [18] and discussed in [16] that the frequency correlation values when the estimators are designed for the worst-case channel environment, i.e., a rectangular PDP, amount to

$$r_{\mathrm{h,f}}\left[\Delta k\right] = \frac{1 - \exp(-2j\pi L\Delta k/N)}{2j\pi L\Delta k/N}, \tag{4.2}$$

where $\Delta k = k - k'$ is the distance between a pilot and estimated tone, N is the DFT size, and L is the PDP spread in discrete time samples. Thus, the designed filter taps will be a function of the pilot separation, as delay spread and DFT size, i.e., $\delta kL/N$. Thus, by controlling the pilot separation, e.g., through merging, one may be able to employ similar filter taps for estimation of the wireless channel. The same principle has been suggested in [16] to use only two sets of filters to address the channel estimation needs of LTE and DVB-H across their different modes of operation. One may observe that if the estimators in [16] were designed based on the extended CP in LTE, only one filter set could cover the channel estimation needs of both standards. A detailed description of such approach is not the intension of this report, though.

5 Filter-tap memory optimized pilot-pattern design in OFDM systems

The presented approach for pilot pattern design is based on filter-coefficient memory optimization in multi-standard environments. Following the memory optimization strategy for the two exemplary standards, i.e., LTE and DVB-H, discussed in [16], the intension is to propose a new approach towards skewed pilot pattern design. Our goal in the suggested strategy is not to take all possible optimization criteria into account. Rather, we would like to shed light on some parameters of interest which can be taken into consideration during pilot pattern design for low-power terminals, specially in multi-mode and multi-standard environments.

The presented ideas in this report for pilot pattern design, with respect to MR-MMSE filter-coefficient optimization, cover two different scenarios. First, pilot pattern design for an arbitrary OFDM systems is discussed in Sec. 5.1. The intension is to provide maximum flexibility in terms of pilot merging schemes such that similar MRMMSE channel estimators can be used while the number of similar OFDM systems selected for co-integration is maximized. Then, it will be shown in Sec. 5.2 that pilot pattern for an arbitrary OFDM system may be designed such that its integration in a multi-standard platform, where one standard is already fixed, makes it possible to employ similar MRMMSE channel estimators. Considering the fact that LTE has been opted as the standard of choice for high speed communications, it is expected that it will be widely deployed and probably replace many of existing commercial wireless communications systems. Thus, pilot pattern design for an exemplary OFDM system, compatible with LTE, will finalize Sec. 5.2.

5.1 Pilot-pattern design for an arbitrary OFDM system

Consider a skewed pilot pattern specified by α, β, γ, and Γ. An example of such pattern is the primary skewed-pilot pattern shown in Fig. 4. Following the merging schemes practiced and elaborated in [14–16], we have restricted ourselves to the ones where an even pilot spacing in the constructed PV can be achieved. As a result, the only skewed patterns of interest are characterized by $\alpha/\gamma = k$, where k is a positive integer. In other words, γ has to be a divisor of α. On the other hand, it can be observed that the number of possible merging schemes equals α/γ for such systems. Thus, the smaller the value of γ, the higher the number of possible merging schemes.

On the other hand, due to efficient FFT/IFFT implementations, the majority of practical OFDM systems are designed such that $N = 2^v$, where v is a positive integer. Also, it can be observed from a number of standardized OFDM systems that the same principle holds with respect to the respective GIs. In other words, the employed GIs in these systems satisfy

$$N_{CP} = 2^x, \tag{5.1}$$

where x is a positive integer. For instance, all the GIs in DVB-H as well as the extended one in LTE satisfy (5.1). In the event of normal GI in LTE, where (5.1) is not held, the estimators need to be designed for a truncated or extended GI such that $L_{\text{design}} = 2^x$ for maximum coefficient memory optimization [16]. Moreover, the standardized GI in Worldwide Interoperability for Microwave Access (WiMAX) [19] follows (5.1). Thus, it is a valid assumption to restrict the proposed pilot pattern to OFDM systems where both N and GIs are powers of 2.

Taking the above mentioned facts into account, the optimal values for α and γ are restricted to the powers of 2 only. Besides, unless prohibited due to fading characteristics of the channel, $\gamma = 2$ is selected as a default design value. Selection of $\gamma = 2$, as the smallest divisor of α, maximizes the number of possible merging schemes which in turn increases the configurations for which similar MRMMSE

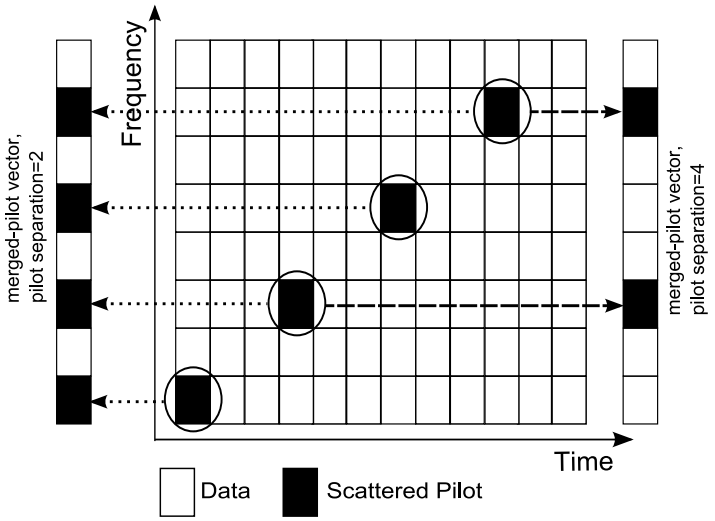

Figure 4: An example of pilot-merging practiced for a primary skewed pilot pattern. The pilot vector to the left is constructed by merging all the available pilots in the tile and exhibits a pilot separation of 2. The merged-pilot vector to the right, however, is constructed by merging the pilots from alternate pilot carrying OFDM symbols and has a pilot separation of 4.

filters can be used, this follows (4.2). Thus, the following procedure may be pursued for pilot pattern design for an arbitrary OFDM system.

- Stage 1:
  First, the parameters α, β, γ, and Γ need to be estimated with respect to the design criteria, i.e., D_{s}, D_{p}, Δf, and N. Taking the Nyquist sampling criteria with a sufficient margin [1] into account and restricting α to powers of 2 only, where

$$\alpha = \max_{q} 2^{q} \tag{5.2}$$

  and

$$\alpha \leqslant \frac{1}{2D_{\mathrm{s}}\Delta f}, \tag{5.3}$$

  it is trivial to conclude that

$$\alpha = 2^{\left\lfloor \log_2 \frac{1}{2D_{\mathrm{s}}\Delta f} \right\rfloor}. \tag{5.4}$$

  Likewise, restricting β to the powers of 2 only, constraint to the adapted sampling criteria,

$$\beta = 2^{\left\lfloor \log_2 \frac{\Delta f}{2D_{\mathrm{p}}} \right\rfloor}. \tag{5.5}$$

[1] The sampling is set to twice as fast as the one required by the Nyquist sampling criteria. It has been shown that [13, 20] it provides an acceptable balance in the channel estimation performance versus pilot overhead for band-limited channels in the presence of AWGN.

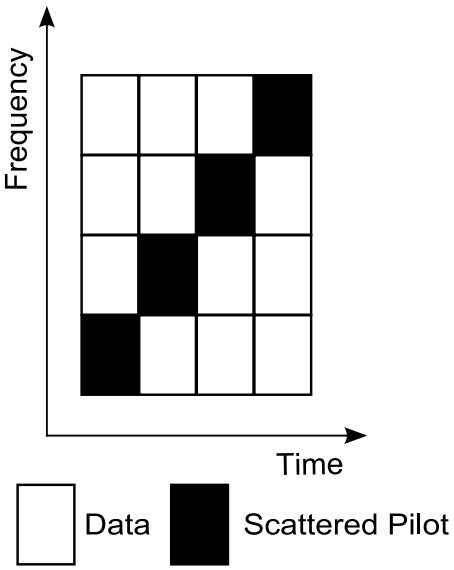

Figure 5: An example of an elementary tile constructed from Fig. 4. Please note that the pilot indexes in frequency monotonically increases as a function of symbol time.

Besides, Γ should be a positive integer such that $\Gamma = \left\lfloor \frac{\gamma\beta}{\alpha} \right\rfloor \geqslant 1$.Thus, $\gamma = 2^i$, where $i = \max\left(1, \left\lceil \log_2 \frac{\alpha}{\beta} \right\rceil\right)$.

- Stage 2:
  Following the design parameters derived from Stage 1, suppose a primary skewed pilot-pattern, similar to Fig. 3, is created. The pattern is arranged such that the pilot frequency shift increases monotonically with respect to the OFDM symbol time index. Although the constructed pattern provides an appropriate alternative from a coefficient-memory optimization principle, one may rearrange the indexes for the pilot-carrying OFDM symbols such that a more optimized pattern with respect to channel estimation performance, in the event of merging in fast fading environments, is provided.

  For instance, if a pilot spacing of 6 in the constructed PV associated with Fig. 4 is desired, the pilots from OFDM symbols 1 and 7 should be merged. As a result, upon the application of merged-pilot MRMMSE channel estimation and respective equalization, a considerable performance degradation may hit the system for fast-fading environments. If, however, the pilot-carrying OFDM symbols selected for merging were placed next to each other, the performance degradation would considerably decrease due to higher correlation among the symbols in time. Meanwhile, the same principle applies in the event of merging more pilot-carrying OFDM symbols. Thus, a more optimized skewed-pilot pattern may be sought such that upon pilot-merging the performance degradation due to fast fading environments is minimized.

  The 2nd stage of our proposed pilot pattern design procedure is illustrated

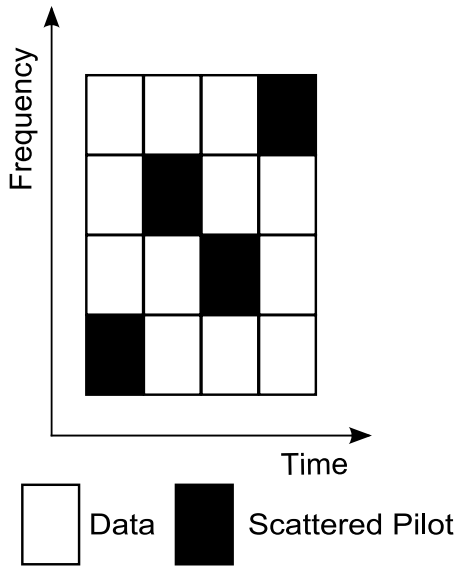

Figure 6: An example of a rearranged elementary tile constructed from Fig. 4. Please note the difference in pilot pattern when compared to Fig. 5.

by the flow-chart shown in Fig. 8. However, it is worthwhile to provide an insight into the operation of the proposed flow-chart by designing an alternative pilot pattern for the example shown in Fig. 4. Let's start by collecting the first four pilot-carrying OFDM symbols and remove the non-pilot carrying tones. The result is a tile (called an elementary tile) depicted in Fig. 5. The resultant elementary tile does not provide the closest distance between pilot-contributing OFDM symbols when merging is practiced. If, instead, the pilot carrying OFDM symbols were rearranged such that a modified elementary tile, shown in Fig. 6, was created, then channel estimation performance in fading environments, in the event of merging, would improve. Finally, the modified elementary tile is expanded by inserting a proper number of non-pilot carrying subcarriers and OFDM symbols such that $\alpha = 8$ and $\Gamma = 3$ are satisfied. The result is a fundamental tile, seen in Fig. 7, which may be used to span the whole time-frequency grid for a given OFDM system according to its specifications.

The design procedure for an arbitrary OFDM system may be initiated by creating an elementary tile by collecting the first α/γ pilot-carrying OFDM symbols in time and removing the non-pilot carrying subcarriers associated with the primary skewed-pilot pattern depicted in Fig. 3. Please observe that the OFDM symbols are arranged such that the pilot frequency shift monotonically increases with respect to the OFDM symbol time index. As mentioned earlier, the outcome is known as an elementary tile and is used in the flow-chart shown in Fig. 8 to finalize the pilot pattern design suggested by this literature. The flow-chart follows an iterative grid search where at each stage the best candidates for pilot merging are grouped together. In fact, the algorithm guarantees the proximity of pilot-contributing OFDM symbols in the event

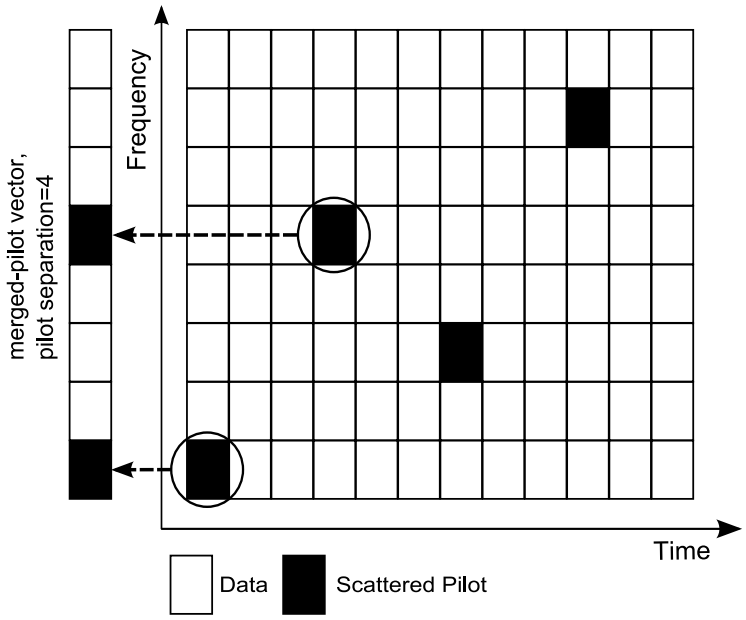

Figure 7: An example of a fundamental tile constructed from Fig. 4. Please note the difference in pilot pattern when compared to Fig. 4. To construct a merged-pilot vector where a pilot separation of 4 is desired, the pilots from two consecutive pilot-carrying OFDM symbols need to be merged. As a result, the performance of the channel estimation, in the event of pilot merging, in fading environments increases when compared to Fig. 4. If a pilot separation of 2 is desired, the channel estimation performance for both patterns is the same.

of pilot merging. The novelty of such pilot arrangement not only guarantees the proximity of two-consecutive pilot-carrying OFDM symbols but also provides the closest distance among pilot-carrying OFDM symbols in case a pilot merging of higher order is sought. For instance, if four pilot-carrying OFDM symbols should be merged, our algorithm makes sure the pilot-contributing OFDM symbols exhibit the shortest distance from each other, when compared to other possible pilot arrangements.

The discussion about the proposed pilot-pattern strategy described by the flowchart in Fig. 8 can be finalized through an example. Assume the proposed approach in Stage 1 results in $\alpha = 16$, $\gamma = 2$, and $\Gamma = 3$ for a given OFDM system. Fig. 9 illustrates the procedure mentioned in Stage 2 and elaborated by Fig. 8 to finalize the proposed pilot pattern design for this system. It is worthwhile to point out that the constructed tile can be used to fill in the time-frequency grid of arbitrary size dictated by the OFDM system requirements and specifications.

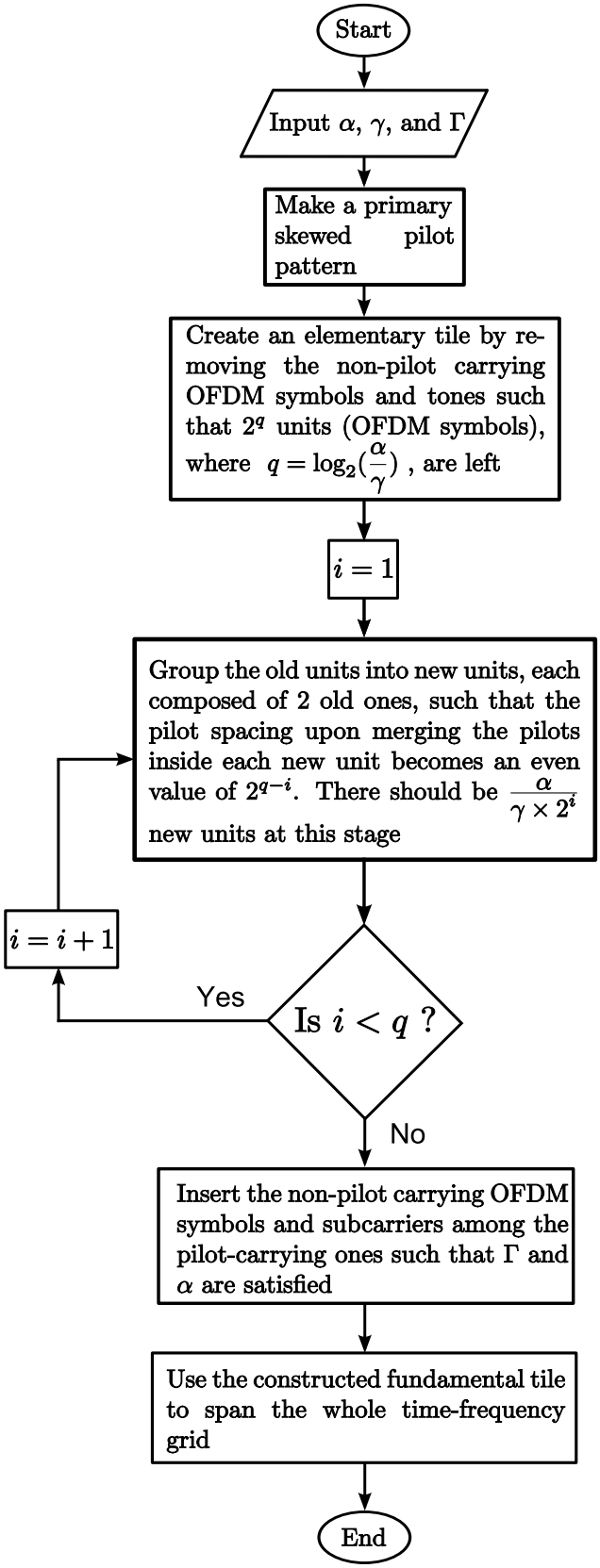

Figure 8: Construction of an optimum tile in terms of filter-memory optimized MRMMSE estimators as well as merging operation. The final pattern looks different from the primary skewed pilot pattern exemplified by Fig. 3 and 4

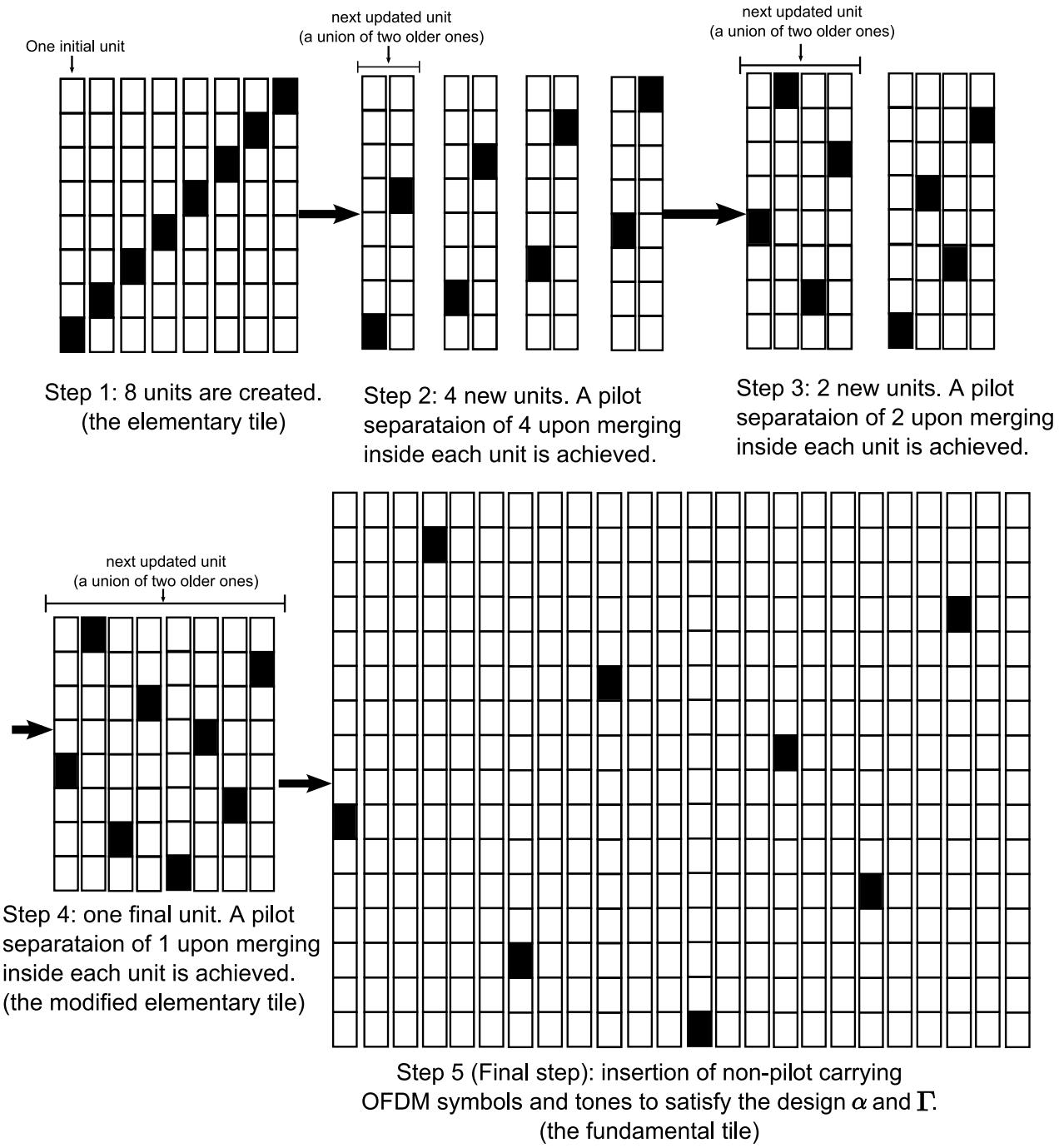

Figure 9: An example of tile construction according to the procedure in Stage 2 as illustrated in Fig. 8.

An alternative approach to the application of the flow-chart shown in Fig. 8, each time a new pilot pattern needs to be designed, is to create a library of modified elementary tiles. Please note that each modified elementary tile is distinctly characterized by the number of pilots it accommodates. Besides, the number of pilots in the fundamental tile for each design equals $(\frac{\alpha}{\gamma})$. Thus, after the proper design values, i.e., α, γ, and Γ are estimated through Stage 1, the appropriate tile is selected from the library and expanded, constraint to α and Γ, to create the target fundamental tile.

5.2 Pilot pattern design for OFDM systems compatible with a standardized OFDM system, e.g., LTE

With the advent of more standards as well as improvements in hardware technology, there is a growing interest in integrating more wireless OFDM standards in one platform. An example of such systems has been elaborated in [17]. Thus, it becomes but inevitable to finalize the pilot pattern design for OFDM systems when the design criteria is constraint by an existing OFDM system, e.g., LTE. However, as discussed in Sec. 5.1 the OFDM systems of interest are restricted to the ones where the number of DFT points as well as GI lengths are powers of 2. However, for systems where some GI lengths happen to disagree with the above presumptions, e.g., the normal CP in LTE, the MRMMSE estimators need to be designed for a truncated or extended CP. The MRMMSE filter design procedure has been discussed in [16] with respect to the normal CP in LTE. Besides, to practice the suggested pilot merging as well as filter-tap memory optimization in the event of co-integration, $\alpha_{\text{std.}} = k \times \gamma_{\text{std.}}$ should hold, where k is a positive integer and subscript $(\cdot)_{\text{std.}}$ denotes the standardized OFDM system parameters.

Imagine a standardized OFDM system with

$$\gamma_{std.} = 2^u r_0^{v_0} ... r_{l-1}^{v_{l-1}}, \tag{5.6}$$

where $\{r_0, ..., r_{l-1}\}$ belong to the set of prime numbers excluding 2 and $\{u, v_0, ..., v_{l-1}\} \in \mathbf{Z}^+$. Furthermore, $\mathbf{Z}^+$ is the set of nonnegative integers. As discussed above, the system should satisfy $\alpha_{\text{std.}} = k \times \gamma_{\text{std.}}$ so that MRMMSE filter-coefficient co-optimization can be performed. As a result, to design a flexible pilot pattern for the compatible OFDM system, two design goals should be pursued in parallel. First, the proposed pilot pattern should allow its co-integration with the standardized system while using similar MRMMSE filter coefficients. Second, it should maximize the number of other OFDM systems which can be integrated in the same platform provided that similar filter coefficients can be used. Moreover, a natural outcome of such strategy is not only maximizing the number of compatible OFDM systems but also maximizing the the number of operation modes, in terms of employing different GIs associated with the same OFDM system.

Similar to Sec. 5.1, the pilot pattern design can be split into two different stages. During the first stage, the parameters of interest, i.e., α, γ, and γ are estimated. The second design stage, however, rearranges the locations of the pilot-carrying

OFDM symbols such that a higher performance in the event of merging in fast-fading environments is achieved. The following procedure can be followed for the first design stage. Suppose

$$\alpha = \max_{q} (\gamma_{\text{ini}} 2^q) \tag{5.7}$$

constraint to (5.3), where q is a positive integer and $\gamma_{\text{ini}} = r_0^{v_0} ... r_{l-1}^{v_{l-1}}$. As a result,

$$\alpha = 2^{\left\lfloor \log_2 \frac{1}{2\gamma_{\text{ini}} D_s \Delta f} \right\rfloor}. \tag{5.8}$$

Meanwhile, β should follow (5.5). Besides, Γ should be a positive integer such that $\Gamma = \left\lfloor \frac{\gamma\beta}{\alpha} \right\rfloor \geqslant 1$.Thus, $\gamma = \gamma_{\text{ini}} 2^i$, where $i = \max(1, \left\lceil \log_2 \frac{\alpha}{\gamma_{\text{ini}}\beta} \right\rceil)$. The second design stage is consistent with the flow-chart in Sec. 5.1 as illustrated in Fig. 8.

An example of the above presented approach is pilot-pattern design for systems compatible with LTE. Being the standard of choice for high-speed wireless communications, it is expected that LTE gradually replaces the existing standards in market and remain a dominant one for the foreseeable future. As a result, it is not far fetched to presume that many multi-standard wireless OFDM platforms integrate LTE as one of their fundamental alternatives. Thus, the future OFDM systems can be designed such that maximum flexibility in terms of MRMMSE channel estimators when co-implemented with LTE is achieved.

For instance, suppose it is desired to design the pilot pattern for systems compatible with LTE. Furthermore, the given OFDM system specifications result in $\alpha = 12$, $\gamma = 3$, and $\Gamma = 1$. Thus, an elementary tile, similar to the one associated with Step 1 in Fig. 10, may be constructed. Moreover, the elementary tile can be further processed by the flow-chart depicted by Fig. 8. The result is a fundamental tile which is more efficient in terms of employing MRMMSE estimators.

One might realize that the advantages are not limited to MRMMSE algorithms only. In fact, in the event of slowly fading environments, the majority of pilot-based channel estimation algorithms may benefit from merging the nearby pilots, because not only the number of effective pilots increases but also the resultant pilot spacing is reduced. Although, one might argue that the same principle holds for a primary skewed pilot pattern, employing the proposed pilot re-indexing facilitates the merging scheme for a higher amount of fading associated with a given wireless environment.

Last but not least, had the pilot pattern for DVB-H been designed according to the fundamental elementary tile shown in Fig. 10, the performance of the merged-pilot channel estimation algorithms would have improved for fading environments. Please observe that the design parameters, i.e., α, Γ, and γ are similar to the ones standardized for DVB-H.

6 Conclusion

We have shown that it is possible to adopt a different approach for pilot pattern design if the co-integration of several OFDM systems is sought. The proposed design

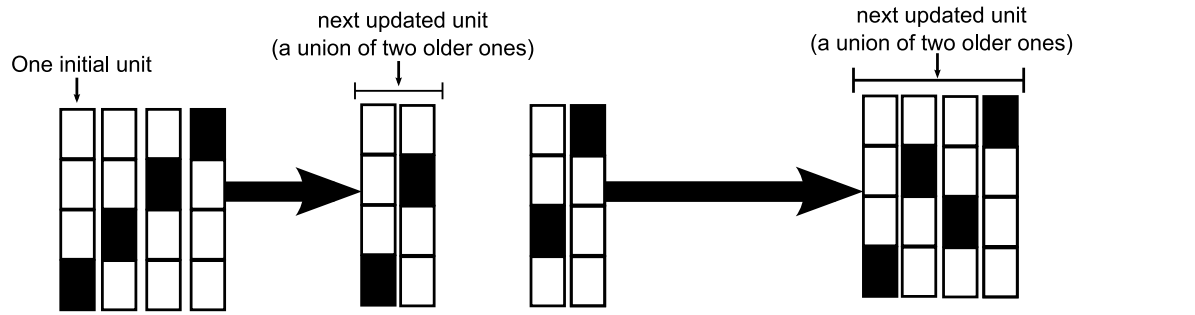

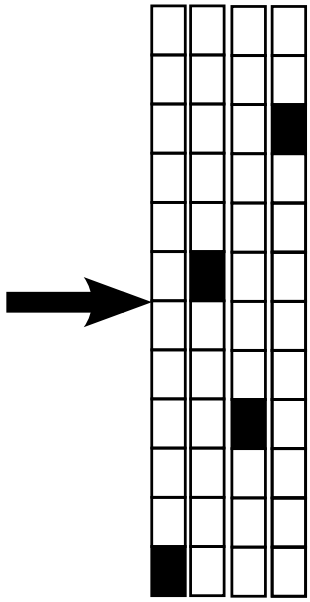

Step 4 (final step): insertion of non-pilot carrying OFDM symbols and tones to satisfy the design α and Γ.

Figure 10: Construction of a fundamental tile for an OFDM system compatible with LTE where $\alpha = 12$, $\gamma = 3$, and $\Gamma = 1$. Compared to the standardized pilot pattern for DVB-H, the result is more optimized for merging practices.

procedure maximizes the performance of the merged-pilot MRMMSE algorithms. Meanwhile, it provides the possibility to employ other estimation approaches. The main merits, however, result from the possibility to change the pilot spacing by either merging or time-domain filtering. As a result, the MRMMSE filters can be shared among a number of different standards. Our approach starts with the pilot pattern design for an arbitrary OFDM system. However, it is shown that it can be modified and adapted to design the pilots for systems which need to remain compatible with a given OFDM standard, such as LTE. Moreover, we showed that by following the proposed strategy, the pilot pattern for an exemplary DVB-H system would look differently when co-implemented with LTE. In other words, the existing pilot pattern may not be optimal if pilot merging upon channel estimation is sought. Although the proposed approach is specifically developed for filter-tap memory optimization as well as high performance in the event of merged-pilot MRMMSE estimation, it provides an alternative insight into pilot pattern design for future OFDM systems.

References

[1] R. W. Chang, "Synthesis of band-limited orthogonal signals for multichannel data transmission," *Bell Syst. Tech. J., 45*, pp. 1775–1796, 1996.

[2] R. Chang and R. Gibby, "A theoretical study of performance of an orthogonal multiplexing data transmission scheme," *IEEE Trans. Commun.*, vol. 16, pp. 529–540, Aug. 1968.

[3] F. Horlin and A. Bourdoux, *Digital Compensation for Analog Front-ends*. West Sussex, United Kingdom: John Wiley & Sons Ltd., 2008.

[4] L. Tong et al., "Blind identification and equalization of multipath channels," in *Proc. IEEE Int. Conf. Commun.,* Chicago, IL, pp. 1513–1517, 1992.

[5] L. Baccala and S. Roy, "A new blind time-domain channel identification method based on cyclostationarity," *IEEE Signal Process. Lett.*, vol. 1, pp. 89–91, June 1994.

[6] H. Zeng and L. Tong, "Blind channel estimation using the second-order statistics: Algorithms," *IEEE Trans. Signal Process.*, vol. 45, pp. 1919–1930, Aug. 1997.

[7] W. Songping and Y. Bar-Ness, "OFDM channel estimation in the presence of frequency offset and phase noise," in *Proc. IEEE Int. Conf. Commun.,* Anchorage, AK, pp. 3366–3370, 2003.

[8] "IEEE Standard for Information technology–Telecommunications and information exchange between systems–Local and metropolitan area networks–Specific requirements Part 11: Wireless LAN Medium Access Control (MAC) and Physical Layer (PHY) Specifications Amendment 5: Enhancements for Higher Throughput," *IEEE Std 802.11n-2009*, pp. c1–502, Sep. 2009.

[9] C. Knievel et al., "2-D graph-based soft channel estimation for MIMO-OFDM," in *Proc. IEEE Int. Conf. Commun.,* Cape Town, pp. 1–5, 2010.

[10] B. Hassibi and B. Hochwald, "How much training is needed in multiple-antenna wireless links?," *IEEE Trans. Inf. Theory*, vol. 49, pp. 951–963, Apr. 2003.

[11] R. Nilsson et al., "An analysis of two-dimensional pilot-symbol assisted modulation for OFDM," in *Proc. IEEE Int. Conf. Personal Wireless Commun.,* Mumbai, pp. 71–74, 1997.

[12] F. Tufvesson and T. Maseng, "Pilot assisted channel estimation for OFDM in mobile cellular systems," in *Proc. IEEE Veh. Tech. Conf.,* Phoenix, AZ, pp. 1639–1643, 1997.

[13] P. Hoeher et al., "Two-dimensional pilot-symbol-aided channel estimation by Wiener filtering," in *Proc. IEEE Int. Conf. Acous., Speech and Signal Process.,* Munich, pp. 1845–1848, 1997.

[14] F. Foroughi Abari et al., "Channel estimation for a mobile terminal in a multi-standard environment (LTE and DVB-H)," in *Proc. IEEE Int. Conf. Signal Process. and Commun. Syst.,* Omaha, NE, pp. 1–9, Sep. 2009.

[15] F. Foroughi Abari et al., "Low complexity channel estimation for LTE in fast fading environments for implementation on Multi-Standard platforms," in *Proc. IEEE Veh. Tech. Conf.,* Ottawa, pp. 1–5, Sep. 2010.

[16] F. Foroughi Abari et al., "On coefficient memory co-optimization for channel estimation in a multi-standard environment (LTE and DVB-H)," in *Proc. IEEE 8th Int. Workshop on MultiCarrier Syst. and Solutions ,* Herssching, pp. 1–5, May 2011.

[17] Ericsson AB et al., "System Requirements Specification (2nd version), incl. scope and time plan," Scalable Multi-tasking Baseband for Mobile Communications, Tech. Rep. D1.2, Jan. 2008. Available: http://www.multibase-project.eu.

[18] O. Edfors et al., "OFDM channel estimation by singular value decomposition," *IEEE Trans. Commun.*, vol. 46, pp. 931–939, July 1998.

[19] "IEEE802.16, in part 16: Local and metropolitian local area networks-air interface for fixed and mobile broadband wireless access systems amendment 2: Physical and medium access control layers for combined and fixed operation in licenced bands and corrigendum 1," Broadband Wireless Access Working Group, Tech. Specifications Final Draft, 2006.

[20] R. Nilsson et al., "An analysis of two-dimensional pilot-symbol assisted modulation for OFDM," in *Proc. IEEE Int. Conf. Personal Wireless Commun.,* Mumbai, pp. 71–74, 1997.